Remote Sensing of Alpine Grassland Ecosystems On the Qinghai-Tibetan Plateau

Dissertation
zur
Erlangung der naturwissenschaftlichen Doktorwürde
(Dr. sc. nat.)
vorgelegt der
Mathematisch-naturwissenschaftlichen Fakultät
der
Universität Zürich

von
Chengxiu Li
aus
China

Promotionskommission
Prof. Dr. Michael E. Schaepman (Vorsitz)
Dr. Hendrik Wulf (Leitung der Dissertation)
Prof. Dr. Bernhard Schmid

Zürich, 2019

Front page: Herding livestock on the Qinghai-Tibetan Plateau. The picture shows the interaction and impact between human activity and environment.
Picture taken by Chengxiu Li in August 2015

Chengxiu Li

Remote Sensing of Alpine Grassland Ecosystems on the Qinghai-Tibetan Plateau

Remote Sensing Series, Vol. 82
Remote Sensing Laboratories, Department of Geography, University of Zurich
Switzerland, 2019

ISBN: 978-3-906894-12-6

This work was approved as a PhD thesis by the Faculty of Science of the University of Zurich in the fall semester of 2019. Doctorate committee: Prof. Dr. Michael E. Schaepman (chair), Dr. Hendrik Wulf (dissertation supervisor), Prof. Dr. Bernhard Schmid.
External examiner: Prof. Dr. Alexander Damm, PD Dr. Karin Schwiter

Abstract

Alpine grassland ecosystems on the Qinghai-Tibetan Plateau (QTP) are critical for global change research and livelihoods of a large part of the world's population who are depending on fresh water coming from the QTP. The harsh environmental conditions on the QTP characterize plant traits reflecting plant adaptation strategies and determining ecosystem functioning. The ecosystem function on the QTP has been influenced by climate change and human activities, showing ecosystem degradation of bare-soil patch development and changes in community composition. Remote Sensing (RS) offers the ability to address challenges of alpine grassland research on understanding ecosystem functioning, human influences and ecosystem degradation. This thesis demonstrates the use of remote sensing to firstly, retrieve plant traits at the canopy level for understanding plant adaptation strategies; secondly, to evaluate the human influence on ecosystems and finally, to monitor ecosystem development and degradation.

The thesis maps three plant traits including canopy Chlorophyll content (CHL), Plant Dry Matter Content (PDMC) and Specific Plant Area (SPA) at the spatial resolutions of 10 m, 30 m and 500 m on the QTP. The remotely sensed traits (SPA and PDMC) are correlated with literature-derived leaf traits of CWMs of SLA and LDMC despite vastly different measurement methods. Alpine meadow plants reveal a wider range and higher averages of CHL and SPA but lower PDMC in comparison to alpine steppe plants. The trait differences among vegetation types indicate faster growth of alpine meadow but higher resilience to harsh conditions of alpine steppe, showing differences in adaptation strategies to environmental conditions.

The thesis further provides a framework for estimating human influence on ecosystems at two spatial scales though mapping the spatial patterns of biomass reduction and gain relating to human activities. At the regional scale of 10 km, we map the potential biomass only driven by environmental variables and actual biomass estimated from satellite data. We assume that human activities contribute to biomass gain if actual biomass is higher than the potential one, indicating positive human influence, and vice versa. We found that higher livestock density contribute to biomass gain at the 10 km scale. However, at the local scale of 500 m within a radius of 8 km distance to settlements, we find biomass decreased closer to settlements in the

regions with higher livestock density, but increased in areas with lower livestock density. These results suggest complex relationships between livestock grazing and biomass, varying between spatial scales and regions. Grazing may boost biomass production across the whole QTP at the 10 km scale; however, overgrazing may reduce biomass near settlements at the 500 m scale.

The thesis further monitors grassland development and degradation stages. Specifically, we develop indicators that are temporal changes in grassland cover and spatial heterogeneity for monitoring grassland development and degradation. We find that grassland cover shows declining trends in the literature-defined degraded areas but increasing trends in the desert areas from 2000–2016. However, spatial heterogeneity generally has increased in 2000-2016. We map the new degradation categories in 2016, including degradation, desertification, and improving categories using differences in the trends of grassland cover and spatial heterogeneity. Most study areas (63%) are classified as degraded and 2% of areas are at risk of desertification. Areas (35%) identified as improving and re-growing occur in steppe-dominated areas, at higher-elevation, or in previously severely degraded grasslands.

The thesis discusses the advantages and limitations of using remote sensing for mapping plant traits, human influence and ecosystem degradation. The proposed future research directions include retrieval of plant traits at different scales, monitoring dynamics of human influence on ecosystem and studying drivers for ecosystem degradation on the QTP.

Zusammenfassung

Die alpinen Graslandökosysteme auf dem Qinghai-Tibet Plateau (QTP) spielen eine wesentliche Rolle für Studien zum globalen Wandel und für die Lebensgrundlage eines grossen Teils der Weltbevölkerung, die von der vom Frischwasser aus dem QTP abhängt. Die rauen Umgebungsbedingungen auf dem QTP charakterisieren pflanzliche Merkmale, die wiederum Anpassungsstrategien widerspiegeln und die Funktionsweisen des Ökosystems mitbestimmen. Die Ökosysteme auf dem QTP verändern sich im Zuge des Klimawandels. Wichtige Funktionen des Ökosystems werden durch die globale Erwärmung beeinflusst und durch menschliche Einwirkungen beeinträchtigt. Diese Entwicklung zieht Prozesse der Bodendegradation nach sich und verändert die Zusammensetzung der Pflanzengemeinschaft. Fernerkundungsmethoden bieten die Möglichkeit die Funktionsweise eines Ökosystems zu charakterisieren, indem sie pflanzliche Merkmale auf der räumlichen Skala eines Pixels bewertet. Darüber hinaus ermöglicht die Fernerkundung den menschlichen Einfluss auf Ökosysteme zu bewerten und deren grossräumigen Veränderungen zu überwachen.

Im Rahmen dieser Arbeit wurden die folgenden drei pflanzlichen Merkmale mit einer räumlichen Auflösung von 10 m, 30 m und 500 m im QTP bestimmt: Chlorophyllgehalt, pflanzlicher Trockengehalt (PDMC), und die spezifische Pflanzenfläche (SPA). Wir fanden heraus, dass die fernerkundlich bestimmten Pflanzenmerkmale SPA und PDMC mit Literaturwerten von Blattmerkmalen für die spezifische Blattfläche (SLA) und dem Trockengehalt der Blätter (LDMC) korrelieren. Diese Korrelation bezieht sich jeweils auf das gewichtete Mittel einer Pflanzengemeinschaft (CWMs) und besteht trotz grundlegend verschiedener Messmethoden. Die Unterschiede zwischen Pflanzeneigenschaften weisen darauf hin, dass alpine Wiesen schneller wachsen während alpine Steppen widerstandsfähiger gegen schwierige Verhältnisse sind. Dies zeigt die unterschiedlichen Anpassungsstrategien der Pflanzen zur Umwelt. Darüber hinaus bietet diese Doktorarbeit einen Rahmen für die Kartierung des menschlichen Einflusses auf Ökosysteme. Diese Analyse wurde auf zwei unterschiedlichen räumlichen Skalen durchgeführt und untersucht räumliche Muster der zeitlichen Zu- bzw. Abnahme von Biomasse im Zusammenhang mit menschlichen Aktivitäten. Auf der regionalen Skala von 10 km kartieren wir die potenzielle Biomasse, welche nur durch Umweltvariablen

beeinflusst wird, sowie die tatsächliche Biomasse, die wir von Satellitendaten ableiten. Wir nehmen an, dass menschliche Aktivitäten zur Zunahme der Biomasse beitragen, wenn die potenzielle Biomasse niedriger als die Tatsächliche ist, und umgekehrt falls das Gegenteil der Fall ist. Wir fanden heraus, dass Gebiete mit höherer Viehdichte eine Zunahme von Biomasse aufweisen, während Gebiete mit niedrigerer Viehdichte eine Abnahme aufweisen. Auf der lokalen Skala von 500 m, im 8-km Umkreis von Siedlungen, stellten wir fest, dass die Biomasse näher an den Siedlungen in den Regionen mit höherer Viehdichte zurückging und die Biomasse näher an den Siedlungen in Regionen mit niedrigerer Viehdichte anstieg. Diese Resultate deuten darauf hin, dass weidendes Vieh die Biomassenproduktion über das ganze QTP auf der 10 km Skala fördert, jedoch in Siedlungsnähe auf der 500 m Skala Überweidung und somit ein Rückgang der Biomasse beobachtet werden kann. Dies deutet auf komplexe Zusammenhänge zwischen Viehzucht und Biomasse hin, die zwischen räumlichen Skalen und Regionen variieren.

Im Rahmen dieser Doktorarbeit haben wir ebenfalls Entwicklungs- und Degradationsstadien des Grasland-Ökosystems untersucht. Im Einzelnen haben wir Indikatoren entwickelt, die die zeitliche Veränderungen in der Grasbedeckung und ihre räumliche Heterogenität abbilden, um die Degradation von Grasflächen zu überwachen. Dabei haben wir festgestellt, dass für die Zeitspanne 2000-2016 die Grasbedeckung einen rückläufigen Trend in den von der Literatur definierten vormals degradierten Gebieten zeigte, aber ein zunehmender Trend in vormaligen Wüstengebieten besteht. Allerdings hat die räumliche Heterogenität zwischen den Jahren 2000-2016 in weiten Teilen zugenommen. Für das Jahr 2016 haben wir neue Degradationsklassen definiert, die Kategorien zur Degradation, Desertifikation und Verbesserung der Grasflächen beinhalten. Diese Einteilung beruht auf Unterschieden in den zeitlichen Trends zur Grasbedeckung und ihrer räumlichen Heterogenität. Die meisten Untersuchungsgebiete (63%) wurden als degradiert eingestuft und 2% der Gesamtfläche waren von der Gefahr zu desertifizieren betroffen. Die als verbessert und wieder wachsend eingestuften Flächen (35%) traten vornehmlich in Steppengebieten, höher gelegenen oder zuvor stark degradierten Graslandschaften auf.

In dieser Arbeit wurden die Vorteile und Grenzen der fernerkundlichen Bestimmung von pflanzlichen Merkmalen, des menschlichen Einflusses auf die Ökosysteme und

des Degradation diskutiert. Mögliche zukünftige Forschungsrichtungen beinhalten die Bestimmung von pflanzlichen Merkmalen auf verschiedenen Skalen, die Beobachtung der Dynamik des menschlichen Einflusses auf das Grasland-Ökosystem, sowie die Untersuchung der Einflussfaktoren für die Degradation des Ökosystems auf dem QTP.

Table of Contents

List of Abbreviations

APHRODITE	Asian Precipitation-Highly Resolved Observational Data Integration Towards Evaluation of the Water Resources
BRDF	Bidirectional Reflectance Distribution Function
CHL	CHLorophyll content
CIgreen	Green chlorophyll index
CIred-edge	Red-edge chlorophyll index
CV	Coefficient of Variation
CWMs	Community-Weighted Means
ESRI	Environmental Systems Research Institute
EVI	Enhanced Vegetation Index
GRF	Gaussian Random Field
GIMMS	Global Inventory Monitoring and Modeling Systems
HydroSHEDS	Global Hydrological data and maps based on Shuttle Elevation Derivatives at multiple Scales
LMA	Leaf Mass per Area
LDMC	Leaf Dry Matter Content
LAI	Leaf Area Index
JRC	Joint Research Center
MODIS	Moderate Resolution Imaging Spectroradiometer
MCD12Q1	MODIS Land Cover Type Yearly - L3 Global - 500m
MCD15A3H	MODIS Leaf Area Index product - 4-Day L4 Global - 500m
MCARI/OSAVI	Modified Chlorophyll Absorption Ratio Index and the Optimized Soil-Adjusted Vegetation Index
MCD43A4	MODIS Albedo Nadir BRDF-Adjusted reflectance product
NASA	National Aeronautics and Space Administration
NPP	Net Primary Productivity
NDVI	Normalized Difference Vegetation Index
QTP	Qinghai-Tibetan Plateau
RS	Remote Sensing
RTMs	Radiation Transfer Models
rRMSE	relative Root Mean Square Error
PDMC	Plant Dry Matter Content
PAI	Plant Area Index
SPAD	Soil Plant Analysis Development
SPA	Specific Plant Area
SLA	Specific Leaf Area
SVM	Support Vector Machines
TOA	Top Of the Atmosphere
TCARI/OSAVI	Transformed Chlorophyll Absorption Ratio Index and the Optimized Soil-Adjusted Vegetation Index
TRMM	Tropical Rainfall Measuring Mission
VI	Vegetation Index
VIF	Variance Inflation Factor

Chapter 1

Introduction

1.1 Alpine ecosystems are critical for global change research

1.1.1 Characteristics of alpine climate and ecosystems

Alpine ecosystems refer to high-altitude ecosystems above the tree line from all parts of the world (Körner, 1995), which cover about 3% (4.5 million km^2) of the world's land area (Körner, 2003). Alpine ecosystems are characteristic of extremes in climate and physical environment, such as low temperature, high solar radiation, nutrient-poor soil, and slow microbial processes (Körner, 2003).

The Qinghai-Tibetan Plateau (QTP) is the highest and largest alpine grassland ecosystem in the world, covering around 2.5 million km^2 with an average elevation of more than 4000 m a.s.l. Climate conditions on the QTP are characteristic of wet summers and cold and dry winters, driven by the South Asian and East Asian monsoons and Westerlies (Miller, 2005). Many major rivers originate on the QTP, including the Yellow, Yangtze, Mekong, Salween, Indus, Sutlej, Ganges and Brahmaputra (Miller, 2005).

Alpine meadow (c. 45%) and alpine steppe (c. 29%) are the main vegetation types on the QTP (Miller, 2005). Alpine meadow is mainly found on the eastern part of the QTP, and alpine steppe lies on the central and western part of the QTP (Miller, 2005). The transitional ecotone, alpine steppe-meadows (c. 4.28%), typically comprises of a mixture of plant species from the above two habitats (Miehe et al., 2013). The other vegetation types, alpine desert steppe (c. 6%) and temperate desert (c. 1.59%) are located on the northwestern and northeastern QTP respectively (Miller, 2005). The temperate mountain meadow (4.6%) is mainly situated on the southeastern part of the QTP (Miller, 2005). Figure 1.1 shows photos of main grassland types on the QTP.

Figure 1.1 Example photos of main grassland types on the QTP. a) and b) Alpine meadow on the northeastern of QTP (2015.07). c) Alpine steppe on the eastern Tibet, Bange county (2016.08) d): Temperate desert on the Qaidam Basin, northeastern part of the QTP (2015.08)

1.1.2 Plant traits to understand plant adaptation strategies

Alpine plants develop adaption strategies of coping with harsh environments of extreme temperatures, drought, and excessive radiation (Körner, 2003). The adaption strategies can be revealed by specific plant morphological, physiological and biochemical features, which are termed as "plant traits" (Pérez-Harguindeguy et al., 2013). For example, alpine dwarfism shows morphological adaptation to the cold and windy environment (Körner, 2003). The study of the plant traits can help to understand how plant lives in such climatic extremes (Harrison et al., 2010); how plant traits respond to various environmental pressures (e.g. changes in climate and land use) and therefore affect on the ecosystem processes (e.g. biogeochemical cycles) (Díaz et al., 2004; Lavorel and Garnier, 2002) and ecosystem functioning (Orwin et al., 2010; Wright et al., 2004).

The QTP is an ideal place for large-scale ecological studies (He et al., 2006a) because of the unique high-altitude environment. Plant morphological and biophysical traits have been studied on the QTP for a better understanding of plant adaptation strategies and ecosystem functioning. The alpine plants on the QTP are characteristic of higher leaf nitrogen concentrations and photosynthetic capacities in comparison to a global dataset (He et al., 2006a). These characteristics can possibly balance the low efficiency of physiological processes at low temperatures (Reich and Oleksyn, 2004). The high Specific Leaf Area on the QTP allows rapid C assimilation during the short growing season, and the low Specific Roots Length with high physical robustness can withstand soil freezing (Geng et al., 2014). Alpine plants on the QTP can compensate carbon gain under low temperature by stabilizing biomass investment to photosynthetic structures and increasing the surface area of fine roots (Ma et al., 2010).

Plant traits in response to climate change (i.e. warming) and land use change (i.e. grazing, fertilization) have also been studied on the QTP based on field experiments. The study found that simulated warming delays the reproductive phenology on the QTP (Dorji et al., 2013). Fertilization increases the extent of traits differences between organisms, i.e. functional diversity, but decreases species diversity on the QTP (Niu et al., 2014). However, these field studies were focused on small areas and therefore provided limited insights on understanding how plant traits respond to climate change and human activities. However, estimating plant traits over the complete QTP remains challenging due to the vast extent and limited accessibility of the area but is critical for global change research.

1.1.3 Alpine ecosystems are sensitive to climate change

Climate change has been more pronounced in alpine ecosystems and therefore the ecosystems are considered particularly vulnerable (Theurillat and Guisan, 2001). The QTP has experienced a global and significant warming with an increase rate of 0.3 °C/10 yr^{-1} (Duan et al., 2006; Li et al., 2010; Piao et al., 2010) which is approximately three times of the global warming rate (Piao et al., 2010; Yao et al., 2012b). The warming was found stronger at higher elevations (Liu and Chen, 2000), at nighttime and in winter and autumn (Li et al., 2010). The precipitation showed a slight increasing trend with high temporal-spatial variations across the whole QTP (Kang et al., 2010; Li et al., 2010). Specifically, the precipitation showed increasing

trends on the central-eastern and southeastern part of the QTP during the winter and spring, but non-significant decreasing trends found in the summer and autumn (Li et al., 2010; Xu et al., 2008).

Warming has caused glacier melting (Yao et al., 2012a, 2007) and permafrost degradation (Yang et al., 2010). Melting glaciers contribute to runoff in the short term, but cause flooding (H. Chen et al., 2013) and affect water supplies of billions of people in the long-term (Cyranoski, 2005). Permafrost degradation has impacts on ecology, hydrology and engineering (Wu et al., 2015), and results in soil moisture and nutrient reduction, leading to vegetation degradation and desertification (Jin et al., 2000; Wang et al., 2006). Furthermore, permafrost degradation caused a huge amount of carbon entering the atmosphere, exacerbating global warming, as permafrost stores one-third of the world's soil carbon (Qiu, 2008).

Ecosystems have been also changed on the QTP, as evidenced by vegetation cover reduction, changes in plant composition and soil properties. All these changes were served as facts and indicators of ecosystem degradation (Gao and Li, 2016; Harris, 2010). The ecosystem degradation is evident over a range of scales across the QTP (X.-L. Li et al., 2013). Plant cover has reduced and bare-soil patches have developed on the QTP by showing increasing vegetation polygonal crack and vegetation fragmentation at a fine scale (Miehe et al., 2019) and soil patch development at a landscape scale. Furthermore, the degraded grasslands showed changes in community composition with the invasion of exotic and toxic species (Gao and Li, 2016) (Figure 1.2). These degraded grasslands are particularly vulnerable to wind and water erosion (X. Li et al., 2018a). Geographically, south Qinghai, north Tibet, and the Qaidam Basin have been identified as the most extensive and severely degraded regions (X. L. Li et al., 2013). In south Qinghai, degradation became more prominent from the mid-1990s onwards (Liu et al., 2008). In north Tibet, degraded grasslands showed plant cover reduction, especially along the railway and highway (X. L. Li et al., 2013). In Qaidam Basin, grassland degradation took the forms of salinization and alkalization and even desertification (X. L. Li et al., 2013; Wang et al., 2003).

However, ecosystem restoration and recovery have been also observed on the QTP at various scales (Peng et al., 2014; Wang et al., 2014). At the large scale, satellite-measured vegetation greenness, as a proxy of vegetation photosynthesis rate and vegetation cover, has increased in past decades (Shen et al., 2015). The field experiment suggested that warming increased primary productivity of in the alpine

meadow, but reduced growth on the alpine steppe (Ganjurjav et al., 2016). Even though ecosystem degradation on the QTP has been widely recognized and discussed, the degraded ecosystems caused the loss of ecosystem services and ecosystem functioning (Körner, 2003), and threatened the water supply for the large human population downstream (Viviroli et al., 2006).

Figure 1.2. Example photos of degraded grasslands. a) Reduced pasture quality with invasive species that are not favored by domestic livestock (Qumalai County, July 2015). b) Degraded grassland with reduced vegetation cover (August 2016, Naqu county).

1.1.4 The impact of human activities on ecosystem change

Land use changes are another relevant part for understanding ecosystem changes. The land use changes involve increasing human activities, such as increasing livestock grazing, tourism, traffic routes development, and hydro-electric constructions (Körner, 2003). Livestock trampling, overgrazing and soil destruction can have dramatic consequences for life conditions down-slope (Körner, 2003). On the QTP, diverse human activities have a complex impact on the grassland ecosystems. Human-induced moderate grazing could support the maintenance and recovery of alpine meadows (X. Li et al., 2018b; Miehe et al., 2019). However, overgrazing is considered an important factor during the early stages of degradation (Gao and Li, 2016), which result in a reduction of palatable grasses and an increase in forbs and poisonous plants (X. Li et al., 2018b). Overgrazing loosens the underlying soil and worsens wind erosion, leading to the increasing of bare-soil patches (Gao and Li, 2016). Management policies of sedentarization and limiting livestock density have been taken to restore degraded grasslands on the QTP (Dong et al., 2013; Nyima, 2015). The impacts of the corresponding projects on social, economic and ecological aspects of grassland ecosystems are still uncertain (Gongbuzeren et al., 2015). Some restoration projects

have shown positive outcomes, as suggested by increasing vegetation activity after launching the projects (Cai et al., 2015). However, complete recovery of degraded pastures (e.g. soil fertility, ecosystem stability) is unfeasible because of the slow vegetation restoration rate, and the continuously increasing climate change and human pressure on the QTP (Liu et al., 2018), for example, natural attractions and cultural landscape have attracted growing tourists on the QTP in the last decades (L. en Wang et al., 2017; Li and Chi, 2014). The influence of human activities on ecosystems is integrated with climatic variables. Disentangling the drivers of ecosystem changes is challenging, however, important for appropriate ecosystem management practices (Harris, 2010; X. Li et al., 2018b; Miehe et al., 2019).

Figure 1.3. Example photos of human activities on the QTP. a) Livestock tramping causes vegetation-cover reduction (Zekog, July 2015). b) Ecosystem restoration project has been developed for recovering degraded grasslands along roads (Madoi county, July 2016). c) Road density has been increased on the northeastern QTP (Haibei, July 2015). d) Increasing tourism activities (Yushu County, August 2016).

1.2 Addressing grassland ecosystems challenges using remote sensing

Remote sensing provides a means of estimation vegetation biophysical variables and plant traits at the large-scale. It enables the quantification of human influences on the grassland ecosystems at varying spatial scales. It further allows for the monitoring of ecosystem changes through regular and long-term satellite observations.

1.2.1 Remote sensing of plant traits and vegetation biophysical variables

Remote sensing offers potentials of estimating plant properties at leaf-, plant- and canopy-level (Ollinger, 2011). At the leaf and plant level, plant physiological, biochemical and structural traits influence spectral properties through leaf absorption properties (Ustin, 2013), and scattering and reflectance (Ollinger, 2011). At the canopy level, leaf spectral properties, canopy structure, and soil background all have an impact on spectral properties (Ollinger, 2011). The distinct optical properties of vegetation in the visible and near-infrared (NIR) regions can be observed at leaf, plant and canopy level (Tucker, 1979). Measurement of the reflectance at visible and infrared wavelengths can characterize grassland plant traits and vegetation biophysical properties (Verrelst et al., 2015).

The quantitative estimation of plant traits, such as pigments, dry matter, leaf structure, and leaf orientation have been assessed using remote sensing data (Homolová et al., 2013). These optically effective plant properties can be retrieved from canopy reflectance, called ‘optical traits’ (Feilhauer et al., 2017). “Optical traits” have been estimated from the canopy reflectance using empirical models (Martin et al., 2008; Ollinger, 2011) and physical canopy reflectance models (A. M. Ali et al., 2016; Feilhauer et al., 2017; Jacquemoud et al., 2009; Ollinger, 2011).

Studies on plant trait estimation using the spectral properties are limited in grassland systems (Roelofsen et al., 2014). Specific Leaf Area, Leaf Dry Matter Content, leaf Nitrogen, and leaf Phosphorus have been retrieved from the spectra in the grassland ecosystem (Homolová et al., 2013; Roelofsen et al., 2014). However, estimating plant traits using the remotely-sensed spectra in grassland ecosystems are difficult because of the small dimension of herbaceous specimens compared to the spatial resolution of satellite image (Verrelst et al., 2009).

Vegetation biophysical variables of Chlorophyll content (CHL), leaf area index (LAI), vegetation cover and aboveground biomass are commonly studied using the remote

sensing data. CHL and LAI control biological and physical processes of vegetation productivity and carbon cycle (Pu et al., 2003), Dash and Curran, 2004, Clevers and Gitelson, 2013). Vegetation cover and biomass are the most widely-investigated variables that are not only important for assessing pasture quantity and grassland degradation (Wang et al., 2010), but also for understanding environmental change and human influence on ecosystems (Lehnert et al., 2015).

Vegetation Index (VI) has been extensively used to estimate these vegetation bio-geophysical properties (Glenn et al., 2008; Jia et al., 2016; Verrelst et al., 2015; Zhang et al., 2016). Reflectance at the red-edge bands has shown to be highly significant to predict CHL (Clevers and Gitelson, 2013; Vincini et al., 2014, Delegido et al., 2013, Clevers and Kooistra, 2012; Ramoelo et al., 2012). The red-edge band has been successfully applied to retrieve CHL in the grassland (Clevers and Gitelson, 2013). LAI was mapped in a heterogeneous grassland from canopy spectral reflectance measurements using empirical statistical models (Darvishzadeh et al., 2008) and physical models (Darvishzadeh et al., 2011). The application of linear spectral unmixing (Gottlicher et al., 2009) and machine-learning algorithms such as support vector machines (SVM) have been used to estimate plant cover (Hostert et al., 2014; Lehnert et al., 2015). Difficulties of estimating grassland biophysical variables include uncertainties of remote sensing data and model parameters (Jia et al., 2016), and mismatch between satellite data and ground truth data (I. Ali et al., 2016; C. Li et al., 2018).

1.2.2 Evaluating human influence on grassland ecosystems using remote sensing

Various human activities including urbanization, overgrazing and intensive management practices have caused grassland degradation (I. Ali et al., 2016). Remote sensing has been used to map, monitor and quantify the diverse human influence on grasslands, for example assessing grazing effects, evaluating ecosystem restoration projects (Cai et al., 2015; Huang et al., 2013) and monitoring changes in land cover (Li et al., 2009; Zeng et al., 2003). The overall human influences on productivity have been estimated by modeling the difference between remotely-sensed actual Net Primary Productivity (NPP) value and climate-driven potential NPP value (Haberl et al., 2007; Xu et al., 2016). Human influences of livestock grazing intensity (I. Ali et al., 2016; Feng and Zhao, 2011) have been monitored using remote sensing, showing

negative correlation between grazing density and vegetation index (NDVI) (Kawamura et al., 2005). The positive grazing exclusion effects have been observed using the long-term remote sensing data (J. Li et al., 2013). On the QTP, effects of restoration programs (Cai et al., 2015; Huang et al., 2013) have been evaluated using the long-term vegetation index dataset (Cai et al., 2015; Huang et al., 2013). Changes in land cover have been mapped to reflect the human influence of management practices on grasslands both at the local scale (I. Ali et al., 2016) and regional scale (Nitze et al., 2015). For example, grassland area had decreased from 1977 to 2004 on the northeastern of QTP, probably related to the increasing built-up area and cropland area (Li et al., 2009; Zeng et al., 2003). On the eastern QTP, significant changes in land use have found at the surroundings of human settlements using the long-term satellite data (Yang et al., 2015).

1.2.3 Monitoring grassland dynamics and degradations using remote sensing

The spatiotemporal trends of vegetation index derived from the satellite data have been widely studied in recent decades on the QTP (Wang, 2016). The vegetation index, served as a proxy of vegetation cover, net primary production (NPP) and grassland biomass, has been used as an indicator of ecosystem functioning. The overall positive trends of these vegetation index have been reported on the QTP (Wang, 2016). For example, alpine grasslands on the eastern QTP showed a significant positive trend accounted for 45% of the area, while only 4% of area show a significant negative trend in 1982-2002 (X. Wang et al., 2016).

However, grassland degradation has also been observed using remote sensing data. Based on grassland cover (Fassnacht et al., 2015; Liu et al., 2008), vegetation index (Li et al., 2017), grassland fragmentation (Liu et al., 2008) and changes in grassland cover and NPP (Liu et al., 2008; Z. Wang et al., 2016), different levels of grassland degradation were identified (Gao and Li, 2017). Study showed that alpine grassland degradation is particularly obvious in the Three-River Source Region, showing relative low values of plant coverage (<50%), and high proportion of palatable herbage (>50%) (Zhou et al., 2005).

1.3 Thesis aims and structure

1.3.1 Key challenges for alpine grassland ecosystem studies

- **Retrieval of plant traits across the QTP using remote sensing**

Remote sensing has been widely used to estimate biophysical variables in the grasslands (section 1.21), however the studies on estimation of plant traits in the alpine grasslands are limited (section 1.21) and difficult because of the small dimension of herbaceous specimens compared to spatial resolution of remote sensed images (Verrelst et al., 2009). The vast extent and limited accessibility of the QTP bring difficulties of estimating plant traits on the whole Plateau. Remote sensing offers a way to estimate the plant traits at the large scale. The estimation of plant traits from the remote sensing will help us to better understand the plant adaptation strategies and ecosystem functioning.

- **Mapping increased human influences on the alpine grasslands**

Increasing diverse human activities and land-use intensity have exerted a complex influence on the alpine grassland ecosystems on the QTP. The human activities have happened at different areas and scales by showing privatization of alpine grasslands and spatially heterogeneous grazing intensity across the whole QTP (Harris, 2010; Y. Wang et al., 2017). Grassland restoration projects and infrastructure development have affected grasslands at the local scale (Li et al., 2017). Quantifying and mapping human influences on ecosystems both at the whole Plateau scale and local scale are important to understand the effects of different human activities.

- **Monitoring grassland degradation and developments in past decades**

Alpine grassland ecosystems have been experienced changes on the QTP by showing changes in community composition, soil properties, and vegetation productivity observed from the field study (section 1.13) and satellite data (section 1.23). Both grassland degradation and vegetation greening trends have been discussed on the QTP. However, criteria and indicators for assessing vegetation changes and identifying grassland degradation are not clear (Chen and Rao, 2008; Feng et al., 2005). Vegetation cover is the most common indicator for monitoring degradation (Li et al., 2014). However, the low vegetation cover does not indicate degraded grasslands because low plant cover is a natural characteristic of the harsh ecosystems

on the most parts of the QTP. The degraded grasslands showed grassland cover reduction and bare-soil patches development causing the changes in vegetation spatial heterogeneity. Therefore, changes in grassland cover and spatial heterogeneity may offer a good indication for grassland development.

1.3.2 Research aims

Remote sensing has potentials to address the challenges of alpine grassland ecosystems on the QTP. Considering the increasing changes in the ecosystems and increasing pressures from human activities, this study aims to provide a broad view of mapping plant traits for understanding of ecosystem functioning, mapping various human influence on the ecosystems and monitoring ecosystem dynamics and identifying ecosystem degradation levels on the QTP. Three main goals have been defined for this thesis:

- Retrieval of plant traits across the QTP using remote sensing.
- Mapping human influences on the alpine grasslands.
- Monitoring grassland degradation and development stages in past decades.

1.3.3 Research questions and hypothesis

Three research questions have been formulated based on the research challenges and research aims identified in the previous sections.

RQ1: Can we estimate plant traits at the canopy level from remote sensing data? Are remotely-sensed plant traits comparable to the plant traits measured at the community level in the field?

Hypothesis 1:

We hypothesize that plant traits estimated from the remote sensing data at the canopy level are comparable to the plant traits measured at the community level in the field. This is because the leaf-level trait measurements are close to plant-level trait measurements for alpine herbaceous plants, given that these plants do not have prominent aboveground stems. Therefore, aboveground part of these plants can be considered as equivalent to “big-leaf structures” when measuring traits (Pérez-Harguindeguy et al., 2013). In this case, remotely sensed plant spectral information corresponds to plant-level traits aggregated to the community level.

RQ2: Can we map the human influence on grassland ecosystems on the QTP? What is the impact of livestock grazing on grasslands at different spatial scales?

Hypothesis 2:

We hypothesize that at the regional scale of 10-km, spatial patterns of grassland biomass that could not be attributed to environmental variables were likely correlated to human activities. At the local scale of 500 m, distance to settlements served as a proxy of human-influence intensity and changes in biomass along the distance could indicate the human influence on the ecosystems.

RQ3: How did the grassland cover and spatial heterogeneity change between 2000 and 2016? Which degradation levels can be extracted from changes in grassland cover and spatial heterogeneity?

Hypothesis 3:

We hypothesize that changes in vegetation cover and in spatial heterogeneity can indicate grassland degradation levels. Based in this hypothesis, we studied their changes (2000 - 2016) at different degradation groups identified from the literature in 2004(Liu et al., 2008). We proposed new degradation categories in 2016 based on changes in grassland cover and spatial heterogeneity.

1.3.4 Datasets

1.3.4.1 Satellite data

Satellite data of Landsat-8 surface reflectance (Roy et al., 2014) in 2015 and 2016, Sentinel-2 Top Of the Atmosphere (TOA) reflectance (Drusch et al., 2012) data from 2016, Moderate Resolution Imaging Spectroradiometer (MODIS) Land Cover Type product (MCD12Q1) (Friedl et al., 2010) from 2013 and MODIS LAI product (MCD15A3H) (Myneni and Y. K., 2015) in 2015 and 2016 were used to map plant traits at the canopy level. All these dataset covered the whole QTP from June to September and were masked cloud, snow and cloud shadow in the Google earth engine platform (Gorelick et al., 2017).

The Normalized Difference Vegetation Index (NDVI) (Tucker, 1979) from the Landsat-8 surface reflectance in 2015 were used to estimate aboveground grassland biomass (Jia et al., 2016; Zhang et al., 2016). The long-term NDVI data (2000-2016) from Moderate Resolution Imaging Spectroradiometer (MODIS) bidirectional

reflectance distribution function (BRDF) Adjusted Reflectance (MCD43A4) (Schaaf et al., 2002) were used to monitor changes in grassland cover and spatial heterogeneity to further identify grassland degradation levels.

1.3.4.2 Field-measured data

We conducted field work in 2015 and 2016 to measure plant traits at the canopy level, they include (1) plant cover of abundant species in quadrat, (2) SPAD leaf absorbance (SPAD-502Plus Chlorophyll Meter, KONICA MINOLTA, INC., Osaka, Japan) of abundant species, (3) Plant Area Index (PAI) using Digital Hemispherical Photographs (DHPs) and calculated with the CAN-EYE software (Mougin et al., 2014; Sea et al., 2011), (4) plot aboveground plant fresh biomass and dry biomass. More information on field measurement can be found in section 2.3.1.

We also derived plant traits value of the QTP from the existing publications (L. Chen et al., 2013; He et al., 2006b; Niu et al., 2016; Zhou et al., 2016). The Literature-derived plant traits included Community Weighted Means (CWMs) of Specific Leaf Area (SLA) and Leaf Dry Matter Content (LDMC). These traits were used to validate satellite estimated plant trait at the canopy level. The detailed description on integrating the published plant traits with this study is also available on section 2.3.1.

1.3.4.3 Environmental data

Climate, soil and topography dataset were used to mapping human influence and monitoring grassland degradation. The climatic data include growing season (June–September) mean air temperature and precipitation in 2015. The dataset were extracted from the China Meteorological Forcing Dataset with a spatial resolution of 0.1° (Chen et al., 2011).

Soil variables including soil organic matter, available nitrogen and total phosphorus were extracted from a 30 × 30 arcsec resolution gridded soil characteristics dataset (Shangguan et al., 2013).

Topographic data of elevation and slope data were based on the NASA Shuttle Radar Topographic Mission (SRTM Version 4) (Farr et al., 2007). All these evnironmental dataset were used to model the contribution of environmental variables to spatial variation in grassland biomass for further mapping biomass related to human activities. The topographic data were used to characterize degradation levels along elevation and slope gradient.

River network data extracted from hydrological data (HydroSHEDS: Hydrological

data and maps based on SHuttle Elevation Derivatives at multiple Scales) (Lehner et al., 2008) were used to mask higher spatial heterogeneity value caused rivers that is not related to grassland degradation.

1.3.4.4 Vegetation data

The vegetation-type data especially main vegetation types of alpine meadow and alpine steppe were from the Chinese vegetation atlas (scale 1:1000 000). This atlas is based on the results of nationwide vegetation surveys and complementary data from aerial remote sensing devices and satellite images, as well as geological, pedological and climatological data (Hou, 2001). The eco-geographical regions (Figure 3.1) of QTP were based on the vegetation types and climatic variables (Gao et al., 2009) were also included as a further environmental explanatory variable for spatial variation in grassland biomass (Section 3.1). Furthermore, a grassland degradation-level dataset for 2004 (Liu et al., 2008) was used as a reference to classify changes in NDVI and spatial heterogeneity into new degradation categories for 2016.

1.3.4.5 Indicators of human influences

Livestock density and distance to settlements were used to as indicators of human influence. These two indicators were used to study they can explain spatial pattern of biomass. Livestock density was assessed in terms of the number of sheep, goats and yak per square kilometer reported in the 2015 statistical yearbook from Qinghai, Xizang (National Bureau of Statistics of China, 2015). The settlement locations of cities, towns, hamlets and villages in 2017 were extracted from OpenStreetMap (Haklay and Weber, 2008) as spatial points (https://download.geofabrik.de/asia/china.html).

1.3.5 Thesis structure

Chapter 1 provides a background to the thesis and introduces its goals and research questions. In Chapter 2, we map plant traits on the canopy level across the whole QTP and explore traits difference among vegetation types. Chapter 3 quantifies the human influence on the grassland biomass. Chapter 4 monitors the dynamics of vegetation cover and spatial heterogeneity to map grassland degradation and improvement stages. Finally, chapter 5 summarizes and synthesizes the major findings of chapters 2-4, and provides concluding remarks and an outlook to the thesis.

1.4 References

Ali, A.M., Darvishzadeh, R., Skidmore, A.K., Duren, I. van, Heiden, U., Heurich, M., 2016. Estimating leaf functional traits by inversion of PROSPECT: Assessing leaf dry matter content and specific leaf area in mixed mountainous forest. Int. J. Appl. Earth Obs. Geoinf. 45, 66–76. doi:10.1016/j.jag.2015.11.004

Ali, I., Cawkwell, F., Dwyer, E., Barrett, B., Green, S., 2016. Satellite remote sensing of grasslands: from observation to management. J. Plant Ecol. 9, 649–671. doi:10.1093/jpe/rtw005

Cai, H., Yang, X., Xu, X., 2015. Human-induced grassland degradation/restoration in the central Tibetan Plateau: The effects of ecological protection and restoration projects. Ecol. Eng. 83, 112–119. doi:10.1016/j.ecoleng.2015.06.031

Chen, H., Zhu, Q., Peng, C., Wu, N., Wang, Y., Fang, X., Gao, Y., Zhu, D., Yang, G., Tian, J., Kang, X., Piao, S., Ouyang, H., Xiang, W., Luo, Z., Jiang, H., Song, X., Zhang, Y., Yu, G., Zhao, X., Gong, P., Yao, T., Wu, J., 2013. The impacts of climate change and human activities on biogeochemical cycles on the Qinghai-Tibetan Plateau. Glob. Chang. Biol. 19, 2940–2955. doi:10.1111/gcb.12277

Chen, L., Niu, K., Wu, Y., Geng, Y., Mi, Z., Flynn, D.F.B., He, J.S., 2013. UV radiation is the primary factor driving the variation in leaf phenolics across Chinese grasslands. Ecol. Evol. 3, 4696–4710. doi:10.1002/ece3.862

Chen, S., Rao, P., 2008. Land degradation monitoring using multi-temporal Landsat TM/ETM data in a transition zone between grassland and cropland of northeast China. Int. J. Remote Sens. 29, 2055–2073. doi:10.1080/01431160701355280

Clevers, J.G.P.W., Gitelson, A.A., 2013. Remote estimation of crop and grass chlorophyll and nitrogen content using red-edge bands on sentinel-2 and-3. Int. J. Appl. Earth Obs. Geoinf. 23, 344–351. doi:10.1016/j.jag.2012.10.008

Cyranoski, D., 2005. The long-range forecast. Nature 438, 275–276. doi:10.1038/438275a

Darvishzadeh, R., Atzberger, C., Skidmore, A., Schlerf, M., 2011. Mapping grassland leaf area index with airborne hyperspectral imagery: A comparison study of statistical approaches and inversion of radiative transfer models. ISPRS J. Photogramm. Remote Sens. 66, 894–906. doi:10.1016/j.isprsjprs.2011.09.013

Darvishzadeh, R., Skidmore, A., Schlerf, M., Atzberger, C., 2008. Inversion of a radiative transfer model for estimating vegetation LAI and chlorophyll in a heterogeneous grassland. Remote Sens. Environ. 112, 2592–2604. doi:10.1016/j.rse.2007.12.003

Dash, J., Curran, P.J., 2004. The MERIS terrestrial chlorophyll index. Int. J. Remote Sens. 25, 5403–5413. doi:10.1080/0143116042000274015

Díaz, S., Hodgson, J.G., Thompson, K., Cabido, M., Cornelissen, J.H.C., Jalili, A., Montserrat-Martí, G., Grime, J.P., Zarrinkamar, F., Asri, Y., Band, S.R., Basconcelo, S., Castro-Díez, P., Funes, G., Hamzehee, B., Khoshnevi, M., Pérez-Harguindeguy, N., Pérez-Rontomé, M.C., Shirvany, A., Vendramini, F., Yazdani, S., Abbas-Azimi, R., Bogaard, A., Boustani, S., Charles, M., Dehghan, M., de Torres-Espuny, L., Falczuk, V., Guerrero-Campo, J., Hynd, A., Jones, G., Kowsary, E., Kazemi-Saeed, F., Maestro-Martínez, M., Romo-Díez, A., Shaw, S., Siavash, B., Villar-Salvador, P., Zak, M.R., 2004. The plant traits that drive ecosystems: Evidence from three continents. J. Veg. Sci. 15, 295. doi:10.1658/1100-9233(2004)015[0295:TPTTDE]2.0.CO;2

Dong, Q.M., Zhao, X.Q., Wu, G.L., Shi, J.J., Ren, G.H., 2013. A review of formation mechanism and restoration measures of “black-soil-type” degraded grassland in the Qinghai-Tibetan Plateau. Environ. Earth Sci. 70, 2359–2370. doi:10.1007/s12665-013-2338-7

Dorji, T., Totland, Ø., Moe, S.R., Hopping, K.A., Pan, J., Klein, J.A., 2013. Plant functional traits mediate reproductive phenology and success in response to experimental warming and snow addition in Tibet. Glob. Chang. Biol. 19, 459–472. doi:10.1111/gcb.12059

Drusch, M., Del Bello, U., Carlier, S., Colin, O., Fernandez, V., Gascon, F., Hoersch, B., Isola, C., Laberinti, P., Martimort, P., Meygret, A., Spoto, F., Sy, O., Marchese, F., Bargellini, P., 2012. Sentinel-2: ESA’s Optical High-Resolution Mission for GMES Operational Services. Remote Sens. Environ. 120, 25–36. doi:10.1016/j.rse.2011.11.026

Duan, A., Wu, G., Zhang, Q., Liu, Y., 2006. New proofs of the recent climate warming over the Tibetan Plateau as a result of the increasing greenhouse gases emissions. Chinese Sci. Bull. 51, 1396–1400. doi:10.1007/s11434-006-1396-6

Farr, T., Rosen, P., Caro, E., Crippen, R., Duren, R., Hensley, S., Kobrick, M., Paller, M., Rodriguez, E., Roth, L., Seal, D., Shaffer, S., Shimada, J., Umland, J., Werner, M., Oskin, M., Burbank, D., Alsdorf, D., 2007. The shuttle radar topography mission. Rev. Geophys. 45, 1–33. doi:10.1029/2005RG000183.1.INTRODUCTION

Fassnacht, F.E., Li, L., Fritz, A., 2015. Mapping degraded grassland on the Eastern Tibetan Plateau with multi-temporal Landsat 8 data - where do the severely degraded areas occur? Int. J. Appl. Earth Obs. Geoinf. 42, 115–127. doi:10.1016/j.jag.2015.06.005

Feilhauer, H., Somers, B., van der Linden, S., 2017. Optical trait indicators for remote sensing of plant species composition: Predictive power and seasonal variability. Ecol. Indic. 73, 825–833.

doi:10.1016/j.ecolind.2016.11.003

Feng, J., Wang, T., Qi, S., Xie, C., 2005. Land degradation in the source region of the Yellow River, northeast Qinghai-Xizang Plateau: Classification and evaluation. Environ. Geol. 47, 459–466. doi:10.1007/s00254-004-1161-6

Feng, X.M., Zhao, Y.S., 2011. Grazing intensity monitoring in Northern China steppe□: Integrating CENTURY model and MODIS data 11, 175–182. doi:10.1016/j.ecolind.2009.07.002

Friedl, M.A., Sulla-Menashe, D., Tan, B., Schneider, A., Ramankutty, N., Sibley, A., Huang, X., 2010. MODIS Collection 5 global land cover: Algorithm refinements and characterization of new datasets. Remote Sens. Environ. 114, 168–182. doi:10.1016/j.rse.2009.08.016

Ganjurjav, H., Gao, Q., Gornish, E.S., Schwartz, M.W., Liang, Y., Cao, X., Zhang, W., Zhang, Y., Li, W., Wan, Y., Li, Y., Danjiu, L., Guo, H., Lin, E., 2016. Differential response of alpine steppe and alpine meadow to climate warming in the central Qinghai–Tibetan Plateau. Agric. For. Meteorol. 223, 233–240. doi:https://doi.org/10.1016/j.agrformet.2016.03.017

Gao, J., Li, S., Zhao, Z., 2009. Validating the demarcation of eco-geographical regions: A geostatistical application. Environ. Earth Sci. 59, 1327–1336. doi:10.1007/s12665-009-0120-7

Gao, J., Li, X., 2016. Degradation of frigid swampy meadows on the Qinghai–Tibet Plateau: Current status and future directions of research. Prog. Phys. Geogr. 40, 794–810. doi:10.1177/0309133316659283

Gao, J., Li, X.L., 2017. A knowledge-based approach to mapping degraded meadows on the Qinghai–Tibet Plateau, China. Int. J. Remote Sens. 38, 6147–6163. doi:10.1080/01431161.2017.1348642

Geng, Y., Wang, L., Jin, D., Liu, H., He, J.S., 2014. Alpine climate alters the relationships between leaf and root morphological traits but not chemical traits. Oecologia 175, 445–455. doi:10.1007/s00442-014-2919-5

Glenn, E.P., Huete, A.R., Nagler, P.L., Nelson, S.G., 2008. Relationship between remotely-sensed vegetation indices, canopy attributes and plant physiological processes: What vegetation indices can and cannot tell us about the landscape. Sensors 8, 2136–2160. doi:10.3390/s8042136

Gongbuzeren, Li, Y., Li, W., 2015. China's Rangeland Management Policy Debates: What Have We Learned? Rangel. Ecol. Manag. 68, 305–314. doi:10.1016/j.rama.2015.05.007

Gorelick, N., Hancher, M., Dixon, M., Ilyushchenko, S., Thau, D., Moore, R., 2017. Google Earth Engine: Planetary-scale geospatial analysis for everyone. Remote Sens. Environ. doi:10.1016/j.rse.2017.06.031

Gottlicher, D., Obregón, A., Homeier, J., Rollenbeck, R., Nauss, T., Bendix, J., 2009. Land-cover classification in the Andes of southern Ecuador using Landsat ETM+ data as a basis for SVAT modelling. Int. J. Remote Sens. 30, 1867–1886. doi:10.1080/01431160802541531

Haberl, H., Erb, K.H., Krausmann, F., Gaube, V., Bondeau, A., Plutzar, C., Gingrich, S., Lucht, W., Fischer-Kowalski, M., 2007. Quantifying and mapping the human appropriation of net primary production in earth's terrestrial ecosystems. Proc. Natl. Acad. Sci. 104, 12942–12947. doi:10.1073/pnas.0704243104

Harris, R.B., 2010. Rangeland degradation on the Qinghai-Tibetan plateau: A review of the evidence of its magnitude and causes. J. Arid Environ. 74, 1–12. doi:10.1016/j.jaridenv.2009.06.014

Harrison, S.P., Prentice, I.C., Barboni, D., Kohfeld, K.E., Ni, J., Sutra, J.P., 2010. Ecophysiological and bioclimatic foundations for a global plant functional classification. J. Veg. Sci. 21, 300–317. doi:10.1111/j.1654-1103.2009.01144.x

He, J.S., Wang, Z., Wang, X., Schmid, B., Zuo, W., Zhou, M., Zheng, C., Wang, M., Fang, J., 2006a. A test of the generality of leaf trait relationships on the Tibetan Plateau. New Phytol. 170, 835–848. doi:10.1111/j.1469-8137.2006.01704.x

He, J.S., Wang, Z., Wang, X., Schmid, B., Zuo, W., Zhou, M., Zheng, C., Wang, M., Fang, J., 2006b. A test of the generality of leaf trait relationships on the Tibetan Plateau. New Phytol. 170, 835–848. doi:10.1111/j.1469-8137.2006.01704.x

Homolová, L., Malenovský, Z., Clevers, J.G.P.W., García-Santos, G., Schaepman, M.E., 2013. Review of optical-based remote sensing for plant trait mapping. Ecol. Complex. 15, 1–16. doi:10.1016/j.ecocom.2013.06.003

Hostert, P., Suess, S., Schwieder, M., Leitão, P., Senf, C., 2014. Estimating Fractional Shrub Cover Using Simulated EnMAP Data: A Comparison of Three Machine Learning Regression Techniques. Remote Sens. 6, 3427–3445. doi:10.3390/rs6043427

Hou, X., 2001. Vegetation Altas of China. Science Press, Beijing.

Huang, L., Xiao, T., Zhao, Z., Sun, C., Liu, J., Shao, Q., Fan, J., Wang, J., 2013. Effects of grassland restoration programs on ecosystems in arid and semiarid China. J. Environ. Manage. 117, 268–275. doi:10.1016/j.jenvman.2012.12.040

Jacquemoud, S., Verhoef, W., Baret, F., Bacour, C., Zarco-Tejada, P.J., Asner, G.P., François, C., Ustin, S.L., 2009. PROSPECT + SAIL models: A review of use for vegetation characterization. Remote Sens. Environ. 113, S56–S66. doi:10.1016/j.rse.2008.01.026

Jia, W., Liu, M., Yang, Y., He, H., Zhu, X., Yang, F., Yin, C., Xiang, W., 2016. Estimation and uncertainty analyses of grassland biomass in Northern China: Comparison of multiple remote sensing data sources and modeling approaches. Ecol. Indic. 60, 1031–1040.

doi:10.1016/j.ecolind.2015.09.001

Jin, H., Li, S., Cheng, G., Shaoling, W., Li, X., 2000. Permafrost and climatic change in China. Glob. Planet. Change 26, 387–404. doi:10.1016/S0921-8181(00)00051-5

Kang, S., Xu, Y., You, Q., Flügel, W.-A., Pepin, N., Yao, T., 2010. Review of climate and cryospheric change in the Tibetan Plateau. Environ. Res. Lett. 5, 015101. doi:10.1088/1748-9326/5/1/015101

Kawamura, K., Akiyama, T., Yokota, H., 2005. Quantifying grazing intensities using geographic information systems and satellite remote sensing in the Xilingol steppe region , Inner Mongolia , China 107, 83–93. doi:10.1016/j.agee.2004.09.008

Körner, C., 2003. Alpine Plant Life: Functional Plant Ecology Of High Mountain Ecosystems, Alpine Plant Life, 2nd Edn. doi:10.1007/978-3-642-18970-8

Körner, C., 1995. Alpine plant diversity: a global survey and functional interpretations, in: Arctic and Alpine Biodiversity. pp. 45–62. doi:10.1007/978-3-642-78966-3_4

Lavorel, S., Garnier, E., 2002. Predicting changes in community composition and ecosystem functioning from plant traits: revisting the Holy Grail. Funct. Ecol. 16, 545–556. doi:Doi 10.1046/J.1365-2435.2002.00664.X

Lehner, B., Verdin, K., Jarvis, A., 2008. New global hydrography derived from spaceborne elevation data. Eos (Washington. DC). 89, 93–94. doi:10.1029/2008EO100001

Lehnert, L.W., Meyer, H., Wang, Y., Miehe, G., Thies, B., Reudenbach, C., Bendix, J., 2015. Retrieval of grassland plant coverage on the Tibetan Plateau based on a multi-scale, multi-sensor and multi-method approach. Remote Sens. Environ. 164, 197–207. doi:10.1016/j.rse.2015.04.020

Li, C., Wulf, H., Schmid, B., He, J., Schaepman, M.E., Member, S., 2018. Estimating Plant Traits of Alpine Grasslands on the Qinghai-Tibetan Plateau Using Remote Sensing 1–13.

Li, J., Yang, X., Jin, Y., Yang, Z., Huang, W., Zhao, L., Gao, T., Yu, H., Ma, H., Qin, Z., Xu, B., 2013. Remote Sensing of Environment Monitoring and analysis of grassland deserti fi cation dynamics using Landsat images in Ningxia , China. Remote Sens. Environ. 138, 19–26. doi:10.1016/j.rse.2013.07.010

Li, L., Fassnacht, F.E., Storch, I., B??rgi, M., 2017. Land-use regime shift triggered the recent degradation of alpine pastures in Nyanpo Yutse of the eastern Qinghai-Tibetan Plateau. Landsc. Ecol. 1–17. doi:10.1007/s10980-017-0510-2

Li, L., Yang, S., Wang, Z., Zhu, X., Tang, H., 2010. Evidence of Warming and Wetting Climate over the Qinghai-Tibet Plateau. Arctic, Antarct. Alp. Res. 42, 449–457. doi:10.1657/1938-4246-42.4.449

Li, R., Chi, X., 2014. Thermal comfort and tourism climate changes in the Qinghai-Tibet Plateau in the last 50 years. Theor. Appl. Climatol. 117, 613–624. doi:10.1007/s00704-013-1027-5

Li, X.-L., Gao, J., Brierley, G., Qiao, Y.-M., Zhang, J., Yang, Y.-W., 2013. Rangeland Degradation on the Qinghai-Tibet Plateau: Implications for Rehabilitation. L. Degrad. Dev. 24, 72–80. doi:10.1002/ldr.1108

Li, X., Gao, J., Zhang, J., 2018a. A topographic perspective on the distribution of degraded meadows and their changes on the Qinghai-Tibet Plateau, West China. L. Degrad. Dev. 29, 1574–1582. doi:10.1002/ldr.2952

Li, X., Perry, G.L.W., Brierley, G.J., 2018b. A spatial simulation model to assess controls upon grassland degradation on the Qinghai-Tibet Plateau, China. Appl. Geogr. 98, 166–176. doi:10.1016/j.apgeog.2018.07.003

Li, X.L., Gao, J., Brierley, G., Qiao, Y.M., Zhang, J., Yang, Y.W., 2013. Rangeland Degradation On The Qinghai-Tibet Plateau: Implications For Rehabilitation. L. Degrad. Dev. 24, 72–80. doi:10.1002/ldr.1108

Li, X.L., Perry, G.L.W., Brierley, G., Sun, H.Q., Li, C.H., Lu, G.X., 2014. Quantitative assessment of degradation classifications for degraded alpine meadows (Heitutan), Sanjiangyuan, western China. L. Degrad. Dev. 25, 417–427. doi:10.1002/ldr.2154

Li, X.Y., Ma, Y.J., Xu, H.Y., Wang, J.H., Zhang, D.S., 2009. Impact of land use and land cover change on environmental degradation in lake Qinghai watershed, Northeast Qinghai-Tibet Plateau. L. Degrad. Dev. 20, 69–83. doi:10.1002/ldr.885

Liu, J., Xu, X., Shao, Q., 2008. Grassland degradation in the “Three-River Headwaters” region, qinghai province. J. Geogr. Sci. 18, 259–273. doi:10.1007/s11442-008-0259-2

Liu, S., Zamanian, K., Schleuss, P.M., Zarebanadkouki, M., Kuzyakov, Y., 2018. Degradation of Tibetan grasslands: Consequences for carbon and nutrient cycles. Agric. Ecosyst. Environ. 252, 93–104. doi:10.1016/j.agee.2017.10.011

Liu, X., Chen, B., 2000. Climatic warming in the Tibetan Plateau during recent decades. Int. J. Climatol. 20, 1729–1742. doi:10.1002/1097-0088(20001130)20:14<1729::AID-JOC556>3.0.CO;2-Y

Ma, W.L., Shi, P.L., Li, W.H., He, Y.T., Zhang, X.Z., Shen, Z.X., Chai, S.Y., 2010. Changes in individual plant traits and biomass allocation in alpine meadow with elevation variation on the Qinghai-Tibetan Plateau. Sci. China Life Sci. 53, 1142–1151. doi:10.1007/s11427-010-4054-9

Martin, M.E., Plourde, L.C., Ollinger, S. V., Smith, M.L., McNeil, B.E., 2008. A generalizable method for remote sensing of canopy nitrogen across a wide range of forest ecosystems. Remote Sens.

Environ. 112, 3511–3519. doi:10.1016/j.rse.2008.04.008

Miehe, G., Miehe, S., Bach, K., Wesche, K., Seeber, E., Behrendes, L., Kaiser, K., Reudenbach, C., Nölling, J., Hanspach, J., Herrmann, M., Yaoming, M., Mosbrugger, V., 2013. Resilience or vulnerability? Vegetation patterns of a Central Tibetan pastoral ecotone. Steppe Ecosyst. Biol. Divers. Manag. Restor. 111–151.

Miehe, G., Schleuss, P.M., Seeber, E., Babel, W., Biermann, T., Braendle, M., Chen, F., Coners, H., Foken, T., Gerken, T., Graf, H.F., Guggenberger, G., Hafner, S., Holzapfel, M., Ingrisch, J., Kuzyakov, Y., Lai, Z., Lehnert, L., Leuschner, C., Li, X., Liu, J., Liu, S., Ma, Y., Miehe, S., Mosbrugger, V., Noltie, H.J., Schmidt, J., Spielvogel, S., Unteregelsbacher, S., Wang, Y., Willinghöfer, S., Xu, X., Yang, Y., Zhang, S., Opgenoorth, L., Wesche, K., 2019. The Kobresia pygmaea ecosystem of the Tibetan highlands – Origin, functioning and degradation of the world's largest pastoral alpine ecosystem: Kobresia pastures of Tibet. Sci. Total Environ. 648, 754–771. doi:10.1016/j.scitotenv.2018.08.164

Miller, D.J., 2005. The Tibetan Steppe. Grasslands of the World 305–342.

Mougin, E., Demarez, V., Diawara, M., Hiernaux, P., Soumaguel, N., Berg, A., 2014. Estimation of LAI, fAPAR and fCover of Sahel rangelands (Gourma, Mali). Agric. For. Meteorol. 198, 155–167. doi:10.1016/j.agrformet.2014.08.006

Myneni, R., Y. K., T.P., 2015. MCD15A2H MODIS/Terra+Aqua Leaf Area Index/FPAR 8?day L4 Global 500m SIN Grid V006. NASA EOSDIS L. Process. DAAC. doi:10.5067/MODIS/MCD15A2H.006

Nitze, I., Barrett, B., Cawkwell, F., 2015. International Journal of Applied Earth Observation and Geoinformation Temporal optimisation of image acquisition for land cover classification with Random Forest and MODIS time-series. Int. J. Appl. Earth Obs. Geoinf. 34, 136–146. doi:10.1016/j.jag.2014.08.001

Niu, K., Choler, P., de Bello, F., Mirotchnick, N., Du, G., Sun, S., 2014. Fertilization decreases species diversity but increases functional diversity: A three-year experiment in a Tibetan alpine meadow. Agric. Ecosyst. Environ. 182, 106–112. doi:10.1016/j.agee.2013.07.015

Niu, K., He, J. sheng, Zhang, S., Lechowicz, M.J., 2016. Tradeoffs between forage quality and soil fertility: Lessons from Himalayan rangelands. Agric. Ecosyst. Environ. 234, 31–39. doi:10.1016/j.agee.2016.04.023

Nyima, Y., 2015. What factors determine carrying capacity? A case study from pastoral Tibet. Area 47, 73–80. doi:10.1111/area.12137

Ollinger, S. V., 2011. Sources of variability in canopy reflectance and the convergent properties of plants. New Phytol. 189, 375–394. doi:10.1111/j.1469-8137.2010.03536.x

Orwin, K.H., Buckland, S.M., Johnson, D., Turner, B.L., Smart, S., Oakley, S., Bardgett, R.D., 2010. Linkages of plant traits to soil properties and the functioning of temperate grassland. J. Ecol. 98, 1074–1083. doi:10.1111/j.1365-2745.2010.01679.x

Peng, F., You, Q., Xu, M., Guo, J., Wang, T., Xue, X., 2014. Effects of warming and clipping on ecosystem carbon fluxes across two hydrologically contrasting years in an alpine meadow of the Qinghai-Tibet Plateau. PLoS One 9. doi:10.1371/journal.pone.0109319

Pérez-Harguindeguy, N., Diaz, S., Garnier, E., Lavorel, S., Poorter, H., Jaureguiberry, P., Bret-Harte, M.S.S., Cornwell, W.K.K., Craine, J.M.M., Gurvich, D.E.E., Urcelay, C., Veneklaas, E.J.J., Reich, P.B.B., Poorter, L., Wright, I.J.J., Etc., Ray, P., Etc., Díaz, S., Lavorel, S., Poorter, H., Jaureguiberry, P., Bret-Harte, M.S.S., Cornwell, W.K.K., Craine, J.M.M., Gurvich, D.E.E., Urcelay, C., Veneklaas, E.J.J., Reich, P.B.B., Poorter, L., Wright, I.J.J., Ray, P., Enrico, L., Pausas, J.G., Vos, A.C. de, Buchmann, N., Funes, G., Quétier, F., Hodgson, J.G., Thompson, K., Morgan, H.D., Steege, H. ter, Heijden, M.G.A. van der, Sack, L., Blonder, B., Poschlod, P., Vaieretti, M. V., Conti, G., Staver, A.C., Aquino, S., Cornelissen, J.H.C., 2013. New Handbook for standardized measurment of plant functional traits worldwide. Aust. J. Bot. 61, 167–234. doi:http://dx.doi.org/10.1071/BT12225

Piao, S., Ciais, P., Huang, Y., Shen, Z., Peng, S., Li, J., Zhou, L., Liu, H., Ma, Y., Ding, Y., Friedlingstein, P., Liu, C., Tan, K., Yu, Y., Zhang, T., Fang, J., 2010. The impacts of climate change on water resources and agriculture in China. Nature 467, 43–51. doi:10.1038/nature09364

Pu, R., Gong, P., Biging, G.S., Larrieu, M.R., 2003. Extraction of red edge optical parameters from hyperion data for estimation of forest leaf area index. IEEE Trans. Geosci. Remote Sens. 41, 916–921. doi:10.1109/TGRS.2003.813555

Qiu, J., 2008. China: The third pole. Nature 454, 393–396. doi:10.1038/454393a

Ramoelo, A., Skidmore, A.K., Cho, M.A., Schlerf, M., Mathieu, R., Heitkönig, I.M.A., 2012. Regional estimation of savanna grass nitrogen using the red-edge band of the spaceborne rapideye sensor. Int. J. Appl. Earth Obs. Geoinf. 19, 151–162. doi:10.1016/j.jag.2012.05.009

Reich, P.B., Oleksyn, J., 2004. Global patterns of plant leaf N and P in relation to temperature and latitude. Proc. Natl. Acad. Sci. 101, 11001–11006. doi:10.1073/pnas.0403588101

Roelofsen, H.D., van Bodegom, P.M., Kooistra, L., Witte, J.P.M., 2014. Predicting leaf traits of herbaceous species from their spectral characteristics. Ecol. Evol. 4, 706–719. doi:10.1002/ece3.932

Roy, D.P., Wulder, M.A., Loveland, T.R., C.E., W., Allen, R.G., Anderson, M.C., Helder, D., Irons, J.R., Johnson, D.M., Kennedy, R., Scambos, T.A., Schaaf, C.B., Schott, J.R., Sheng, Y., Vermote, E.F., Belward, A.S., Bindschadler, R., Cohen, W.B., Gao, F., Hipple, J.D., Hostert, P., Huntington, J., Justice, C.O., Kilic, A., Kovalskyy, V., Lee, Z.P., Lymburner, L., Masek, J.G., McCorkel, J., Shuai, Y., Trezza, R., Vogelmann, J., Wynne, R.H., Zhu, Z., 2014. Landsat-8: Science and product vision for terrestrial global change research. Remote Sens. Environ. 145, 154–172. doi:10.1016/j.rse.2014.02.001

Sea, W.B., Choler, P., Beringer, J., Weinmann, R.A., Hutley, L.B., Leuning, R., 2011. Documenting improvement in leaf area index estimates from MODIS using hemispherical photos for Australian savannas. Agric. For. Meteorol. 151, 1453–1461. doi:10.1016/j.agrformet.2010.12.006

Shangguan, W., Dai, Y., Liu, B., Zhu, A., Duan, Q., Wu, L., Ji, D., Ye, A., Yuan, H., Zhang, Q., Chen, D., Chen, M., Chu, J., Dou, Y., Guo, J., Li, H., Li, J., Liang, L., Liang, X., Liu, H., Liu, S., Miao, C., Zhang, Y., 2013. A China data set of soil properties for land surface modeling. J. Adv. Model. Earth Syst. 5, 212–224. doi:10.1002/jame.20026

Shen, M., Piao, S., Jeong, S.-J., Zhou, L., Zeng, Z., Ciais, P., Chen, D., Huang, M., Jin, C.-S., Li, L.Z.X., Li, Y., Myneni, R.B., Yang, K., Zhang, G., Zhang, Y., Yao, T., 2015. Evaporative cooling over the Tibetan Plateau induced by vegetation growth. Proc. Natl. Acad. Sci. 112, 9299–9304. doi:10.1073/pnas.1504418112

Theurillat, J., Guisan, A., 2001. Potential impact of climate change on vegetation in the european alps-a review (Theurillat & Guisan, 2001).pdf 77–109.

Tucker, C.J., 1979. Red and photographic infrared linear combinations for monitoring vegetation. Remote Sens. Environ. 8, 127–150. doi:10.1016/0034-4257(79)90013-0

Ustin, S.L., 2013. Remote sensing of canopy chemistry. Proc. Natl. Acad. Sci. 110, 804–805. doi:10.1073/pnas.1219393110

Verrelst, J., Camps-Valls, G., Muñoz-Marí, J., Rivera, J.P., Veroustraete, F., Clevers, J.G.P.W., Moreno, J., 2015. Optical remote sensing and the retrieval of terrestrial vegetation bio-geophysical properties - A review. ISPRS J. Photogramm. Remote Sens. 108, 273–290. doi:10.1016/j.isprsjprs.2015.05.005

Verrelst, J., Geerling, G.W., Sykora, K. V., Clevers, J.G.P.W., 2009. Mapping of aggregated floodplain plant communities using image fusion of CASI and LiDAR data. Int. J. Appl. Earth Obs. Geoinf. 11, 83–94. doi:10.1016/j.jag.2008.09.001

Vincini, M., Amaducci, S., Frazzi, E., 2014. Empirical estimation of leaf chlorophyll density in winter wheat canopies using Sentinel-2 spectral resolution. IEEE Trans. Geosci. Remote Sens. 52, 3220–3235. doi:10.1109/TGRS.2013.2271813

Viviroli, D., Weingartner, R., Messerli, B., 2006. Assessing the Hydrological Significance of the World's Mountains. Mt. Res. Dev. 23, 32–40. doi:10.1659/0276-4741(2003)023[0032:athsot]2.0.co;2

Wang, C., 2016. A remote sensing perspective of alpine grasslands on the Tibetan Plateau: Better or worse under "Tibet Warming"? Remote Sens. Appl. Soc. Environ. 3, 36–44. doi:10.1016/j.rsase.2015.12.002

Wang, G., Ding, Y., Shen, Y., Lai, Y., 2003. Environmental degradation in the Hexi Corridor region of China over the last 50 years and comprehensive mitigation and rehabilitation strategies. Environ. Geol. 44, 68–77. doi:10.1007/s00254-002-0736-3

Wang, G., Li, Y., Wu, Q., Wang, Y., 2006. Impacts of permafrost changes on alpine ecosystem in Qinghai-Tibet Plateau. Sci. China, Ser. D Earth Sci. 49, 1156–1169. doi:10.1007/s11430-006-1156-0

Wang, J., Wang, G., Hu, H., Wu, Q., 2010. The influence of degradation of the swamp and alpine meadows on CH4and CO2fluxes on the Qinghai-Tibetan Plateau. Environ. Earth Sci. 60, 537–548. doi:10.1007/s12665-009-0193-3

Wang, L. en, Zeng, Y., Zhong, L., 2017. Impact of climate change on tourism on the Qinghai-Tibetan Plateau: Research based on a literature review. Sustain. 9. doi:10.3390/su9091539

Wang, X., Dong, S., Gao, Q., Zhou, H., Liu, S., Su, X., Li, Y., 2014. Effects of short-term and long-term warming on soil nutrients, microbial biomass and enzyme activities in an alpine meadow on the Qinghai-Tibet Plateau of China. Soil Biol. Biochem. 76, 140–142. doi:10.1016/j.soilbio.2014.05.014

Wang, X., Yi, S., Wu, Q., Yang, K., Ding, Y., 2016. The role of permafrost and soil water in distribution of alpine grassland and its NDVI dynamics on the Qinghai-Tibetan Plateau. Glob. Planet. Change 147, 40–53. doi:10.1016/j.gloplacha.2016.10.014

Wang, Y., Heberling, G., Görzen, E., Miehe, G., Seeber, E., Wesche, K., 2017. Combined effects of livestock grazing and abiotic environment on vegetation and soils of grasslands across Tibet. Appl. Veg. Sci. 20, 327–339. doi:10.1111/avsc.12312

Wang, Z., Zhang, Yanzhen, Yang, Y., Zhou, W., Gang, C., Zhang, Ying, Li, J., An, R., Wang, K., Odeh, I., Qi, J., 2016. Quantitative assess the driving forces on the grassland degradation in the Qinghai-Tibet Plateau, in China. Ecol. Inform. 33, 32–44. doi:10.1016/j.ecoinf.2016.03.006

Wright, I.J., Reich, P.B., Westoby, M., Ackerly, D.D., Baruch, Z., Bongers, F., Cavender-Bares, J., Chapin, T., Cornelissen, J.H.C., Diemer, M., Flexas, J., Garnier, E., Groom, P.K., Gulias, J., Hikosaka, K., Lamont, B.B., Lee, T., Lee, W., Lusk, C., Midgley, J.J., Navas, M.-L., Niinemets, Ülo, Oleksyn, J., Osada, N., Poorter, H., Poot, P., Prior, L., Pyankov, V.I., Roumet, C., Thomas, S.C., Tjoelker, M.G., Veneklaas, E.J., Villar, R., 2004. The worldwide leaf economics spectrum. Nature 428, 821–827. doi:10.1038/nature02403

Wu, Q., Hou, Y., Yun, H., Liu, Y., 2015. Changes in active-layer thickness and near-surface permafrost between 2002 and 2012 in alpine ecosystems, Qinghai-Xizang (Tibet) Plateau, China. Glob. Planet. Change 124, 149–155. doi:10.1016/j.gloplacha.2014.09.002

Xu, H. jie, Wang, X. ping, Zhang, X. xiao, 2016. Alpine grasslands response to climatic factors and anthropogenic activities on the Tibetan Plateau from 2000 to 2012. Ecol. Eng. 92, 251–259. doi:10.1016/j.ecoleng.2016.04.005

Xu, Z.X., Gong, T.L., Li, J.Y., 2008. Decadal trend of climate in the Tibetan plateau - Regional temperature and precipitation. Hydrol. Process. 22, 3056–3065. doi:10.1002/hyp.6892

Yang, J., Wang, Y.C., Guo, L., Xue, D., 2015. Patterns and structures of land use change in the three rivers headwaters region of China. PLoS One 10. doi:10.1371/journal.pone.0119121

Yang, M., Nelson, F.E., Shiklomanov, N.I., Guo, D., Wan, G., 2010. Permafrost degradation and its environmental effects on the Tibetan Plateau: A review of recent research. Earth-Science Rev. 103, 31–44. doi:10.1016/j.earscirev.2010.07.002

Yao, T., Pu, J., Lu, A., Wang, Y., Yu, W., 2007. Recent Glacial Retreat and Its Impact on Hydrological Processes on the Tibetan Plateau, China, and Surrounding Regions. Arctic, Antarct. Alp. Res. 39, 642–650. doi:10.1657/1523-0430(07-510)[YAO]2.0.CO;2

Yao, T., Thompson, L., Yang, W., Yu, W., Gao, Y., Guo, X., Yang, X., Duan, K., Zhao, H., Xu, B., Pu, J., Lu, A., Xiang, Y., Kattel, D.B., Joswiak, D., 2012a. Different glacier status with atmospheric circulations in Tibetan Plateau and surroundings. Nat. Clim. Chang. 2, 663–667. doi:10.1038/nclimate1580

Yao, T., Thompson, L.G., Mosbrugger, V., Zhang, F., Ma, Y., Luo, T., Xu, B., Yang, X., Joswiak, D.R., Wang, W., Joswiak, M.E., Devkota, L.P., Tayal, S., Jilani, R., Fayziev, R., 2012b. Third Pole Environment (TPE). Environ. Dev. 3, 52–64. doi:10.1016/j.envdev.2012.04.002

Zeng, Y.. b, Feng, Z.. c, Cao, G.., 2003. Land cover change and its environmental impact in the upper reaches of the Yellow River, northeast Qinghai-Tibetan Plateau. Mt. Res. Dev. 23, 353–361. doi:10.1659/0276-4741(2003)023[0353:LCCAIE]2.0.CO;2

Zhang, B., Zhang, L., Xie, D., Yin, X., Liu, C., Liu, G., 2016. Application of synthetic NDVI time series blended from landsat and MODIS data for grassland biomass estimation. Remote Sens. 8, 10. doi:10.3390/rs8010010

Zhou, H., Zhao, X., Tang, Y., Gu, S., Zhou, L., 2005. Alpine grassland degradation and its control in the source region of the Yangtze and Yellow Rivers, China. Grassl. Sci. 51, 191–203. doi:10.1111/j.1744-697X.2005.00028.x

Zhou, X., Wang, Y., Zhang, P., Guo, Z., Chu, C., Du, G., 2016. The effects of fertilization on the trait-abundance relationships in a Tibetan alpine meadow community. J. Plant Ecol. 9, 144–152. doi:10.1093/jpe/rtv043

Chapter 2

Estimating Plant Traits of Alpine Grasslands on the Qinghai-Tibetan Plateau using Remote Sensing

This chapter is based on the peer-reviewed article:
Li, C., Wulf, H., Schmid, B., He, J.S., Schaepman, M.E., 2018. Estimating plant traits of alpine grasslands on the qinghai-tibetan plateau using remote sensing. IEEE J. Sel. Top. Appl. Earth Obs. Remote Sens. 11, 2263–2275

Paper reprinted with permission from IEEE, 2019

Authors' contributions (alphabetical order): BS, CL, HW, MES designed the study and developed the methodology. CL collected the data. BS, CL, HW, MES performed the analysis. BS, CL, HW, MES wrote the manuscript. HJS provided critical feedback and helped shape the research, analysis and manuscript.

2.1 Abstract

Mapping plants traits on the Qinghai-Tibetan Plateau grassland is important for understanding ecosystem functions and how plants respond to global change. Detailed trait maps for the complete Qinghai-Tibetan Plateau are missing. Here, we addressed this issue by combining Sentinel-2 and Landsat multispectral satellite data with field measurements to map and compare plant traits of meadow and steppe communities across the complete Qinghai-Tibetan Plateau. We measured in-situ plant-level traits of CHLorophyll content (CHL), Specific Plant Area (SPA= plant area / plant dry mass) and Plant Dry Matter Content (PDMC = plant dry mass / fresh mass). We hypothesized that plant-level traits of SPA and PDMC are close to Community-Weighted Means (CWMs) of Specific Leaf Area (SLA) and Leaf Dry Matter Content (LDMC) because leaves represent the largest fraction of aboveground biomass in the Qinghai-Tibetan Plateau grasslands. Despite vastly different measurement methods, we found that the remotely-sensed traits (SPA and PDMC) correlated with literature-derived leaf traits of CWMs of SLA and LDMC. Both remotely-sensed and field-measured results showed that alpine meadow plants reveal a wider range and higher averages of CHL and SPA but lower PDMC compared with alpine steppe plants. These trait differences between vegetation types indicate faster growth of alpine meadow but higher resilience to harsh conditions of alpine steppe, representing differences in adaptation strategies to environmental conditions. Our study demonstrates that remote sensing can be used to estimate plant traits in alpine grasslands with potential applications to retrieve functional diversity and correlated ecosystem functions in future studies.

2.2 Introduction

Plant traits are physiological and morphological features of an organism (Violle et al., 2007). Plant traits such as leaf nitrogen concentration, specific leaf area (SLA) and leaf dry matter content (LDMC) are related to plant physiological processes such as light capture and photosynthetic rate and can hence provide indications of functional strategies of plants in different environmental conditions (Gitelson et al., 2014a; Wu et al., 2008). These correlations make these traits key to predict ecosystem functions, such as primary productivity (Forrestel et al., 2017). Within the recently emerging discussion on Essential Biodiversity Variables (EBVs) derived by remote-sensing techniques (Pettorelli et al., 2016), these traits have been listed as key plant functional traits (Skidmore et al., 2015). Their relevance for plant and ecosystem functioning is reflected by their incorporation into dynamic global vegetation models to simulate ecosystem functions such as vegetation carbon dynamics and hydrological processes (Pappas et al., 2016; Sakschewski et al., 2015). Therefore the retrieval of these plant traits is important, in particular for grasslands, which cover more than 40% of the terrestrial land surface and are responsible for important ecosystem services such as carbon sequestration and forage production (Forrestel et al., 2017).

In alpine grasslands, leaf-level trait measurements are close to plant-level trait measurements, because herbaceous plants do not have prominent aboveground stems and in addition stems are green and thus are physiologically similar to leaves. This is especially the case for the grassland on the Qinghai-Tibetan Plateau, where aboveground vegetation is dominated by graminoids and rosette- and cushion-forming plants (Georg Miehe et al., 2011; Miehe et al., 2008). For these types of vegetation, aboveground part of plants can therefore be considered as equivalent to ‘big-leaf structures’ when measuring traits (Pérez-Harguindeguy et al., 2013). Regarding photosynthesis and primary productivity it is hence appropriate to work with aboveground plant-level traits rather than leaf-level traits in these vegetation types. Plant-level traits aggregated to the community level allow for an easier integration with spaceborne remote sensing datasets, which typically collect spectral information of grasslands on the canopy-level.

Remotely-sensed vegetation spectra provide information on plant physiological (e.g. pigment, SLA, and LDMC) and morphological traits (e.g. Leaf Area) (Feilhauer et al., 2017; Homolová et al., 2013). Physical radiative-transfer models and empirical

statistical models have been developed to estimate plant physiological and morphological traits (Ali et al., 2016b; Feilhauer et al., 2017; Féret et al., 2011; Homolová et al., 2013; Jacquemoud et al., 2009; le Maire et al., 2008) using remotely-sensed data. Employing these models, plant traits like CHLorophyll content (CHL) (Schlemmera et al., 2013; Ustin et al., 2009; Vincini et al., 2014), SLA (Ali et al., 2017b, 2017a; Asner et al., 2011; Asner and Martin, 2008; Féret et al., 2011) and LDMC (Ali et al., 2016a, 2016b; Roelofsen et al., 2014) were successfully derived. Although LDMC and SLA are crucial plant traits for understanding plant functioning, studies on estimating CHL, SLA and LDMC for grassland ecosystems using spectral data are relatively rare (Capolupo et al., 2015; Feilhauer et al., 2017; Punalekar et al., 2016; Roelofsen et al., 2014, 2013; Vohland and Jarmer, 2008). In an earlier study a radiative transfer model was inverted to estimate CHL and leaf mass per area (LMA = 1 / SLA) for a grassland ecosystem, but the retrieved plant traits were not validated with field-measured traits (Feilhauer et al., 2017). A further local study applied partial least squares regressions to estimate plant physiological traits at leaf and canopy level using field spectroradiometer data (Roelofsen et al., 2013). To our knowledge, no study so far has estimated plant traits of LDMC and SLA for grassland ecosystems using remote sensing data. Furthermore, we are not aware of studies that attempted to estimate plant traits using remote sensing across the whole Qinghai-Tibetan Plateau. Existing studies from the Qinghai-Tibetan Plateau working with plant traits typically remained at a plot scale and explored the relationships between local plant traits and environmental variables such as soil and climatic variables (He et al., 2009, 2006a); grazing level (Niu et al., 2015; Sun et al., 2014; Zhu et al., 2012); and elevation (Ma et al., 2010).

We hypothesize that selected plant traits can be estimated for extensive areas from remotely-sensed spectra using field data aggregated to the canopy level. The aggregation to canopy level is motivated by the fact that grassland spectra observed from spaceborne multispectral satellites inherently represent a mixed signal of the plant community. Applying such an approach to estimate plant traits over the complete Tibetan Plateau can help to characterize the current ecosystem state in terms of plant functioning. Such an assessment cannot be realized on the ground with a realistic financial budget due to the vast extent and limited accessibility of the Qinghai-Tibetan Plateau. Furthermore, remote sensing enables repeated assessments over time, which can help to identify changes of plant traits. Tracing changes of plant

traits on the Qinghai-Tibetan Plateau is particularly important as the area is prone to be affected by climate-change due to its very high altitude and corresponding harsh conditions (Yao et al., 2012). This is also mirrored in grassland degradation processes that have been observed in different intensities over the Plateau and have been related to anthropogenic activities (e.g., overgrazing) but also natural processed triggered by a changing climate (Harris, 2010). Besides such monitoring activities, spatially continuous data on plant traits can also help to better understand the current distribution of plant functional types and plant strategy groups over the the Plateau. The latter could be crucial to understand potential threats for certain plant communities under climate change scenarios.

In this study, we use field-measured values of canopy CHL, Specific Plant Area (SPA) and Plant Dry Matter Content (PDMC) aggregated to the canopy level to derive remotely-sensed proxies of these traits for the entire Qinghai-Tibetan Plateau. Furthermore, we show how remotely-sensed traits of SPA and PDMC correspond to literature-derived Community-Weighted Means (CWMs) of SLA and LDMC in alpine grasslands. Finally, based on the plant traits estimated via remote sensing, we investigate plant trait differences between four vegetation types to identify differences in plant adaptation strategies

2.2.1 Data

2.2.1.1 The Study Area and Vegetation Types

The Qinghai-Tibetan Plateau covers an area of approximately 2.5×106 km2 with complex terrain and an average elevation of more than 4000 m a.s.l (Figure 2.1). The area shows a decreasing thermal and moisture gradient from southeast to northwest (Chen et al., 2015), where the mean annual temperature ranges from 15.5 °C to –5.0 °C and the precipitation ranges from more than 1000 mm yr-1 to less than 100 mm yr-1 (Chen et al., 2015; Miehe et al., 2008).

The most dominant vegetation types are alpine steppe and alpine meadow, which occupy 22.4% and 23% of the total Plateau area, respectively (Hou, 2001). Both vegetation types are predominantly located at elevations above 4000 m (Li et al., 2014; Georg Miehe et al., 2011; Miehe et al., 2008). Alpine meadow occurs in the south-eastern humid highlands (Li et al., 2014; Miehe et al., 2008). Alpine steppe prevails in the more (semi-) arid central and western highlands with low precipitation (< 350 mm yr^{-1}) (Georg Miehe et al., 2011). Transitional zones with mixed alpine meadow and

alpine steppe occur in the central part of the Qinghai-Tibetan Plateau (Miehe et al., 2013). Montane steppe and montane meadow are less dominant grassland vegetation types, occupying only 4% and 1% of the whole Plateau area (Hou, 2001). These vegetation types occur predominantly at altitudes < 4000 m. Montane meadow mainly occurs in the northeast Qaidam Basin. Montane steppe is distributed on the northern margin of the Plateau and around the Qaidam Basin (Ni and Herzschuh, 2011).

2.2.1.2 Satellite Data

We used the Google Earth Engine (Gorelick et al., 2017) to process all available satellite data of Landsat-8 surface reflectance (Roy et al., 2014), Sentinel-2 Top Of the Atmosphere (TOA) reflectance (Drusch et al., 2012), Moderate Resolution Imaging Spectroradiometer (MODIS) Land Cover Type product (MCD12Q1) (Friedl et al., 2010) and MODIS LAI product (MCD15A3H) (Myneni and Y. K., 2015). We refer to MODIS LAI as PAI in our context. We applied the Landsat-8 surface reflectance Quality Assurance band (CFmask) (Foga et al., 2017; Zhu and Woodcock, 2012) and the MCD15A3H quality control band (FparLai_QC) to mask cloud, snow and cloud shadow (Yan et al., 2016; Yang et al., 2006). We used an adjusted Landsat cloud-score algorithm to mask clouds in Sentinel-2 TOA reflectance data (Irish et al., 2006).

Given the availability of the red-edge bands in Sentinel-2, we used Sentinel-2 data to estimate canopy CHL. In the study area, Sentinel-2 data are available in the Google Earth Engine as Level 1C TOA reflectance data from 2016 onwards. In all, 3560 Sentinel-2 TOA reflectance scenes spanning from July to August 2016 were selected to calculate red-edge band vegetation indices (Table 2.1) for estimating canopy CHL. Landsat-8 surface reflectance data were available for both years, 2015 and 2016, which enabled us to link Landsat-8 data to all our field measurements. Therefore, we used Landsat-8 surface reflectance data to calculate vegetation indices (Table 2.2) for predicting dry aboveground biomass and PDMC. In total, 1542 Landsat-8 surface reflectance scenes were selected, which covered the whole study area from June to September in 2015 and 2016. We used the MCD15A3H LAI product with 4-day time-steps and 500 m resolution from June to September in 2015 and 2016 to calculate the SPA, and MODIS Land Cover Type product (MCD12Q1) from 2013 to mask out all land cover types other than grasslands.

2.2.1.3 Data on Vegetation Types

The vegetation-type data were acquired from the Chinese vegetation atlas (scale 1:1000 000). This atlas is based on the results of nationwide vegetation surveys and complementary data from aerial remote sensing devices and satellite images, as well as geological, pedological and climatological data (Hou, 2001). The atlas provides a complete map of vegetation types and is frequently used in studies on the Qinghai-Tibetan Plateau (Chen et al., 2015; Lehnert et al., 2015). This dataset was used to build the link between plant traits and vegetation types to further evaluate how plant traits differed among vegetation types.

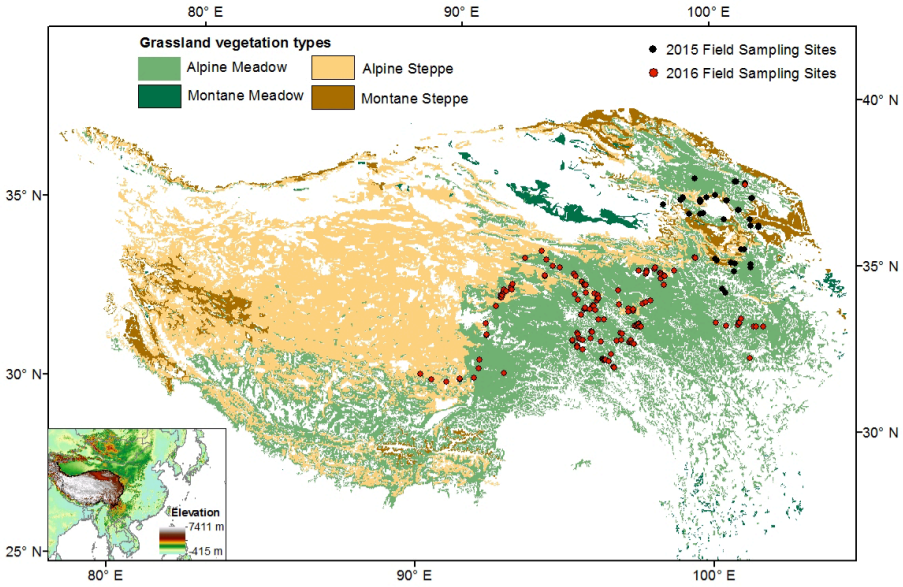

Figure 2.1 Distribution of grassland vegetation types (Hou, 2001) on the Chinese part of the Qinghai-Tibetan Plateau and sampling site locations used in this study (2015 = black dots, 2016 = red dots). Inset indicates elevation data of the extended area based on the NASA Shuttle Radar Topographic Mission (SRTM Version 4) (Farr et al., 2007).

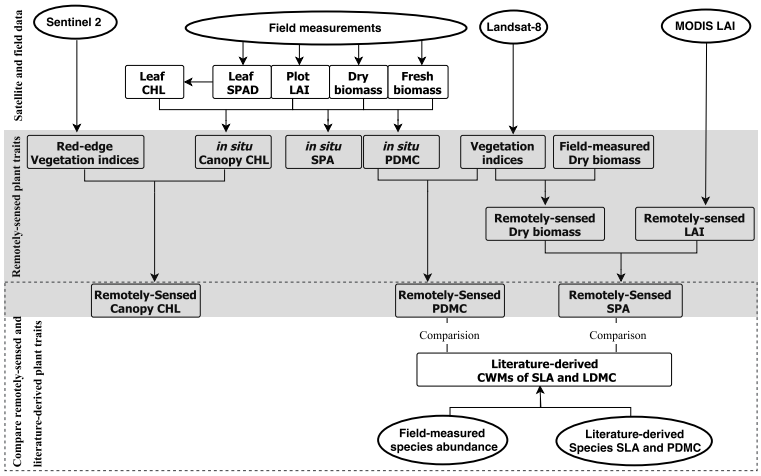

Figure 2.2 Flowchart displaying data and methods to derive plant traits

2.3 Methods

2.3.1 Field-Measured Plant Trait

Field data were collected on 59 sites over an area extending 1225 km in north-south and 695 km in east-west direction (Figure 2.1). The sampling sites cover three vegetation types (i.e. alpine meadow, alpine steppe and montane steppe) along an east-west gradient (Figure 2.1). Montane meadow was not considered in the study because of its limited distribution area. The data acquisition date coincided with the peak of the growing season (late July to mid-August) in 2015 and 2016. The montane steppe sampling sites were located at lower altitudes (around 3200 m) compared to the alpine steppe sampling sites (around 4800 m). Alpine meadow sampling sites were distributed along an elevation gradient ranging from 2800 to 5200 m. All sampling sites were selected to have homogeneous vegetation cover. At each site, four quadrats of one square meter were sampled within an area of 250 × 250 m. Each of the four quadrats was representative of the wider surrounding (30 × 30 m) to represent approximately the extent of a Landsat satellite image pixel.

In each quadrat, we conducted field measurements of (1) species cover, (2) SPAD leaf absorbance (SPAD-502Plus Chlorophyll Meter, KONICA MINOLTA, INC., Osaka, Japan) of abundant species, (3) Plant Area Index (PAI) and (4) plot aboveground plant fresh biomass and dry biomass. Species cover was averaged from 2–3 investigator estimations. For each species, 12–15 SPAD recordings were taken from different leaves and averaged as species SPAD value (Darvishzadeh et al., 2008a; Ghosh et al., 2016). The CWM of SPAD values was obtained by averaging the coverage-weighted species-level SPAD values for each plot. CWMs of SPAD values were converted to CHL values using equation (1) (Ghosh et al., 2016):

$$\text{Leaf CHL}\ (\text{mg} / \text{m}^2) = \text{SPAD} \times 16.844 - 192.84 \quad (1)$$

This model was calibrated from grass 14 CHL measurements in the lab and corresponding SPAD values collected in the field (Ghosh et al., 2016). Finally, CHL values were upscaled to canopy CHL by multiplication with PAI values (Darvishzadeh et al., 2008a, 2008b; Gitelson et al., 2005; Peng and Gitelson, 2011; Wu et al., 2012):

$$\text{Canopy CHL} = \text{leaf CHL} \times \text{PAI} \quad (2)$$

We refer PAI to LAI because all aboveground green parts of a plant were measured instead of only leaves. The PAI measurements were based on Digital Hemispherical Photographs (DHPs) and calculated with the CAN-EYE software (Mougin et al., 2014; Sea et al., 2011). In each quadrat, 8–10 downward pointing photos were taken with automatic exposure settings. Aboveground peaking plant fresh biomass was measured by clipping, weighing to an accuracy of ±0.01 g, and then drying 48 hours at 65°C to obtain a constant dry aboveground biomass. In total, PAI was measured in 228 plots, and plant fresh and dry aboveground biomass was measured in 172 plots.

To estimate traits in a mixed-species community, leaf traits are typically measured for all species and aggregated to the community mean weighted by species abundances in terms of plant cover or above-ground plant biomass proportions (community-weighted means = CWMs) (Lavorel et al., 2008). Ideally, CWMs of traits would be averaged from traits of all plants within a community without requiring taxonomic information of plant species (Schneider et al., 2017). This way of trait measurements within a community is more efficient and accurate because it is independent of taxonomic information and measures all plants within a community. Here, we measured traits within a community directly from vegetation harvests, to average plant-level traits of all plants of a community without requiring taxonomic information. Specifically, we derived the ratio of aboveground plant area and plant dry mass within a community and used it as a proxy of the CWM of SLA. Similarly, we used the ratio of aboveground plant fresh mass and dry mass within a community as a proxy of the CWMs of LDMC. In other words, we refer to the ratio between Plant Area Index (PAI) and aboveground plant dry biomass within a field plot as Specific Plant Area (SPA) and to the ratio between aboveground plant fresh biomass and dry biomass as Plant Dry Matter Content (PDMC) throughout this study. We hypothesize that in alpine grasslands, SPA and PDMC are close to CWMs of SLA and LDMC because leaves represent a large part of aboveground biomass and aboveground non-leaf structures in this vegetation (e.g., stems or graminoid inflorescences) are also green and photosynthesizing. The SPA and PDMC refer to the measurement at the community level, which match the plant traits estimate from remote sensing at the canopy level.

Literature-derived CWMs of SLA and LDMC were calculated using our field-measured species abundance values (cover proportions of dominant species) and SLA

and LDMC values of these species as reported in earlier studies conducted on the Qinghai-Tibetan Plateau (Chen et al., 2013; He et al., 2006b; Niu et al., 2016; Zhou et al., 2016). In total 121 species were recorded in 198 plots. For 42 species SLA values and 29 species LDMC values were averaged from the same species values in the literature (Chen et al., 2013; He et al., 2006b; Niu et al., 2016; Zhou et al., 2016), and 101 species SLA values and 94 species LDMC values were averaged from the same genus values in the literature (Chen et al., 2013; He et al., 2006b; Niu et al., 2016; Zhou et al., 2016). For 19 and 26 species no published SLA and LDMC values, respectively, were available form the literature. To represent the community means of the plots, CWMs of SLA and LDMC were calculated for all plots where SLA and LDMC values for more than 4 species were available. Using this rule, we could derive CWMs of SLA for 18 plots and CWMs of LDMC for 28 plots. In these plots, the species for which SLA and LDMC values were available accounted for more than 38% of plant coverage in all cases. Considering the homogeneity rule that was applied to select the field plots, we hypothesized that these coverages were sufficient to derive a meaningful estimate of the CWMs of the two traits.

2.3.2 Remotely-Sensed Plant Traits

2.3.2.1 CHL

The reflectance in the red-edge region is mainly affected by chlorophyll density (Vincini et al., 2014) and remains highly sensitive to a wide range of chlorophyll-content variability (Gitelson et al., 2014b; Schlemmera et al., 2013). The empirical red-edge indices adapted for Sentinel-2 data have been successfully applied to predict CHL in different ecosystem types (le Maire et al., 2008; Ramoelo et al., 2013; Vincini et al., 2014; Zarco-Tejada et al., 2001). In this study, we used the red-edge bands to predict canopy CHL. These red-edge vegetation indices include the MCARI/OSAVI (the ratio of the Modified Chlorophyll Absorption Ratio Index and the Optimized Soil-Adjusted Vegetation Index), the TCARI/OSAVI (the ratio of the Transformed Chlorophyll Absorption Ratio Index and the Optimized Soil-Adjusted Vegetation Index), the green chlorophyll index (CIgreen) and the red-edge chlorophyll index (CI red-edge) (Clevers and Kooistra, 2012; Schlemmera et al., 2013) (Table 2.1). We compared the performance of these indices and chose the best index to predict canopy CHL throughout the Qinghai-Tibetan Plateau.

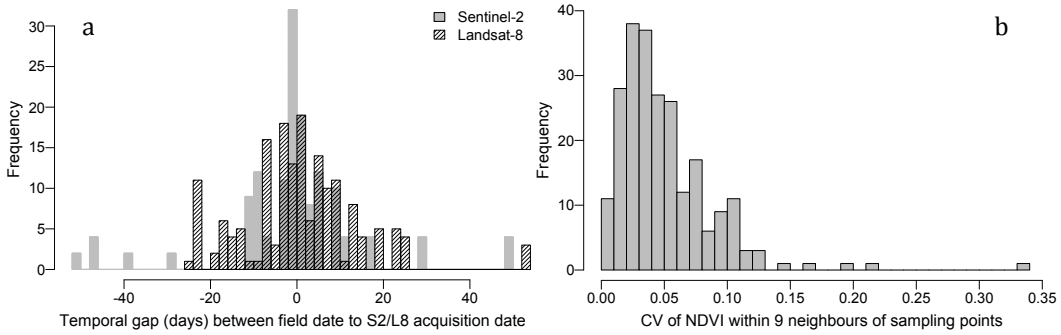

Figure 2.3 Linking field and satellite measurements spatially and temporally. (a) Frequency histogram of the Coefficient of Variation (CV) of Sentinel-2 NDVI (10 m) within 9 neighboring sample points. (b) Frequency histogram of temporal gaps (days) between field measurement date and Sentinel-2 (S2) MCARI/OSAVI acquisition date.

Table 2.1 Sentinel-2 vegetation indices for canopy CHL estimation

Vegetation indices	Formula	Reference
CIred-edge	$R_{783}/R_{705} - 1$	(Gitelson et al., 2006, 2003; Ramoelo et al., 2013)
CIgreen	$R_{783}/R_{560} - 1$	(Gitelson et al., 2006, 2003; Ramoelo et al., 2013)
MCARI/OSAVI	$\frac{[(R_{740} - R_{705}) - 0.2(R_{740} - R_{560})](R_{740}/R_{705})}{(1 + 0.16)\,(R_{740} - R_{705})/(R_{740} - R_{705} + 0.16)}$	(Haboudane et al., 2008, 2002; Wu et al., 2008)
TCARI/OSAVI	$\frac{3[(R_{740} - R_{705}) - 0.2(R_{740} - R_{560})(R_{740}/R_{705})]}{(1 + 0.16)\,(R_{740} - R_{705})/(R_{740} - R_{705} + 0.16)}$	(Haboudane et al., 2002; Wu et al., 2008)

Table 2.2 Landsat-8 vegetation indices for PDMC and aboveground biomass estimation

Rx refers to the reflectance at wavelength x nm

Vegetation indices	Formula	Reference
EVI	$(R_{851} - R_{655})/(R_{851} + 6R_{655} - 7.5R_{482} + 1)$	(Huete et al., 1997)
SAVI	$(R_{851} - R_{655})/(R_{851} + R_{655} + 0.5) * (1.5)$	(Huete and Jackson, 1988)
NDVI	$(R_{851} - R_{655})/(R_{851} + R_{655})$	(Tucker, 1979)
MSAVI	$(2R_{851} + 1 - \sqrt{(2R_{851} + 1)^2 - 8(R_{851} - R_{655})})/2$	(Qi et al., 1994)

2.3.2.2 Specific Plant Area (SPA)

SPA was calculated from the ratio between Plant Area Index (PAI) and aboveground plant dry biomass. PAI values were taken from the MODIS product MCD15A3H at 500 m spatial resolution. Aboveground biomass was estimated using an empirical model developed from Landsat-8 vegetation indices (Table 2.2) and field-measured aboveground biomass. To match the spatial resolution of PAI (500 m) and aboveground biomass (30 m), the aboveground biomass was resampled to 500 m using a bilinear approach. Therefore, SPA was retrieved at a 500 m spatial scale.

2.3.2.3 Plant Dry Matter Content (PDMC)

An empirical model was developed from Landsat-8 vegetation indices and field-

measured PDMC to estimate PDMC for the whole Qinghai-Tibetan Plateau.

2.3.3 Linking Field and Satellite Measurements

We linked remotely-sensed vegetation indices and field-measured plant traits temporally and spatially by extracting the closest satellite pixels with respect to the individual field sampling locations and dates. To evaluate how satellite and field measurements match temporally, we calculated temporal gaps (days) between the satellite acquisition dates and field-measured dates. For 90% of the sampling sites, Sentinel-2 and Landsat-8 images were available within 20 days of field measurements. To test the representativeness of field samples (1 × 1 m) for the satellite pixels (30 × 30 m), we evaluated the homogeneity of the neighborhoods (30 × 30 m) of sampling locations by calculating the coefficient of variation of NDVI. Taking advantage of the 10-m spatial resolution of Sentinel-2 reflectance in the visible bands, coefficients of variation of NDVI of nine neighbors for each sampling point were calculated (Figure 2.3). Lower coefficients of variation values indicate a higher homogeneity of neighborhoods. The coefficient of NDVI variation within 30-m neighborhoods of sampling points showed that 85% of sampling points were located in homogenous neighborhoods with a coefficient of surrounding NDVI variation less than 0.1 (Figure 2.3).

2.3.4 Statistical Modeling and Validation Methods for Remotely-Sensed Plant Traits

We applied linear regression models to quantitatively link the field-measured plant traits with Sentinel-2 red-edge vegetation indices and Landsat-8 vegetation indices (Table 2.1 and Table 2.2). To evaluate model performance, the data were randomly split into two parts, using three-quarters of the data for model calibration and one-quarter for validation. After 500 model runs, we calculated the mean R2 and the relative Root-Mean-Square Error (rRMSE (%)) as the ratio between RMSE and the mean of measured plant traits. The models with the highest accuracy (highest R2 and lowest rRMSE) were applied to the Sentinel-2 red-edge and Landsat-8 vegetation index to generate the canopy CHL, aboveground dry biomass and PDMC maps for the whole study area.

2.3.5 Kernel Density Estimation for Visualization of Plant Traits of Different Vegetation Types

To assess potential plant trait differences between the four examined vegetation types, we applied a kernel density estimation to visualize the distribution of plant traits for the examined vegetation types and visually compare their trait differences (Díaz et al., 2015; Duong, 2007). This analysis was conducted for both field-measured and remotely-sensed plant traits, namely at a 1-m scale based on field-measured plant traits and vegetation types, and at a 1-km scale based on the remotely-sensed plant traits and vegetation types from the Chinese vegetation atlas. We used the 1-km scale to optimize the computation-time. We provided a general overview of the applied data and methods as flowchart (Figure 2.2).

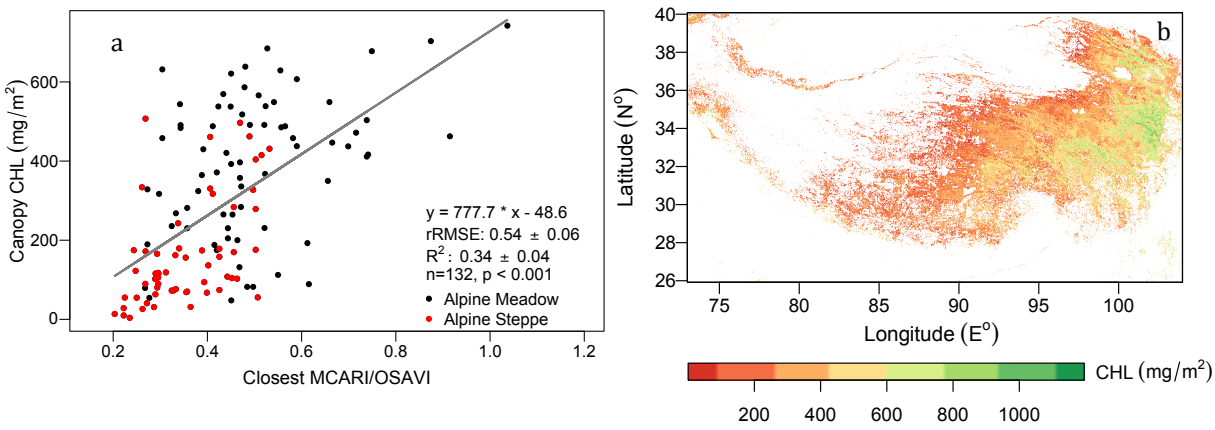

Figure 2.4. Remotely-sensed canopy CHL on the Qinghai-Tibetan Plateau grasslands (a) Linear calibration model of MCARI/OSAVI to predict canopy CHL. (b) Canopy CHL with a spatial resolution of 20 m in the 2016 peak-growing season

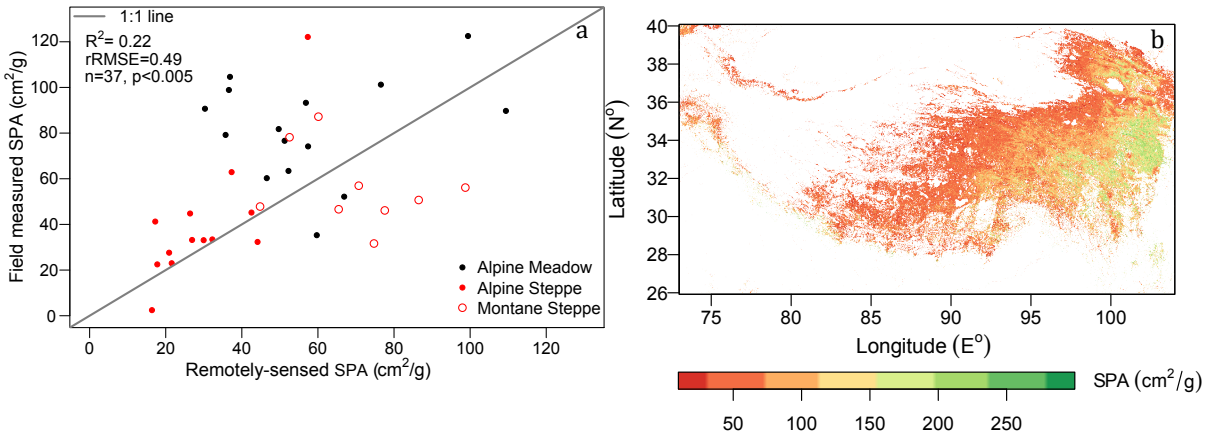

Figure 2.5. Remotely-sensed SPA on the Qinghai-Tibetan Plateau grasslands (a) Scatter plot of field-measured SPA and Remotely-sensed SPA (b) SPA with a spatial resolution of 500 m in the 2016 peak-growing season

2.4 Results

2.4.1 Plant Traits

2.4.1.1 Canopy CHL

The red-edge vegetation index MCARI/OSAVI was able to predict 34% of field-measured canopy CHL variation with an rRMSE of 0.54 outscoring the CIgreen (R^2 = 0.25, rRMSE = 0.57), CI red edge (R^2 = 0.31, rRMSE = 0.55) and the TCARI/OSAVI (R^2 = 0.05, rRMSE = 0.65) indices (Figure 2A.1). The MCARI/OSAVI underestimated the field-measured canopy CHL at lower MCARI/OSAVI values (MCARI/OSAVI < 0.5) but overestimated the field-measured canopy CHL at higher MCARI/OSAVI values (MCARI/OSAVI > 0.5) (Figure 2.4). Based on the MCARI/OSAVI index, we predicted the canopy CHL in the study area (Figure 2.4). The mean Canopy CHL of the entire Plateau in the 2016 peak growing-season was 342 mg/m^2. The CHL map illustrates the decreasing gradient of canopy CHL from the eastern meadow-dominated part to the western steppes-dominant part on the Qinghai-Tibetan Plateau (Figure 2.4).

2.4.1.2 Specific Plant Area (SPA)

The regression model developed from Landsat-8 NDVI (R^2 = 0.55, rRMSE = 0.23) (Figure 2A.2) showed the highest accuracy in predicting field-measured aboveground dry biomass in comparison with the model developed from vegetation indices MSAVI (R^2 = 0.53, rRMSE = 0.24), EVI (R^2 = 0.54, rRMSE = 0.23), and SAVI (R^2 = 0.53, rRMSE = 0.24). The NDVI model was hence used to generate an aboveground biomass map, which was combined with the Plant Area Index (PAI) product to predict Specific Plant Area (SPA). The remotely-sensed SPA calculated from a ratio between PAI (MCD15A3H) and aboveground dry biomass (Landsat-8 NDVI) showed moderate consistency with the field-measured SPA (rRMSE = 0.49 and R^2 = 0.22) (Figure 2.5). Remotely-sensed Specific Plant Area (SPA) also correlated with CWMs of SLA calculated form literature data on the Qinghai-Tibetan Plateau, with R^2 of 0.2 and rRMSE of 0.15 (Figure 2.6). However, remotely-sensed SPA values were on average 53 g/cm^2 lower than CWMs of SLA.

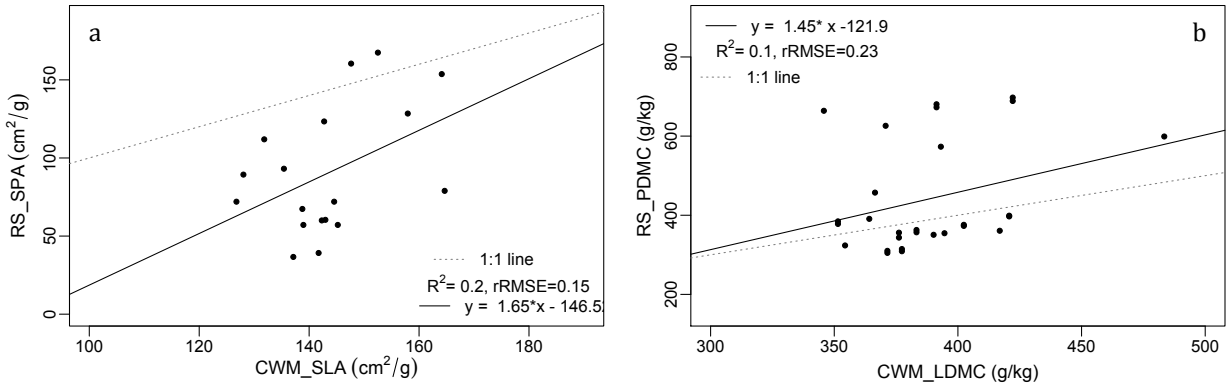

Figure 2.6. Remotely-sensed plant traits and literature-derived plant traits (a) Relationship between remotely-sensed Specific Plant Area (SPA) and literature-derived CWMs of SLA (b) Relationship between remotely-sensed Plant Dry Matter Content (PDMC) and literature-derived CWMs of PDMC.

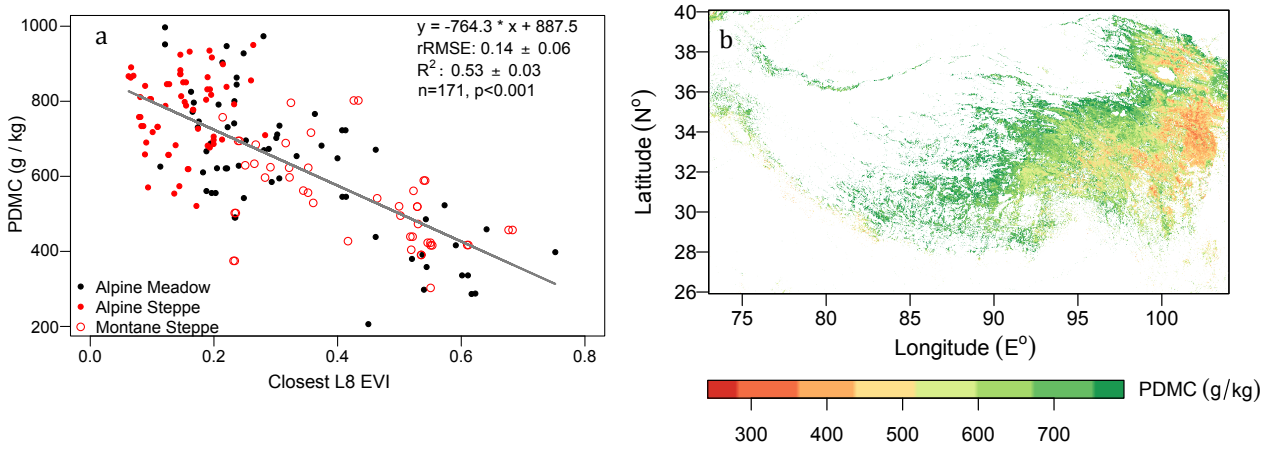

Figure 2.7. Remotely-sensed PDMC on the Qinghai-Tibetan Plateau grasslands. (a) Linear calibration model of EVI to predict PDMC. (b) PDMC with a spatial resolution of 30 m in the 2016 peak-growing season

2.4.2 Plant Dry Matter Content (PDMC)

The regression model developed from Landsat-8 EVI (Figure 2.7) (R^2 = 0.53, rRMSE = 0.144) showed the highest accuracy in predicting field-measured PDMC in comparison with the models that used MSAVI (R^2 = 0.525, rRMSE = 0.144), NDVI (R^2 = 0.522, rRMSE = 0.144) and SAVI (R^2 = 0.526, rRMSE = 0.145) vegetation indices (Figure 2A.3). The predicted PDMC in the 2016 peak growing season showed an opposite spatial pattern compared with predicted canopy CHL and SPA, with lower values in the northeast of the meadow grassland and higher values in sparsely vegetated alpine steppe area in the West (Figure 2.7). We found that remotely-sensed PDMC correlated with literature-derived CWMs of LDMC with R^2 of 0.1 and rRMSE of 0.23 (Figure 2.6).

2.4.3 Differences in plant traits between vegetation types

CHL, SPA and PDMC varied widely among different vegetation types (Figure 2.8). Alpine meadow had higher values and spanned a broader range of canopy CHL and SPA than alpine and montane steppe (Figure 2.8). The alpine steppe had the highest PDMC but the lowest variability, whereas alpine meadow had the highest variability but lower PDMC (Figure 2.8). This pattern was consistent at both scales (1-m and 1-km).

2.5 Discussions

In this study, we found that plant traits of CHL, SPA and PDMC can be retrieved over the complete Qinghai-Tibetan Plateau by statistical models developed from field-measured plant traits and vegetation indices derived from Landsat-8 and Sentinel-2 data. Below, we discuss: 1) the prediction accuracy of remotely-sensed plant traits and their relation with literature-derived CWMs of SLA and LDMC; 2) plant adaptation strategies of vegetation types as indicated by the observed trait differences; 3) potential implications of remotely-sensed plant traits for ecosystem functioning in future studies.

2.5.1 Plant Traits

2.5.1.1 Canopy CHL

We tested the capability of Sentinel-2 red-edge vegetation indices to estimate canopy CHL on the Qinghai-Tibetan Plateau. We estimated canopy CHL through multiplying leaf CHL by PAI, a method often applied in croplands (Darvishzadeh et al., 2008a, 2008b; Gitelson et al., 2005; Peng and Gitelson, 2011; Wu et al., 2012). The method seems also applicable to diverse alpine grasslands on the Qinghai-Tibetan Plateau even though the prediction accuracy (R^2 = 34%, rRMSE of 0.54) is lower than prediction accuracies typically reported for mono-species croplands (Schlemmera et al., 2013; Wu et al., 2008). It is likely that the higher plant species diversity and corresponding higher spatial heterogeneity in PAI in natural grasslands are a main reason for this. Additionally, difficulties of measuring SPAD for small grass leaves may have affected the prediction accuracy.

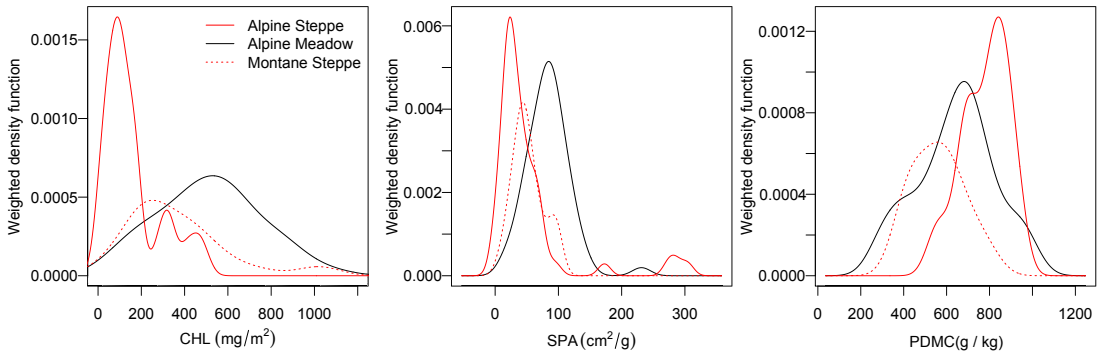

(a) One meter scale

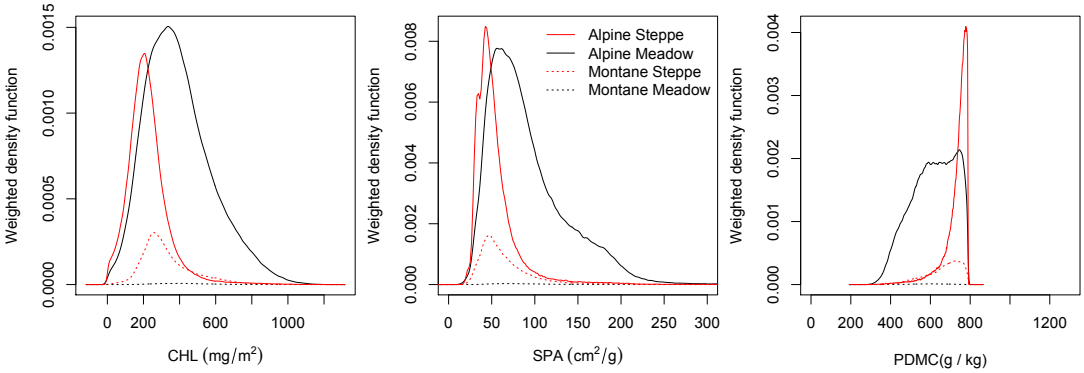

(b) One kilometer scale

Figure 2.8. Probability density functions of plant traits in different vegetation types

We found that among the tested red-edge vegetation indices MCARI/ OSAVI was the best estimator of canopy CHL in alpine grasslands, presumably because it minimizes soil background effects and is resistant to PAI variation for low PAI values while still being sensitive to high CHL values (Wu et al., 2008). TCARI/OSAVI had the lowest accuracy in predicting canopy CHL presumably because it was more affected by background information for PAI values < 0.5 (Wu et al., 2008). A further explanation could be that that TCARI/OSAVI was found to have a non-linear relationship with PAI, changing from positive to negative at PAI = 0.5 (Wu et al., 2008). This characteristic of TCARI/OSAVI might result in lower accuracy when applying a linear model for predicting canopy CHL.

2.5.1.2 Specific Plant Area (SPA)

We found that remotely-sensed Specific Plant Area (SPA) correlated to the field-measured values of SPA (R^2 = 0.22) and the literature-based CWMs of SLA (R^2 = 0.2). We found both field-measured and remotely-sensed SPA were generally lower (-73 g/cm^2 and -53g/cm^2) than the reference CWMs of SLA. The reason for this

underestimation was probably that SPA includes plant parts that have a lower surface to volume ratio than leaves. Even though remotely-sensed SPA and literature-derived CWMs of SLA were obtained with vastly different methods we still found that they were correlated (Figure 2.6).

We showed that remotely-sensed SPA at 500 m scale ranges from 10 to 231.2 cm^2/g over the entire Qinghai-Tibetan Plateau, leading to a wider range of values compared to existing studies (Chen et al., 2013; Li et al., 2017; Ma et al., 2010). This range is within the scope of CWMs of SLA values reported in the literature at a global scale. Kattge et al (Kattge et al., 2011) found that field-measured herb and grass CWMs of SLA ranged from 70–500 cm^2/g with an average of 200 cm^2/g in the northern hemisphere.

2.5.1.3 Plant Dry Matter Content (PDMC)

Remotely-sensed PDMC (R^2 = 0.53, rRMSE = 13%) was estimated with higher prediction accuracy than canopy CHL (R^2 = 0.33, rRMSE = 50%) and SPA (R^2 = 0.22, rRMSE = 49%). This study found that vegetation indices (e.g., EVI) correlated negatively with PDMC (Figure 2.7). The study area covers a large spatial gradient of precipitation (from more than 1000 to less than 100 mm yr^{-1}) (Chen et al., 2015), which influences leaf water content and biomass. Humid areas are characterized by higher leaf water content as well as biomass, leading to higher EVI compared with dry area. Therefore, EVI is positively correlated with leaf water content. The PDMC has an inverse relationship to leaf water content (Roelofsen et al., 2014), thus EVI is negatively correlated with PDMC. This study found that differences in the visible and near-infrared regions of the spectra could explain variations of PDMC in alpine grasslands. Remotely-sensed PDMC correlated with literature-derived CWMs of LDMC on the Qinghai-Tibetan Plateau (Figure 2.6). However, the correlation was rather low and remotely-sensed PDMC values were on average 54.7 g/kg higher than the literature-derived CWM of LDMC, presumably because non-leaf structures – which were considered as part of LDMC in this study - have lower water content than leaves.

2.5.2 Implication of Trait Relationships and Trait Variations among Vegetation Types under Global Change

Trait differences among vegetation types indicate different plant adaptation strategies (Kattenborn et al., 2017). Understanding these different plant strategies may help to

predict how ecosystems will respond to global change, especially for alpine plants on the Qinghai-Tibetan Plateau, which have adapted to low temperatures, and are expected to have developed unique survival strategies (He et al., 2006a).

The trait differences between vegetation types indicate a trade-off between plant productivity and persistence. We found a general East-to-West pattern of decreasing canopy CHL and SPA values and increasing PDMC values across the Qinghai-Tibetan Plateau. These spatial patterns of plant traits are related to the spatial distribution of vegetation types, and further correspond to decreasing rainfall and increasing aridity towards the West (G. Miehe et al., 2011). Vegetation types shift from meadow to steppe along the East-West gradient on the Qinghai-Tibetan Plateau. Alpine meadows occur in environments beneficial to plant growth in terms of water availability and temperature (Miehe et al., 2013), allowing plants to be fast in resource capturing and nutrient turnover (Chapin, 1980; He et al., 2010), leading to high photosynthetic rates and fast growth rates but low tissue density. This adaptation accounts for high CHL and SLA but low LDMC (Díaz et al., 2004; Pierce et al., 2017; Schweiger et al., 2017) of plants in alpine meadow and indicates a trade-off between plant productivity and persistence (Diemer, 1998; He et al., 2009). Alpine steppe grows in arid areas with low water availability and low soil fertility (Miehe et al., 2013), where plants adapt to this resource-limited environment by decreasing leaf area in order to decrease evaporation, increase tissue density and slow down photosynthesis and growth rate (Pierce et al., 2017; Schweiger et al., 2017). This characteristic makes plants invest less in resource acquisition and more in structural tissue, which results in higher LDMC but lower SLA and canopy CHL content (Pierce et al., 2017; Schweiger et al., 2017). In accordance with these hypotheses, we found that plants from alpine meadows had higher CHL and SPA but lower PDMC values than plants from alpine steppe for both field-measured and remotely-sensed traits (Figure 2.8). Montane steppe and montane meadow grow at lower elevations and thus in warmer areas and are exposed to intermediate resource availability. These environmental conditions might explain why their trait values ranged between the values of alpine meadow and alpine steppe.

Potential changes of the vegetation type distributions and plant traits on the Qinghai Tibetan Plateau due to warming and increased precipitation (Kang et al., 2010; Yao et al., 2012; You et al., 2013) could be indicated by the natural spatial gradient of vegetation type distributions and plant traits towards the East. Because the warming

and wetting trend on the Qinghai-Tibetan Plateau (Kang et al., 2010; Yao et al., 2012; You et al., 2013) are comparable to the spatial gradient of increasing temperature and water availability towards the East, this spatial pattern may enable a space-for-time approach to predict the potential changes of plant traits and vegetation types under global change. Because meadows occur in warmer and wetter environments, we speculate that the warming and increasing precipitation are more favorable for alpine meadows. Previous studies found that vegetation activity has increased in recent decades on the Qinghai-Tibetan Plateau because of the increased temperature (Peng et al., 2012; Piao et al., 2006). This trend of increased vegetation activity is more significant for alpine meadow than for the other vegetation types (Zhang et al., 2013). For the reasons stated above, we deduced that alpine meadows might benefit most on the Qinghai-Tibetan Plateau in a global-change setting. This suggests higher CHL and SLA but lower LDMC over the eastern part of the Qinghai-Tibetan Plateau in the future.

2.5.3 Potential Implication of Remotely-Sensed Plant Traits on the Qinghai-Tibetan Plateau

We demonstrated that remotely-sensed SPA and PDMC were related to CWMs of SLA and LDMC reported in earlier studies. Therefore, approximations between plant- and leaf-level traits may be a straightforward way to simplify trait measurement in alpine grasslands. Furthermore, maps of remotely-sensed plant traits as presented in this study, can lay the foundation for further ecological trait studies over large regions under global change.

Remotely-sensed plant traits of CHL, SPA and PDMC are predictors of ecosystem functioning and services on the Qinghai-Tibetan Plateau. CHL and SPA are closely related to plant nitrogen and define the photosynthetic capacity of vegetation (Ali et al., 2016a; ter Steege et al., 2013); they therefore also affect the amount of carbon uptake of the ecosystem. Photosynthetic capacity and carbon uptake are especially important for the ecosystem on the Qinghai-Tibetan Plateau, where the photosynthetic rate is limited by low temperature, low air pressure, high wind speed and high UV-B radiation (He et al., 2006a). LDMC has been shown to correlate negatively with potential relative growth rate and positively with leaf lifespan, which serves as an indicator of plant resistance to physical hazards and disturbance, plant digestibility and rangeland quality (ter Steege et al., 2013). Plants with higher LDMC tend to be

physically tougher and thus are assumed to have higher resistance but lower plant digestibility.

Remotely-sensed plant traits can hence facilitate future studies on how plants traits correlate to environmental variables and land-use related variables such as grazing intensity. Traits and trait combinations vary with temperature, aridity, soil fertility, and grazing level (He et al., 2010), (Niu et al., 2010). The prominent gradient in climate, soil properties, and grazing intensity on the Qinghai-Tibetan Plateau offers a convenient way to study how these different environmental factors correlate to plant traits. Previous studies for example suggested that SLA can express strong traits plasticity (Shipley et al., 2016) and LDMC is sensitive to rainfall (Pakeman, 2014). In another study, CHL was found to be positively correlated with grazing intensity up to medium grazing intensities because cattle excrement is the only external source of nutrients in these ecosystem (Lehnert et al., 2014) and increases nutrient availability for plants. These findings identified in local studies could be re-examined over larger spatial extent and in a spatially continuous way by making use of trait maps as presented in this study. This is particularly interesting as the environmental conditions and land use management strategies vary widely over the Qinghai-Tibetan Plateau and it would hence be interesting to study how the relationships between plant traits and environmental and land-use variables depend on the location on the Plateau.

2.6 Conclusions and Outlook

Based on statistical models between vegetation indices and field-measured plant traits, and by taking advantage of the Google Earth Engine cloud-computing platform, we derived the plant traits CHL, SPA and PDMC across the entire Qinghai-Tibetan Plateau at the fine resolutions of 20 m, 500 m and 30 m respectively. Our results showed that the plant traits of CHL, SPA and PDMC could be predicted using satellite data of Sentinel-2 (20 m) and Landsat-8 (30 m) as well as the MODIS LAI product (500 m), with R^2 of 0.34, 0.22 and 0.53 respectively.

We found that the canopy CHL and SPA values of alpine meadows were higher and had a wider range than the values observed for the alpine steppe. On the contrary, PDMC values were lower and more narrowly distributed in alpine meadow than in alpine steppe. These plant trait differences among vegetation types indicate trade-offs between plant productivity and persistence, describing different plant strategies.

We demonstrated that remotely-sensed and field-measured SPA and PDMC

correlated with literature-derived CWMs of SLA and LDMC even though the correlations were not very strong most likely because the datasets were measured at different times and spatial scales. It is conceivable that the correlations could be improved if measurements were conducted at the same time and spatial scale. More research is needed to further test the hypothesis that leaf-level trait measurement of CWMs of SLA and LDMC are comparable to field-measured and remotely-sensed SPA and PDMC in grassland. Strengthening the hypothesis would be beneficial for simplifying the study of plant traits and also facilitate trait estimation using remote-sensing technologies. The latter would also enable repeated trait assessments via remote sensing, which would enable the monitoring of plant traits. This could be key for a timely identification of potential ecosystem degradations on the Qinghai-Tibetan Plateau.

2.7 Appendix

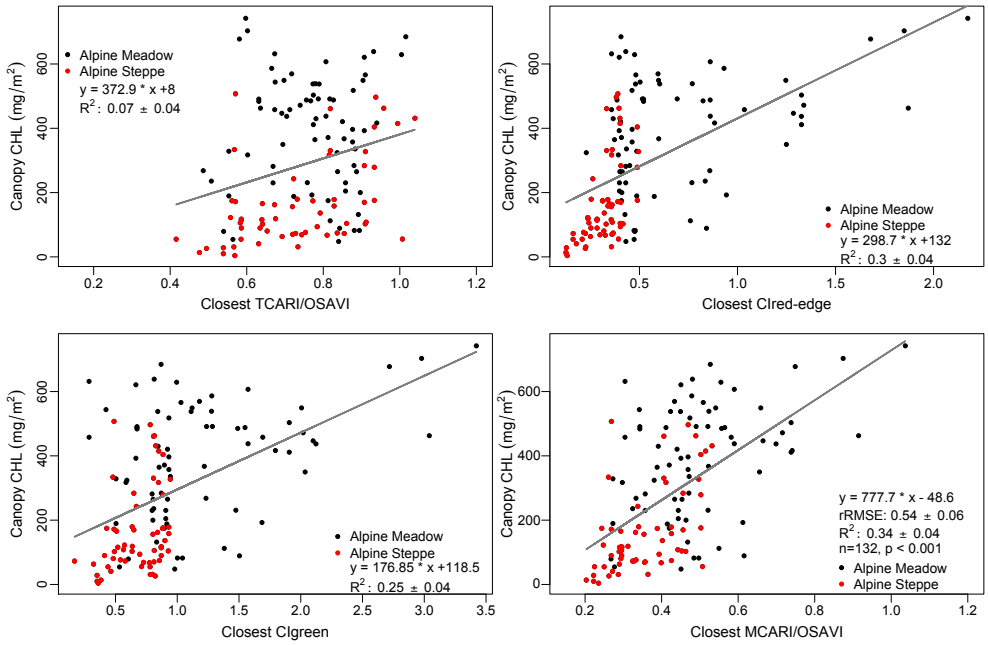

Figure 2A.1 Linear regression between vegetation indices and canopy CHL

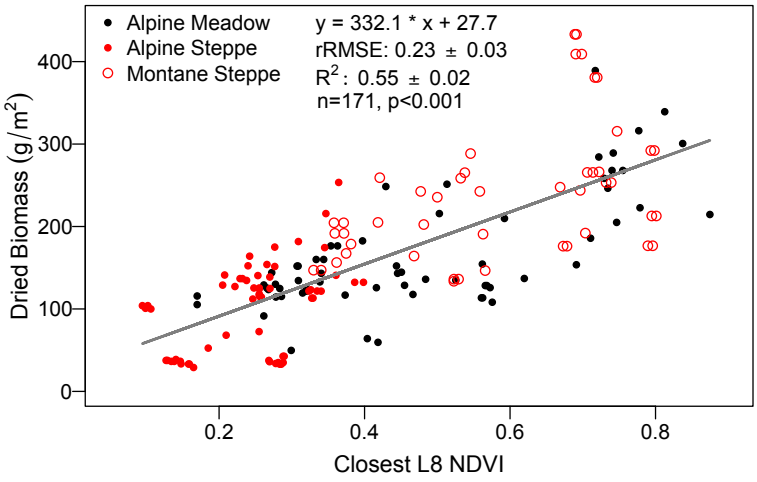

Figure 2A.2 Linear calibration model of Landsat-8 NDVI to predict aboveground biomass

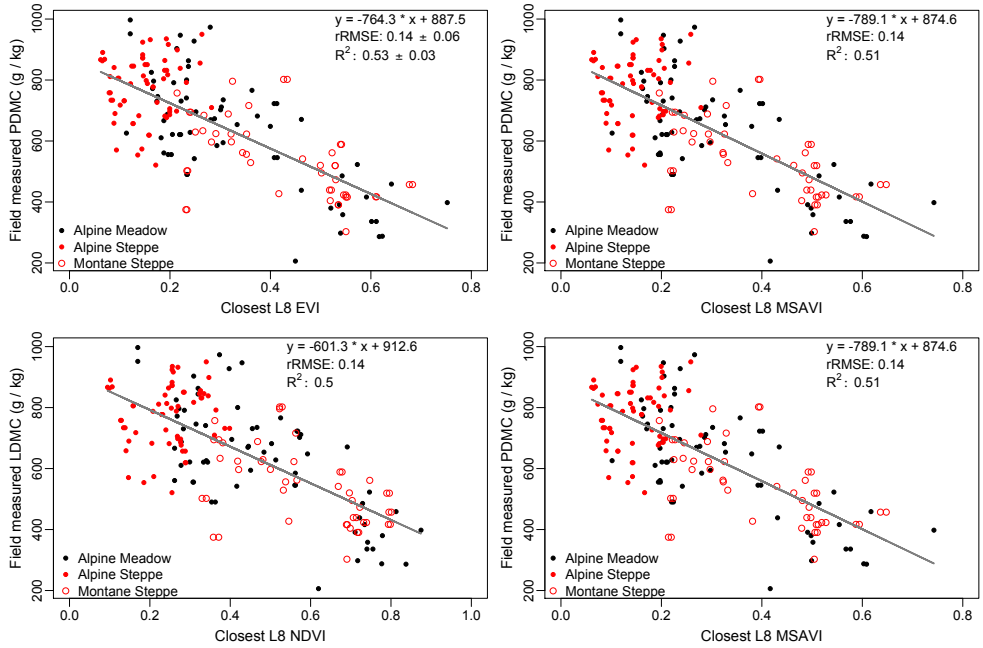

Figure 2A.3 Linear regression between vegetation indices and Plant Dry Matter Content (PDMC)

2.8 Acknowledgment

We are very grateful to Guozhen Du (Lanzhou University), Wei Qi (Lanzhou University), Kechang Niu (Nanjing Unviersity) and Wenying Wang (Qinghai Normal University) for their help and support with field-data collection. We thanks Dominic Fawcett, Fabian Schneider and Daniela Braun for their language corrections and helpful comments. We acknowledge anonymous reviewers who provided useful comments to the manuscript. This study was funded and supported by the China Scholarship council and the University of Zurich Research Priority Program on Global Change and Biodiversity (URPP GCB).

2.9 References

Ali, A.M., Darvishzadeh, R., Skidmore, A.K., 2017a. Retrieval of Specific Leaf Area From Landsat-8 Surface Reflectance Data Using Statistical and Physical Models. IEEE J. Sel. Top. Appl. Earth Obs. Remote Sens. 1–8. doi:10.1109/JSTARS.2017.2690623

Ali, A.M., Darvishzadeh, R., Skidmore, A.K., Duren, I. Van, 2016a. Effects of Canopy Structural Variables on Retrieval of Leaf Dry Matter Content and Specific Leaf Area from Remotely Sensed Data. IEEE J. Sel. Top. Appl. Earth Obs. Remote Sens. 9, 898–909. doi:10.1109/JSTARS.2015.2450762

Ali, A.M., Darvishzadeh, R., Skidmore, A.K., Duren, I. van, Heiden, U., Heurich, M., 2016b. Estimating leaf functional traits by inversion of PROSPECT: Assessing leaf dry matter content and specific leaf area in mixed mountainous forest. Int. J. Appl. Earth Obs. Geoinf. 45, 66–76. doi:10.1016/j.jag.2015.11.004

Ali, A.M., Darvishzadeh, R., Skidmore, A.K., van Duren, I., 2017b. Specific leaf area estimation from leaf and canopy reflectance through optimization and validation of vegetation indices. Agric. For. Meteorol. 236, 162–174. doi:10.1016/j.agrformet.2017.01.015

Asner, G.P., Martin, R.E., 2008. Spectral and chemical analysis of tropical forests: Scaling from leaf to canopy levels. Remote Sens. Environ. 112, 3958–3970. doi:10.1016/j.rse.2008.07.003

Asner, G.P., Martin, R.E., Tupayachi, R., Emerson, R., Martinez, P., Sinca, F., Powell, G.V.N., Wright, S.J., Lugo, A.E., 2011. Taxonomy and remote sensing of leaf mass per area (LMA) in humid tropical forests. Ecol. Appl. 21, 85–98. doi:10.1890/09-1999.1

Capolupo, A., Kooistra, L., Berendonk, C., Boccia, L., Suomalainen, J., 2015. Estimating Plant Traits of Grasslands from UAV-Acquired Hyperspectral Images: A Comparison of Statistical Approaches. ISPRS Int. J. Geo-Information 4, 2792–2820. doi:10.3390/ijgi4042792

Chapin, F.S., 1980. The Mineral Nutrition of Wild Plants 11, 233–260.
Chen, L., Niu, K., Wu, Y., Geng, Y., Mi, Z., Flynn, D.F.B., He, J.S., 2013. UV radiation is the primary factor driving the variation in leaf phenolics across Chinese grasslands. Ecol. Evol. 3, 4696–4710. doi:10.1002/ece3.862

Chen, X., An, S., Inouye, D.W., Schwartz, M.D., 2015. Temperature and snowfall trigger alpine vegetation green-up on the world's roof. Glob. Chang. Biol. 21, 3635–3646. doi:10.1111/gcb.12954

Clevers, J.G.P.W., Kooistra, L., 2012. Using hyperspectral remote sensing data for retrieving canopy chlorophyll and nitrogen content. IEEE J. Sel. Top. Appl. Earth Obs. Remote Sens. 5, 574–583. doi:10.1109/JSTARS.2011.2176468

Darvishzadeh, R., Skidmore, A., Schlerf, M., Atzberger, C., 2008a. Inversion of a radiative transfer model for estimating vegetation LAI and chlorophyll in a heterogeneous grassland. Remote Sens. Environ. 112, 2592–2604. doi:10.1016/j.rse.2007.12.003

Darvishzadeh, R., Skidmore, A., Schlerf, M., Atzberger, C., Corsi, F., Cho, M., 2008b. LAI and chlorophyll estimation for a heterogeneous grassland using hyperspectral measurements. ISPRS J. Photogramm. Remote Sens. 63, 409–426. doi:10.1016/j.isprsjprs.2008.01.001

Díaz, S., Hodgson, J.G., Thompson, K., Cabido, M., Cornelissen, J.H.C., Jalili, A., Montserrat-Martí, G., Grime, J.P., Zarrinkamar, F., Asri, Y., Band, S.R., Basconcelo, S., Castro-Díez, P., Funes, G., Hamzehee, B., Khoshnevi, M., Pérez-Harguindeguy, N., Pérez-Rontomé, M.C., Shirvany, A., Vendramini, F., Yazdani, S., Abbas-Azimi, R., Bogaard, A., Boustani, S., Charles, M., Dehghan, M., de Torres-Espuny, L., Falczuk, V., Guerrero-Campo, J., Hynd, A., Jones, G., Kowsary, E., Kazemi-Saeed, F., Maestro-Martínez, M., Romo-Díez, A., Shaw, S., Siavash, B., Villar-Salvador, P., Zak, M.R., 2004. The plant traits that drive ecosystems: Evidence from three continents. J. Veg. Sci. 15, 295. doi:10.1658/1100-9233(2004)015[0295:TPTTDE]2.0.CO;2

Díaz, S., Kattge, J., Cornelissen, J.H.C., Wright, I.J., Lavorel, S., Dray, S., Reu, B., Kleyer, M., Wirth, C., Colin Prentice, I., Garnier, E., Bönisch, G., Westoby, M., Poorter, H., Reich, P.B., Moles, A.T., Dickie, J., Gillison, A.N., Zanne, A.E., Chave, J., Joseph Wright, S., Sheremet'ev, S.N., Jactel, H., Baraloto, C., Cerabolini, B., Pierce, S., Shipley, B., Kirkup, D., Casanoves, F., Joswig, J.S., Günther, A., Falczuk, V., Rüger, N., Mahecha, M.D., Gorné, L.D., 2015. The global spectrum of plant form and function. Nature 529, 167–171. doi:10.1038/nature16489

Diemer, M., 1998. Leaf lifespans of high-elevation, aseasonal Andean shrub species in relation to leaf traits and leaf habit. Glob. Ecol. Biogeogr. 7, 457–465. doi:10.1046/j.1466-822X.1998.00318.x

Drusch, M., Del Bello, U., Carlier, S., Colin, O., Fernandez, V., Gascon, F., Hoersch, B., Isola, C.,

Laberinti, P., Martimort, P., Meygret, A., Spoto, F., Sy, O., Marchese, F., Bargellini, P., 2012. Sentinel-2: ESA's Optical High-Resolution Mission for GMES Operational Services. Remote Sens. Environ. 120, 25–36. doi:10.1016/j.rse.2011.11.026

Duong, T., 2007. ks: Kernel Density Estimation and Kernel Discriminant Analysis for Multivariate Data in R. J. Stat. Softw. 21, 1–16. doi:10.18637/jss.v068.c02

Farr, T., Rosen, P., Caro, E., Crippen, R., Duren, R., Hensley, S., Kobrick, M., Paller, M., Rodriguez, E., Roth, L., Seal, D., Shaffer, S., Shimada, J., Umland, J., Werner, M., Oskin, M., Burbank, D., Alsdorf, D., 2007. The shuttle radar topography mission. Rev. Geophys. 45, 1–33. doi:10.1029/2005RG000183.1.INTRODUCTION

Feilhauer, H., Somers, B., van der Linden, S., 2017. Optical trait indicators for remote sensing of plant species composition: Predictive power and seasonal variability. Ecol. Indic. 73, 825–833. doi:10.1016/j.ecolind.2016.11.003

Féret, J.-B., François, C., Gitelson, A., Asner, G.P., Barry, K.M., Panigada, C., Richardson, A.D., Jacquemoud, S., 2011. Optimizing spectral indices and chemometric analysis of leaf chemical properties using radiative transfer modeling. Remote Sens. Environ. 115, 2742–2750. doi:10.1016/j.rse.2011.06.016

Foga, S., Scaramuzza, P.L., Guo, S., Zhu, Z., Dilley, R.D., Beckmann, T., Schmidt, G.L., Dwyer, J.L., Joseph Hughes, M., Laue, B., 2017. Cloud detection algorithm comparison and validation for operational Landsat data products. Remote Sens. Environ. 194, 379–390. doi:10.1016/j.rse.2017.03.026

Forrestel, E.J., Donoghue, M.J., Edwards, E.J., Jetz, W., du Toit, J.C.O., Smith, M.D., 2017. Different clades and traits yield similar grassland functional responses. Proc. Natl. Acad. Sci. 114, 705–710. doi:10.1073/pnas.1612909114

Friedl, M.A., Sulla-Menashe, D., Tan, B., Schneider, A., Ramankutty, N., Sibley, A., Huang, X., 2010. MODIS Collection 5 global land cover: Algorithm refinements and characterization of new datasets. Remote Sens. Environ. 114, 168–182. doi:10.1016/j.rse.2009.08.016

Ghosh, S., Mishra, D.R., Gitelson, A.A., 2016. Long-term monitoring of biophysical characteristics of tidal wetlands in the northern Gulf of Mexico - A methodological approach using MODIS. Remote Sens. Environ. 173, 39–58. doi:10.1016/j.rse.2015.11.015

Gitelson, A.A., Gritz †, Y., Merzlyak, M.N., 2003. Relationships between leaf chlorophyll content and spectral reflectance and algorithms for non-destructive chlorophyll assessment in higher plant leaves. J. Plant Physiol. 160, 271–282. doi:10.1078/0176-1617-00887

Gitelson, A.A., Keydan, G.P., Merzlyak, M.N., 2006. Three-band model for noninvasive estimation of chlorophyll, carotenoids, and anthocyanin contents in higher plant leaves. Geophys. Res. Lett. 33, 2–6. doi:10.1029/2006GL026457

Gitelson, A.A., Peng, Y., Arkebauer, T.J., Schepers, J., 2014a. Relationships between gross primary production, green LAI, and canopy chlorophyll content in maize: Implications for remote sensing of primary production. Remote Sens. Environ. 144, 65–72. doi:10.1016/j.rse.2014.01.004

Gitelson, A.A., Peng, Y., Huemmrich, K.F., 2014b. Relationship between fraction of radiation absorbed by photosynthesizing maize and soybean canopies and NDVI from remotely sensed data taken at close range and from MODIS 250m resolution data. Remote Sens. Environ. 147, 108–120. doi:10.1016/j.rse.2014.02.014

Gitelson, A.A., Viña, A., Ciganda, V., Rundquist, D.C., Arkebauer, T.J., 2005. Remote estimation of canopy chlorophyll content in crops. Geophys. Res. Lett. 32, 1–4. doi:10.1029/2005GL022688

Gorelick, N., Hancher, M., Dixon, M., Ilyushchenko, S., Thau, D., Moore, R., 2017. Google Earth Engine: Planetary-scale geospatial analysis for everyone. Remote Sens. Environ. doi:10.1016/j.rse.2017.06.031

Haboudane, D., Miller, J.R., Tremblay, N., Zarco-Tejada, P.J., Dextraze, L., 2002. Integrated narrow-band vegetation indices for prediction of crop chlorophyll content for application to precision agriculture. Remote Sens. Environ. 81, 416–426. doi:10.1016/S0034-4257(02)00018-4

Haboudane, D., Tremblay, N., Miller, J.R., Vigneault, P., 2008. Remote estimation of crop chlorophyll content using spectral indices derived from hyperspectral data. IEEE Trans. Geosci. Remote Sens. 46, 423–436. doi:10.1109/TGRS.2007.904836

Harris, R.B., 2010. Rangeland degradation on the Qinghai-Tibetan plateau: A review of the evidence of its magnitude and causes. J. Arid Environ. 74, 1–12. doi:10.1016/j.jaridenv.2009.06.014

He, J.S., Wang, X., Flynn, D.F.B., Wang, L., Schmid, B., Fang, J., 2009. Taxonomic, phylogenetic, and environmental trade-offs between leaf productivity and persistence. Ecology 90, 2779–2791.

doi:10.1890/08-1126.1

He, J.S., Wang, X., Schmid, B., Flynn, D.F.B., Li, X., Reich, P.B., Fang, J., 2010. Taxonomic identity, phylogeny, climate and soil fertility as drivers of leaf traits across Chinese grassland biomes. J. Plant Res. 123, 551–561. doi:10.1007/s10265-009-0294-9

He, J.S., Wang, Z., Wang, X., Schmid, B., Zuo, W., Zhou, M., Zheng, C., Wang, M., Fang, J., 2006a. A test of the generality of leaf trait relationships on the Tibetan Plateau. New Phytol. 170, 835–848. doi:10.1111/j.1469-8137.2006.01704.x

He, J.S., Wang, Z., Wang, X., Schmid, B., Zuo, W., Zhou, M., Zheng, C., Wang, M., Fang, J., 2006b. A test of the generality of leaf trait relationships on the Tibetan Plateau. New Phytol. 170, 835–848. doi:10.1111/j.1469-8137.2006.01704.x

Homolová, L., Malenovský, Z., Clevers, J.G.P.W., García-Santos, G., Schaepman, M.E., 2013. Review of optical-based remote sensing for plant trait mapping. Ecol. Complex. 15, 1–16. doi:10.1016/j.ecocom.2013.06.003

Hou, X., 2001. Vegetation Altas of China. Science Press, Beijing.

Huete, A.R., Jackson, R.D., 1988. Soil and atmosphere influences on the spectra of partial canopies. Remote Sens. Environ. 25, 89–105. doi:10.1016/0034-4257(88)90043-0

Huete, A.R., Liu, H.Q., Batchily, K., Van Leeuwen, W., 1997. A comparison of vegetation indices over a global set of TM images for EOS-MODIS. Remote Sens. Environ. 59, 440–451. doi:10.1016/S0034-4257(96)00112-5

Irish, R.R., Barker, J.L., Goward, S.N., Arvidson, T., 2006. Characterization of the Landsat-7 ETM+ Automated Cloud-Cover Assessment (ACCA) Algorithm. Photogramm. Eng. Remote Sens. 72, 1179–1188. doi:10.14358/PERS.72.10.1179

Jacquemoud, S., Verhoef, W., Baret, F., Bacour, C., Zarco-Tejada, P.J., Asner, G.P., François, C., Ustin, S.L., 2009. PROSPECT + SAIL models: A review of use for vegetation characterization. Remote Sens. Environ. 113, S56–S66. doi:10.1016/j.rse.2008.01.026

Kang, S., Xu, Y., You, Q., Flügel, W.-A., Pepin, N., Yao, T., 2010. Review of climate and cryospheric change in the Tibetan Plateau. Environ. Res. Lett. 5, 015101. doi:10.1088/1748-9326/5/1/015101

Kattenborn, T., Fassnacht, F.E., Pierce, S., Lopatin, J., Grime, J.P., Schmidtlein, S., 2017. Linking plant strategies and plant traits derived by radiative transfer modelling. J. Veg. Sci. 28, 717–727. doi:10.1111/jvs.12525

Kattge, J., Díaz, S., Lavorel, S., Prentice, I.C., Leadley, P., Bönisch, G., Garnier, E., Westoby, M., Reich, P.B., Wright, I.J., Cornelissen, J.H.C., Violle, C., Harrison, S.P., Van Bodegom, P.M., Reichstein, M., Enquist, B.J., Soudzilovskaia, N.A., Ackerly, D.D., Anand, M., Atkin, O., Bahn, M., Baker, T.R., Baldocchi, D., Bekker, R., Blanco, C.C., Blonder, B., Bond, W.J., Bradstock, R., Bunker, D.E., Casanoves, F., Cavender-Bares, J., Chambers, J.Q., Chapin, F.S., Chave, J., Coomes, D., Cornwell, W.K., Craine, J.M., Dobrin, B.H., Duarte, L., Durka, W., Elser, J., Esser, G., Estiarte, M., Fagan, W.F., Fang, J., Fernández-Méndez, F., Fidelis, A., Finegan, B., Flores, O., Ford, H., Frank, D., Freschet, G.T., Fyllas, N.M., Gallagher, R. V., Green, W.A., Gutierrez, A.G., Hickler, T., Higgins, S.I., Hodgson, J.G., Jalili, A., Jansen, S., Joly, C.A., Kerkhoff, A.J., Kirkup, D., Kitajima, K., Kleyer, M., Klotz, S., Knops, J.M.H., Kramer, K., Kühn, I., Kurokawa, H., Laughlin, D., Lee, T.D., Leishman, M., Lens, F., Lenz, T., Lewis, S.L., Lloyd, J., Llusià, J., Louault, F., Ma, S., Mahecha, M.D., Manning, P., Massad, T., Medlyn, B.E., Messier, J., Moles, A.T., Müller, S.C., Nadrowski, K., Naeem, S., Niinemets, Ü., Nöllert, S., Nüske, A., Ogaya, R., Oleksyn, J., Onipchenko, V.G., Onoda, Y., Ordoñez, J., Overbeck, G., Ozinga, W.A., Patiño, S., Paula, S., Pausas, J.G., Peñuelas, J., Phillips, O.L., Pillar, V., Poorter, H., Poorter, L., Poschlod, P., Prinzing, A., Proulx, R., Rammig, A., Reinsch, S., Reu, B., Sack, L., Salgado-Negret, B., Sardans, J., Shiodera, S., Shipley, B., Siefert, A., Sosinski, E., Soussana, J.F., Swaine, E., Swenson, N., Thompson, K., Thornton, P., Waldram, M., Weiher, E., White, M., White, S., Wright, S.J., Yguel, B., Zaehle, S., Zanne, A.E., Wirth, C., 2011. TRY - a global database of plant traits. Glob. Chang. Biol. 17, 2905–2935. doi:10.1111/j.1365-2486.2011.02451.x

Lavorel, S., Grigulis, K., McIntyre, S., Williams, N.S.G., Garden, D., Dorrough, J., Berman, S., Quétier, F., Thébault, A., Bonis, A., 2008. Assessing functional diversity in the field - Methodology matters! Funct. Ecol. 22, 134–147. doi:10.1111/j.1365-2435.2007.01339.x

le Maire, G., François, C., Soudani, K., Berveiller, D., Pontailler, J.Y., Bréda, N., Genet, H., Davi, H., Dufrêne, E., 2008. Calibration and validation of hyperspectral indices for the estimation of broadleaved forest leaf chlorophyll content, leaf mass per area, leaf area index and leaf canopy biomass. Remote Sens. Environ. 112, 3846–3864. doi:10.1016/j.rse.2008.06.005

Lehnert, L.W., Meyer, H., Meyer, N., Reudenbach, C., Bendix, J., 2014. A hyperspectral indicator

system for rangeland degradation on the Tibetan Plateau: A case study towards spaceborne monitoring. Ecol. Indic. 39, 54–64. doi:10.1016/j.ecolind.2013.12.005

Lehnert, L.W., Meyer, H., Wang, Y., Miehe, G., Thies, B., Reudenbach, C., Bendix, J., 2015. Retrieval of grassland plant coverage on the Tibetan Plateau based on a multi-scale, multi-sensor and multi-method approach. Remote Sens. Environ. 164, 197–207. doi:10.1016/j.rse.2015.04.020

Li, W., Epstein, H.E., Wen, Z., Zhao, J., Jin, J., Jing, G., Cheng, J., Du, G., 2017. Community-weighted mean traits but not functional diversity determine the changes in soil properties during wetland drying on the Tibetan Plateau. Solid Earth 8, 137–147. doi:10.5194/se-8-137-2017

Li, X., Yang, Y., Ma, L., Sun, X., Yang, S., Kong, X., Hu, X., Yang, Y., 2014. Comparative proteomics analyses of Kobresia pygmaea adaptation to environment along an elevational gradient on the central Tibetan Plateau. PLoS One 9. doi:10.1371/journal.pone.0098410

Ma, W.L., Shi, P.L., Li, W.H., He, Y.T., Zhang, X.Z., Shen, Z.X., Chai, S.Y., 2010. Changes in individual plant traits and biomass allocation in alpine meadow with elevation variation on the Qinghai-Tibetan Plateau. Sci. China Life Sci. 53, 1142–1151. doi:10.1007/s11427-010-4054-9

Miehe, G., Bach, K., Miehe, S., Kluge, J., Yongping, Y., Duo, L., Co, S., Wesche, K., 2011. Alpine steppe plant communities of the Tibetan highlands. Appl. Veg. Sci. 14, 547–560. doi:10.1111/j.1654-109X.2011.01147.x

Miehe, G., Miehe, S., Bach, K., Nölling, J., Hanspach, J., Reudenbach, C., Kaiser, K., Wesche, K., Mosbrugger, V., Yang, Y.P., Ma, Y.M., 2011. Plant communities of central Tibetan pastures in the Alpine Steppe/Kobresia pygmaea ecotone. J. Arid Environ. 75, 711–723. doi:10.1016/j.jaridenv.2011.03.001

Miehe, G., Miehe, S., Bach, K., Wesche, K., Seeber, E., Behrendes, L., Kaiser, K., Reudenbach, C., Nölling, J., Hanspach, J., Herrmann, M., Yaoming, M., Mosbrugger, V., 2013. Resilience or vulnerability? Vegetation patterns of a Central Tibetan pastoral ecotone. Steppe Ecosyst. Biol. Divers. Manag. Restor. 111–151.

Miehe, G., Miehe, S., Kaiser, K., Liu, J., Zhao, X., 2008. Status and dynamics of the Kobresia pygmaea ecosystem on the Tibetan plateau. Ambio 37, 272–279. doi:10.1579/0044-7447(2008)37[272:SADOTK]2.0.CO;2

Mougin, E., Demarez, V., Diawara, M., Hiernaux, P., Soumaguel, N., Berg, A., 2014. Estimation of LAI, fAPAR and fCover of Sahel rangelands (Gourma, Mali). Agric. For. Meteorol. 198, 155–167. doi:10.1016/j.agrformet.2014.08.006

Myneni, R., Y. K., T.P., 2015. MCD15A2H MODIS/Terra+Aqua Leaf Area Index/FPAR 8?day L4 Global 500m SIN Grid V006. NASA EOSDIS L. Process. DAAC. doi:10.5067/MODIS/MCD15A2H.006

Ni, J., Herzschuh, U., 2011. Simulating Biome Distribution on the Tibetan Plateau Using a Modified Global Vegetation Model. Arctic, Antarct. Alp. Res. 43, 429–441. doi:10.1657/1938-4246-43.3.429

Niu, K., He, J. sheng, Zhang, S., Lechowicz, M.J., 2016. Tradeoffs between forage quality and soil fertility: Lessons from Himalayan rangelands. Agric. Ecosyst. Environ. 234, 31–39. doi:10.1016/j.agee.2016.04.023

Niu, K., Messier, J., He, J.-S.J.-S., Lechowicz, M.J.M.J., 2015. The effects of grazing on foliar trait diversity and niche differentiation in Tibetan alpine meadows. Ecosphere 6, 1–15. doi:10.1890/ES14-00547.1

Niu, K., Zhang, S., Zhao, B., Du, G., 2010. Linking grazing response of species abundance to functional traits in the Tibetan alpine meadow. Plant Soil 330, 215–223. doi:10.1007/s11104-009-0194-8

Pakeman, R.J., 2014. Leaf dry matter content predicts herbivore productivity, but its functional diversity is positively related to resilience in grasslands. PLoS One 9, 1–6. doi:10.1371/journal.pone.0101876

Pappas, C., Fatichi, S., Burlando, P., 2016. Modeling terrestrial carbon and water dynamics across climatic gradients: Does plant trait diversity matter? New Phytol. 209, 137–151. doi:10.1111/nph.13590

Peng, J., Liu, Z., Liu, Y., Wu, J., Han, Y., 2012. Trend analysis of vegetation dynamics in Qinghai-Tibet Plateau using Hurst Exponent. Ecol. Indic. 14, 28–39. doi:10.1016/j.ecolind.2011.08.011

Peng, Y., Gitelson, A.A., 2011. Application of chlorophyll-related vegetation indices for remote estimation of maize productivity. Agric. For. Meteorol. 151, 1267–1276. doi:10.1016/j.agrformet.2011.05.005

Pérez-Harguindeguy, N., Diaz, S., Garnier, E., Lavorel, S., Poorter, H., Jaureguiberry, P., Bret-Harte, M.S.S., Cornwell, W.K.K., Craine, J.M.M., Gurvich, D.E.E., Urcelay, C., Veneklaas, E.J.J., Reich, P.B.B., Poorter, L., Wright, I.J.J., Etc., Ray, P., Etc., Díaz, S., Lavorel, S., Poorter, H., Jaureguiberry, P., Bret-Harte, M.S.S., Cornwell, W.K.K., Craine, J.M.M., Gurvich, D.E.E., Urcelay, C., Veneklaas, E.J.J., Reich, P.B.B., Poorter, L., Wright, I.J.J., Ray, P., Enrico, L., Pausas, J.G., Vos, A.C. de, Buchmann, N., Funes, G., Quétier, F., Hodgson, J.G., Thompson, K., Morgan, H.D., Steege, H. ter, Heijden, M.G.A. van der, Sack, L., Blonder, B., Poschlod, P., Vaieretti, M. V., Conti, G., Staver, A.C., Aquino, S., Cornelissen, J.H.C., 2013. New Handbook for standardized measurment of plant functional traits worldwide. Aust. J. Bot. 61, 167–234. doi:http://dx.doi.org/10.1071/BT12225

Pettorelli, N., Wegmann, M., Skidmore, A., Mücher, S., Dawson, T.P., Fernandez, M., Lucas, R., Schaepman, M.E., Wang, T., O'Connor, B., Jongman, R.H.G., Kempeneers, P., Sonnenschein, R., Leidner, A.K., Böhm, M., He, K.S., Nagendra, H., Dubois, G., Fatoyinbo, T., Hansen, M.C., Paganini, M., de Klerk, H.M., Asner, G.P., Kerr, J.T., Estes, A.B., Schmeller, D.S., Heiden, U., Rocchini, D., Pereira, H.M., Turak, E., Fernandez, N., Lausch, A., Cho, M.A., Alcaraz-Segura, D., McGeoch, M.A., Turner, W., Mueller, A., St-Louis, V., Penner, J., Vihervaara, P., Belward, A., Reyers, B., Geller, G.N., 2016. Framing the concept of satellite remote sensing essential biodiversity variables: challenges and future directions. Remote Sens. Ecol. Conserv. 2, 122–131. doi:10.1002/rse2.15

Piao, S., Fang, J., Jinsheng, H.E., 2006. Variations in vegetation net primary production in the Qinghai-Xizang Plateau, China, from 1982 to 1999. Clim. Change 74, 253–267. doi:10.1007/s10584-005-6339-8

Pierce, S., Negreiros, D., Cerabolini, B.E.L., Kattge, J., Díaz, S., Kleyer, M., Shipley, B., Wright, S.J., Soudzilovskaia, N.A., Onipchenko, V.G., van Bodegom, P.M., Frenette-Dussault, C., Weiher, E., Pinho, B.X., Cornelissen, J.H.C., Grime, J.P., Thompson, K., Hunt, R., Wilson, P.J., Buffa, G., Nyakunga, O.C., Reich, P.B., Caccianiga, M., Mangili, F., Ceriani, R.M., Luzzaro, A., Brusa, G., Siefert, A., Barbosa, N.P.U., Chapin, F.S., Cornwell, W.K., Fang, J., Fernandes, G.W., Garnier, E., Le Stradic, S., Peñuelas, J., Melo, F.P.L., Slaviero, A., Tabarelli, M., Tampucci, D., 2017. A global method for calculating plant CSR ecological strategies applied across biomes world-wide. Funct. Ecol. 31, 444–457. doi:10.1111/1365-2435.12722

Punalekar, S., Verhoef, A., Tatarenko, I. V., Van Der Tol, C., Macdonald, D.M.J., Marchant, B., Gerard, F., White, K., Gowing, D., 2016. Characterization of a highly biodiverse floodplain meadow using hyperspectral remote sensing within a plant functional trait framework. Remote Sens. 8. doi:10.3390/rs8020112

Qi, J., Chehbouni, A., Huete, A.R., Kerr, Y.H., Sorooshian, S., 1994. A modified soil adjusted vegetation index. Remote Sens. Environ. 48, 119–126. doi:10.1016/0034-4257(94)90134-1

Ramoelo, A., Skidmore, A.K., Schlerf, M., Heitkönig, I.M.A., Mathieu, R., Cho, M.A., 2013. Savanna grass nitrogen to phosphorous ratio estimation using field spectroscopy and the potential for estimation with imaging spectroscopy. Int. J. Appl. Earth Obs. Geoinf. 23, 334–343. doi:10.1016/j.jag.2012.10.008

Roelofsen, H.D., van Bodegom, P.M., Kooistra, L., Witte, J.P.M., 2014. Predicting leaf traits of herbaceous species from their spectral characteristics. Ecol. Evol. 4, 706–719. doi:10.1002/ece3.932

Roelofsen, H.D., van Bodegom, P.M., Kooistra, L., Witte, J.P.M., 2013. Trait Estimation in Herbaceous Plant Assemblages from in situ Canopy Spectra. Remote Sens. 5, 6323–6345. doi:10.3390/rs5126323

Roy, D.P., Wulder, M.A., Loveland, T.R., C.E., W., Allen, R.G., Anderson, M.C., Helder, D., Irons, J.R., Johnson, D.M., Kennedy, R., Scambos, T.A., Schaaf, C.B., Schott, J.R., Sheng, Y., Vermote, E.F., Belward, A.S., Bindschadler, R., Cohen, W.B., Gao, F., Hipple, J.D., Hostert, P., Huntington, J., Justice, C.O., Kilic, A., Kovalskyy, V., Lee, Z.P., Lymburner, L., Masek, J.G., McCorkel, J., Shuai, Y., Trezza, R., Vogelmann, J., Wynne, R.H., Zhu, Z., 2014. Landsat-8: Science and product vision for terrestrial global change research. Remote Sens. Environ. 145, 154–172. doi:10.1016/j.rse.2014.02.001

Sakschewski, B., von Bloh, W., Boit, A., Rammig, A., Kattge, J., Poorter, L., Peñuelas, J., Thonicke, K., 2015. Leaf and stem economics spectra drive diversity of functional plant traits in a dynamic global vegetation model. Glob. Chang. Biol. 21, 2711–2725. doi:10.1111/gcb.12870

Schlemmera, M., Gitelson, A., Schepersa, J., Fergusona, R., Peng, Y., Shanahana, J., Rundquist, D., 2013. Remote estimation of nitrogen and chlorophyll contents in maize at leaf and canopy levels.

Int. J. Appl. Earth Obs. Geoinf. 25, 47–54. doi:10.1016/j.jag.2013.04.003

Schneider, F.D., Morsdorf, F., Schmid, B., Petchey, O.L., Hueni, A., Schimel, D.S., Schaepman, M.E., 2017. Mapping functional diversity from remotely sensed morphological and physiological forest traits. Nat. Commun. 8. doi:10.1038/s41467-017-01530-3

Schweiger, A.K., Schütz, M., Risch, A.C., Kneubühler, M., Haller, R., Schaepman, M.E., 2017. How to predict plant functional types using imaging spectroscopy: linking vegetation community traits, plant functional types and spectral response. Methods Ecol. Evol. 8, 86–95. doi:10.1111/2041-210X.12642

Sea, W.B., Choler, P., Beringer, J., Weinmann, R.A., Hutley, L.B., Leuning, R., 2011. Documenting improvement in leaf area index estimates from MODIS using hemispherical photos for Australian savannas. Agric. For. Meteorol. 151, 1453–1461. doi:10.1016/j.agrformet.2010.12.006

Shipley, B., De Bello, F., Cornelissen, J.H.C., Laliberté, E., Laughlin, D.C., Reich, P.B., 2016. Reinforcing loose foundation stones in trait-based plant ecology. Oecologia 180, 923–931. doi:10.1007/s00442-016-3549-x

Skidmore, A.K., Pettorelli, N., Coops, N.C., Geller, G.N., Hansen, M., Lucas, R., Mücher, C.A., O'Connor, B., Paganini, M., Pereira, H.M., Schaepman, M.E., Turner, W., Wang, T., Wegmann, M., 2015. Environmental science: Agree on biodiversity metrics to track from space. Nature 523, 403–405. doi:10.1038/523403a

Sun, J., Wang, X., Cheng, G., Wu, J., Hong, J., Niu, S., 2014. Effects of grazing regimes on plant traits and soil nutrients in an alpine steppe, northern Tibetan Plateau. PLoS One 9. doi:10.1371/journal.pone.0108821

ter Steege, H., Reich, P.B., Bret-Harte, M.S., Buchmann, N., Aquino, S., Pausas, J.G., Urcelay, C., Hodgson, J.G., Funes, G., Quétier, F., Garnier, E., Veneklaas, E.J., Cornwell, W.K., Cornelissen, J.H.C., Conti, G., Vaieretti, M. V., Jaureguiberry, P., de Vos, A.C., Sack, L., Thompson, K., Pérez-Harguindeguy, N., Blonder, B., Wright, I.J., Poorter, H., Díaz, S., Ray, P., Poschlod, P., Morgan, H.D., Craine, J.M., Gurvich, D.E., Staver, A.C., Enrico, L., Poorter, L., Lavorel, S., 2013. New handbook for standardised measurement of plant functional traits worldwide. Aust. J. Bot. 61, 167. doi:10.1071/bt12225

Tucker, C.J., 1979. Red and photographic infrared linear combinations for monitoring vegetation. Remote Sens. Environ. 8, 127–150. doi:10.1016/0034-4257(79)90013-0

Ustin, S.L., Gitelson, A.A., Jacquemoud, S., Schaepman, M., Asner, G.P., Gamon, J.A., Zarco-Tejada, P., 2009. Retrieval of foliar information about plant pigment systems from high resolution spectroscopy. Remote Sens. Environ. 113, S67–S77. doi:10.1016/j.rse.2008.10.019

Vincini, M., Amaducci, S., Frazzi, E., 2014. Empirical estimation of leaf chlorophyll density in winter wheat canopies using Sentinel-2 spectral resolution. IEEE Trans. Geosci. Remote Sens. 52, 3220–3235. doi:10.1109/TGRS.2013.2271813

Violle, C., Navas, M.L., Vile, D., Kazakou, E., Fortunel, C., Hummel, I., Garnier, E., 2007. Let the concept of trait be functional! Oikos 116, 882–892. doi:10.1111/j.2007.0030-1299.15559.x

Vohland, M., Jarmer, T., 2008. Estimating structural and biochemical parameters for grassland from spectroradiometer data by radiative transfer modelling (PROSPECT+SAIL). Int. J. Remote Sens. 29, 191–209. doi:10.1080/01431160701268947

Wu, C., Niu, Z., Gao, S., 2012. The potential of the satellite derived green chlorophyll index for estimating midday light use efficiency in maize, coniferous forest and grassland. Ecol. Indic. 14, 66–73. doi:10.1016/j.ecolind.2011.08.018

Wu, C., Niu, Z., Tang, Q., Huang, W., 2008. Estimating chlorophyll content from hyperspectral vegetation indices: Modeling and validation. Agric. For. Meteorol. 148, 1230–1241. doi:10.1016/j.agrformet.2008.03.005

Yan, K., Park, T., Yan, G., Liu, Z., Yang, B., Chen, C., Nemani, R.R., Knyazikhin, Y., Myneni, R.B., 2016. Evaluation of MODIS LAI/FPAR product collection 6. Part 2: Validation and intercomparison. Remote Sens. 8, 359. doi:10.3390/rs8060460

Yang, W., Huang, D., Tan, B., Stroeve, J.C., Shabanov, N. V., Knyazikhin, Y., Nemani, R.R., Myneni, R.B., 2006. Analysis of leaf area index and fraction of PAR absorbed by vegetation products from the terra MODIS sensor: 2000-2005. IEEE Trans. Geosci. Remote Sens. 44, 1829–1841. doi:10.1109/TGRS.2006.871214

Yao, T., Thompson, L.G., Mosbrugger, V., Zhang, F., Ma, Y., Luo, T., Xu, B., Yang, X., Joswiak, D.R., Wang, W., Joswiak, M.E., Devkota, L.P., Tayal, S., Jilani, R., Fayziev, R., 2012. Third

Pole Environment (TPE). Environ. Dev. 3, 52–64. doi:10.1016/j.envdev.2012.04.002

You, Q., Fraedrich, K., Ren, G., Pepin, N., Kang, S., 2013. Variability of temperature in the Tibetan Plateau based on homogenized surface stations and reanalysis data. Int. J. Climatol. 33, 1337–1347. doi:10.1002/joc.3512

Zarco-Tejada, P.J., Miller, J.R., Noland, T.L., Mohammed, G.H., Sampson, P.H., 2001. Scaling-up and model inversion methods with narrowband optical indices for chlorophyll content estimation in closed forest canopies with hyperspectral data. IEEE Trans. Geosci. Remote Sens. 39, 1491–1507. doi:10.1109/36.934080

Zhang, G., Zhang, Y., Dong, J., Xiao, X., 2013. Green-up dates in the Tibetan Plateau have continuously advanced from 1982 to 2011. Proc. Natl. Acad. Sci. 110, 4309–4314. doi:10.1073/pnas.1210423110

Zhou, X., Wang, Y., Zhang, P., Guo, Z., Chu, C., Du, G., 2016. The effects of fertilization on the trait-abundance relationships in a Tibetan alpine meadow community. J. Plant Ecol. 9, 144–152. doi:10.1093/jpe/rtv043

Zhu, Z., Woodcock, C.E., 2012. Object-based cloud and cloud shadow detection in Landsat imagery. Remote Sens. Environ. 118, 83–94. doi:10.1016/j.rse.2011.10.028

Zhu, Z.H., Wang, X.A., Li, Y.N., Wang, G., Guo, H., 2012. Predicting plant traits and functional types response to grazing in an alpine shrub meadow on the Qinghai-Tibet Plateau. Sci. China Earth Sci. 55, 837–851. doi:10.1007/s11430-012-4381-8

Chapter 3

Spatial variation of human influences on grassland biomass on the Qinghai-Tibetan Plateau

This chapter is based on the peer-reviewed article:
Li, C., de Jong, R., Schmid, B., Wulf, H., Schaepman, M.E., 2019. Spatial variation of human influences on grassland biomass on the Qinghai-Tibetan plateau. Sci. Total Environ. 665, 678–689

Authors' contributions (alphabetical order): BS, CL, HW, MES, RJ designed the study and developed the methodology. CL collected the data. All authors performed the analysis, verified the analytical methods and wrote the manuscript.

3.1 Abstract

An improved understanding of increased human influence on ecosystems is needed for predicting ecosystem processes and sustainable ecosystem management. We studied spatial variation of human influence on grassland ecosystems at two scales across the Qinghai-Tibetan Plateau (QTP), where increased human activities may have led to ecosystem degradation. At the 10 km scale, we mapped human-influenced spatial patterns based on a hypothesis that spatial patterns of biomass that could not be attributed to environmental variables were likely correlated to human activities. In part this hypothesis could be supported via a positive correlation between biomass unexplained by environmental variables and livestock density. At the 500 m scale, using distance to settlements within a radius of 8 km as a proxy of human-influence intensity, we found both negatively human-influenced areas where biomass decreased closer to settlements (regions with higher livestock density) and positively human-influenced areas where biomass increased closer to settlements (regions with lower livestock density). These results suggest complex relationships between livestock grazing and biomass, varying between spatial scales and regions. Grazing may boost biomass production across the whole QTP at the 10 km scale. However, overgrazing may reduce it near settlements at the 500 m scale. Our approach of mapping and understanding human influence on ecosystems at different scales could guide pasture management to protect grassland in vulnerable regions on the QTP and beyond.

3.2 Introduction

More than three-quarters of the terrestrial biosphere has been altered by human activities (Ellis and Ramankutty, 2008) which has also caused unprecedented changes in many Earth-system processes during the last decades (Chen et al., 2013; Ellis, 2015), including regional and local ecological processes (Ellis and Haff, 2009). It is necessary to understand the consequences of human influence on ecosystems to better explain spatial patterns of ecosystems and their responses to climate and other environmental changes (Ellis, 2015). Ecosystem functioning and services have been most affected in arid and semi-arid areas, where recent degradation has taken place (Chen et al., 2014; Harris, 2010; Wessels et al., 2004). The grassland ecosystems in these areas cover a large portion of the Earths' surface and contain substantial amounts of soil organic carbon. Grassland degradation and land-use changes, including conversion of grassland to cropland, result in a loss of grassland ecosystem carbon stocks (Conant et al., 2017; Guo and Gifford, 2002). This is also the case on the Qinghai-Tibetan Plateau (QTP) (Chen et al., 2013), where vast grassland ecosystems store a large amount of carbon, thus playing a significant role in global carbon cycle (Liu et al., 2016; Ni, 2002).

The grassland ecosystems on the QTP also influence the local (Xu et al., 2009) and even global climate, e.g. by triggering South Asian monsoon activity (Duan and Wu, 2005). In addition, the QTP is the source region of Asia's major rivers (Figure 3.1), which supply fresh water for a large part of the world's population downstream (Foggin, 2008; Xu et al., 2008). The stability of ecosystems on the QTP is thus not only of regional importance but also of global relevance for water supply, radiation feedbacks and global climatic patterns (Meyer et al., 2013).

The grassland ecosystems on the QTP, characterized by slow plant growth and recovery rate after disturbance (Shang and Long, 2007), are particularly vulnerable and threatened by pressures from climatic changes and human activities. Degradation of alpine grasslands has indeed been observed on the QTP, which has led to productivity declines, land desertification and an increase of noxious weeds (Fassnacht et al., 2015; Lehnert et al., 2014a). Such degradation not only damages the livelihoods of local people but also threatens biodiversity and the ecological services of the QTP at large (Harris, 2010). However, the causes of the grassland degradation on the QTP are still unclear and have been related to warming-caused desiccation and

permafrost degradation (Harris, 2010; Lehnert et al., 2016) or to increasing human activities (Harris, 2010; P. Wang et al., 2016; Zhaoli et al., 2005).

Increasing human activities may have affect grassland biomass production on the QTP, which is mostly covered by rangeland and livestock grazing as the main land-use type (Chen et al., 2013). Privatization of rangeland and semi-nomadic pastoralism have caused increasing grazing pressure (Harris, 2010; Meyer et al., 2013; Wang et al., 2017) and overgrazing of winter pastures (Harris et al., 2015, 2016; L. Li et al., 2017). Moreover, infrastructure development such as highways and townships, tourism and mining exert increasing pressure on the QTP grassland ecosystems (S. Li et al., 2017). Human activities of grassland conservation programs (L. Li et al., 2017) and nature reserve programs (S. Li et al., 2018), however, have been launched to protect ecosystems and secure biodiversity and ecosystem services. All these human activities happened at different areas and scales. For example, livestock grazing is widely spread across the whole QTP whereas the grazing pressures are higher in low areas and near human settlements. Construction works are site-based and ecosystem protection programs are widely located in the "Three-Rivers headwater regions" in the southern part of Qinghai province. These human activities indicate that human influences on grassland ecosystems are spatially heterogeneous and scale-dependent.

The various human activities and land-use intensity on the QTP, combined with clear environmental and productivity gradients (Chen et al., 2015), imply that the grasslands respond differently to diverse human activities on the QTP. For example, the different levels of grassland productivity translate into different carrying capacities for livestock (Miehe et al., 2008), indicating different levels of resistance to grazing and different grazing effects (Milchunas et al., 1988). Previous studies involved quantifying human influence on grassland dynamics (Chen et al., 2014; Lehnert et al., 2016; L. Li et al., 2018) and mapping of human-influence intensity on the QTP (S. Li et al., 2017). However, quantifying and mapping spatially heterogeneous human influence on grassland ecosystems has not been done so far, yet this would be key to understand how ecosystems respond to environmental changes and to help distinguishing climatic and anthropogenic contributions to spatial variation in grassland biomass. We aimed to map human-influenced spatial patterns of grassland biomass on the QTP at two spatial scales, i.e. at the 10 km scale across the whole QTP and at the 500 m scale near human settlements.

3.3 Data

3.3.1 Observed aboveground biomass

Grassland aboveground biomass was assessed using an empirical model based on Landsat-8 satellite data and field-measured data (C. Li et al., 2018). Grasslands with higher biomass shows stronger reflectance in near-infrared bands but lower reflectance in visible bands than grassland with lower biomass. The Normalized Difference Vegetation Index (NDVI) was developed to characterize the vegetation (Tucker, 1979) and has been extensively used to estimate aboveground grassland biomass (Jia et al., 2016; Zhang et al., 2016). The 172 biomass plots were measured in the field during peak growing season (late July to mid-August) in 2015 and 2016. The closest Landsat-8 NDVI values were extracted with respect to the individual field sampling locations and dates. The field-measured biomass data were randomly split into two parts, using three-quarters of the data for model calibration and one-quarter for validation. The developed empirical model (R^2 = 0.55, rRMSE = 0.23) was applied to the Landsat-8 NDVI in 2015 to map grassland biomass with the Google Earth Engine (Gorelick et al., 2017) across the whole QTP. The aboveground biomass map was scaled to a spatial resolution of 10 km and 500 m, which further were used to map human influences on biomass at 10 km and 500 m scale.

3.3.2 Climatic variables

The climatic variables used to model the contribution of environmental variables to spatial variation in grassland biomass included growing season (June–September) mean air temperature in 2015 and precipitation in 2015. These variables were extracted from the China Meteorological Forcing Dataset with a spatial resolution of 0.1° (Chen et al., 2011). The temperature variable was constructed by merging observations from 740 meteorological stations and corresponding Princeton meteorological forcing data (Sheffield et al., 2006). The precipitation variable was constructed by combining three precipitation data sets, including observations from the same 740 meteorological stations, the Tropical Rainfall Measuring Mission (TRMM) 3B42 precipitation products (Huffman et al., 2007) and the Asian Precipitation-Highly Resolved Observational Data Integration Towards Evaluation of the Water Resources project (APHRODITE) (Yatagai et al., 2009). This climatic dataset has been widely used in soil moisture modeling and ecosystem studies (Guo

and Wang, 2013; Liu and Xie, 2013; Wang et al., 2017).

3.3.3 Soil properties

Soil variables of soil organic matter, available nitrogen and total phosphorus were selected from eight soil variables (available phosphorus, available potassium, available nitrogen, total phosphorus, total potassium, total nitrogen, soil organic matter and soil PH) to estimate aboveground biomass. The selected soil variables have lowest co-linearity (Variance Inflation Factor <10) with other variables (section 3.2). The soil variables were extracted from a 30×30 arcsec resolution gridded soil characteristics dataset (Shangguan et al., 2013). This dataset includes physical and chemical attributes of soils derived from 8979 soil profiles and the Soil Map of China (1:1,000,000). This soil properties dataset has been widely used in soil and ecological studies (Bi et al., 2016; Maire et al., 2015; Sun et al., 2016; Wang et al., 2015).

3.3.4 Data on eco-geographical regions

The classification of the QTP into eco-geographical regions (Figure 3.1) was included as a further environmental explanatory variable for spatial variation in grassland biomass (Section 3.1). The eco-geographical regions have been defined based on a combination of climatic factors and vegetation types (Gao et al., 2009). We included the classification of eco-geographical regions as an explanatory variable because it reflects the effects of broad differences in species composition between vegetation types on biomass (Chuang et al., 2014). The eco-region data were converted from a polygon-shape file to a raster with 10 km using the statistical software R (R Core Team, 2018).

3.3.5 Indicators of human influences

Two indicators of human influence, livestock density and distance to settlements, were used to explain the potentially human-influenced spatial patterns at the 10 km and 500 m scale. The settlement locations of cities, towns, hamlets and villages in 2017 were extracted from OpenStreetMap (Haklay and Weber, 2008) as spatial points (https://download.geofabrik.de/asia/china.html). The size of settlements was considered when analyzing the correlation between biomass and distance to settlements as described below (section 3.2). The Euclidean distance to the closest of these points was calculated for each grid cell of the QTP (Figure 3.2).

Pasture is the main land-use type on the QTP. Livestock grazing is an important

human-influenced activity. Livestock density can serve as an indicator of such human influence. Livestock density was assessed in terms of the number of sheep, goats and yak per square kilometer reported in the 2015 statistical yearbook from Qinghai, Xizang (National Bureau of Statistics of China, 2015). The absolute numbers of different animal species were converted to livestock units using conversion factors of 0.6 for yak and 0.1 for sheep and goats (Lehnert et al., 2016). In the end, livestock densities of 100 counties at the county level were calculated (Figure 3.2), which decreased from the east to the west of the QTP. The livestock density is suitable to evaluate the human influence on grassland biomass via livestock grazing on the whole QTP scale as demonstrated in previous studies (Lehnert et al., 2016; S. Li et al., 2017). The livestock density data were converted from a polygon shape file to 10 km and 500 m raster in ESRI ArcMap software (http://desktop.arcgis.com/en/arcmap/).

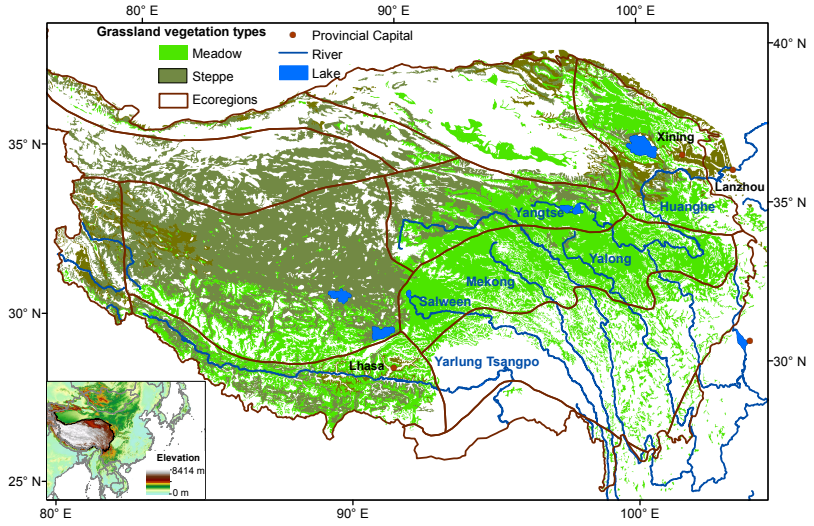

Figure 3.1. Distribution of main grassland vegetation types, eco-regions and major rivers (with names) on the Qinghai-Tibetan Plateau (QTP). Inset indicates elevation data of the extended area based on the NASA Shuttle Radar Topographic Mission (SRTM Version 4; Farr et al., 2007).

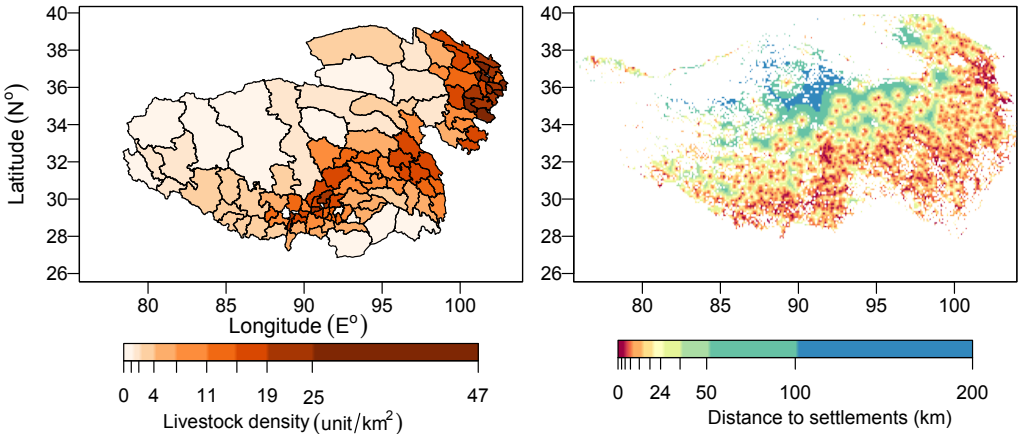

Figure 3.2. Livestock density at county level and distance to settlements at the 500 m scale.

3.4 Methods

3.4.1 Model for environmental and human-influenced spatial patterns of biomass at 10 km scale

We hypothesized that the human-influenced biomass could be calculated from the difference between potential biomass in the absence of human activities and actual biomass estimated from the satellite data. This hypothesis and framework is widely used to quantify human contribution on ecosystem biomass production both at the global scale (Haberl et al., 2014, 2007; Krausmann et al., 2013) and at the regional scale of the QTP (Chen et al., 2014; Z. Wang et al., 2016). The potential biomass is the biomass that would be predicted solely by environmental factors without the interference of human activities. Here this potential biomass was defined based on a deterministic empirical model with environmental explanatory variables (x) with regression coefficients β (fixed effects). The actual aboveground biomass, which is influenced by both environmental variables and human activities, was measured from remote sensing NDVI data (y). The difference between potential biomass and actual biomass involves a spatial process (h) that is potentially correlated with human influences (random effects) and a residual noise component ε (Eqn 1) (de Jong et al., 2013). This analysis was conducted at the 10 km scale across the whole QTP by rescaling all environmental explanatory variables to 10 km resolution using the *projectRaster* function in R with bilinear interpolation:

$$h = y - x^T \beta - \varepsilon \qquad \textit{(Eqn 1)}$$

3.4.2 Deterministic model (xTβ) attributing biomass to environmental drivers

Temperature, precipitation and soil properties are considered to be the most important variables that may explain spatial biomass variation across the whole QTP (Luo et al., 2004; Sun et al., 2013; Yang et al., 2009). In addition, elevation can account for microclimatic variation and influence grassland biomass (Fisk et al., 1998). Therefore these environmental variables were used to estimate potential biomass.

We used each environmental variable's Variance Inflation Factor (VIF) to quantify co-linearity between variables. VIFs are positive values representing the overall correlation of each predictor with all others in a model. Generally, VIF >10 indicate "severe" co-linearity (Neter et al., 1996; Smith et al., 2009). In the end, six environmental variables including temperature, precipitation, available soil nitrogen,

total soil phosphorus, soil organic matter, elevation (Table 3.1) and eco-regions (multi-level factor) were used to develop a multiple linear regression model to predict potential biomass. The VIF of selected environmental variables was 2.4 showing low co-linearity.

A bootstrapping method was applied when estimating model coefficients to avoid spatial dependency in the training data (de Jong et al., 2013). Five thousand samples were randomly selected from 13574 observations to estimate model coefficients. Three-quarter the samples were used for model calibration and one-quarter of samples were used for model validation. This sampling step was repeated five thousand times to include all data into the model. The relative Root-Mean-Square Errors (rRMSEs (%)), that is the ratio between RMSE and the mean of actual biomass, were averaged to estimate model accuracy. Finally, model coefficients were averaged to estimate environmental-driven biomass at the 10 km scale. In addition, to quantify the relative contribution of each variable to biomass, the relative importance of each environmental variables in the multiple linear regressions was investigated using hierarchical variation partitioning as implemented in the R package *relaimpo* (Grömping, 2006) (Table 3.1).

3.4.3 Spatial process (h) and residuals (ε)

We used a Gaussian random field (GRF) to model the spatial patterns of unexplained effects (de Jong et al., 2013). A GRF is described by three elements: 1) a mean function, 2) a range that determines the length scale of the spatial dependency and 3) a sill that determines the marginal variance. The estimated parameter set was used to model the spatial field *h*. The detailed description of the model can be found in de Jong et al. (2013). Based on our assumption, the modeled spatial patterns are correlated to human activities. We further tested the spatial patterns (h) for correlations with the human-influenced variable livestock density at the county level.

The residual component ε contains the remaining spatial variation of biomass that was neither captured by the environmental variables (fixed-effects components fitted in the first step) nor by the spatial process (random-effect components fitted in the second step). In the ideal case, these residuals are spatially uncorrelated (de Jong et al., 2013). This component may contain small-scale human interventions (de Jong et al., 2013; Zhou et al., 2001). To find out whether potential small-scale human interventions could be visible, we also related the residuals to the human-influence

variable livestock density (county level).

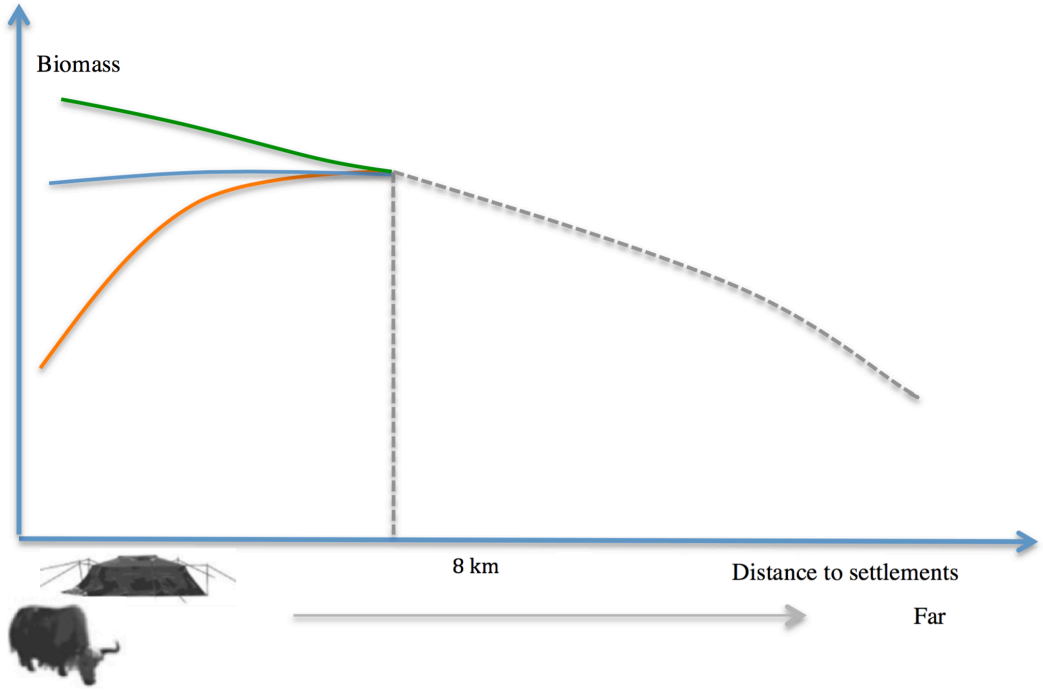

Figure 3.3. Three scenarios of relationships between distance to settlements and grassland biomass: 1 (orange) – biomass decreases near settlements potentially showing a negative human influence on biomass, 2 (blue) – no clear human influence on biomass and 3 (green) – biomass increases near settlements suggesting a positive human influence on biomass. All scenarios hold up to a certain distance (8 km) after which the relationship between biomass and distance tends to be negative (see Figure 3A.1).

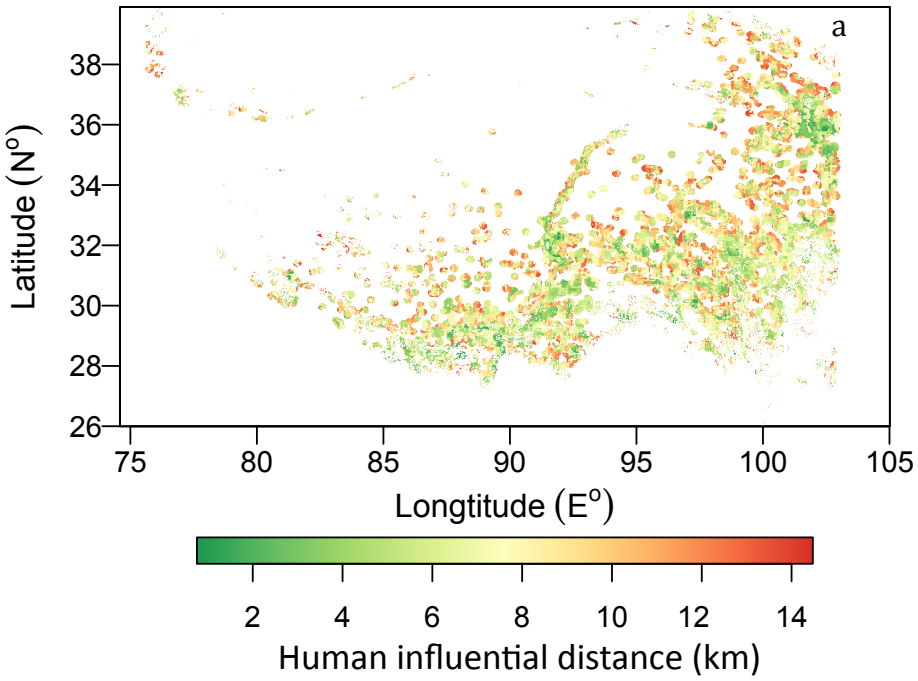

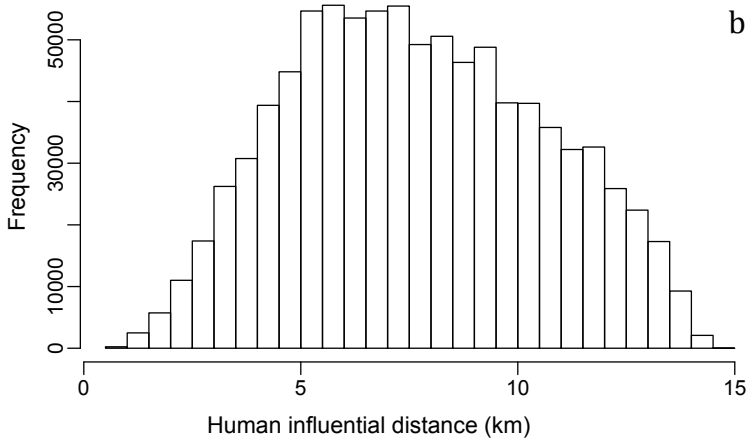

Figure 3.4. The human influential distances on the Qinghai-Tibetan Plateau (a) and their distribution (b). The distances were calculated for local areas using *breakpoints* analysis in R (see Methods). The histogram shows that the average human influential distance is about 8 km.

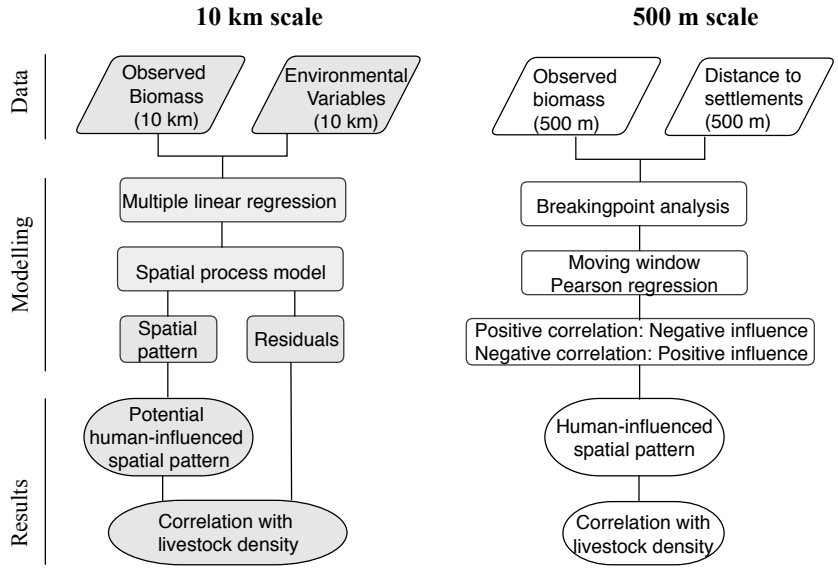

Figure 3.5. Flowchart displaying data and methods used to map the influence of human activities on biomass at 10 km and 500 m scales.

Table 3.1 Environmental variable's Variance Inflation Factor (VIF) and their relative importance for explaining biomass

Parameter	Unit	VIF	Relative importance
Elevation	m	3.95	0.32
Precipitation	mm	2.59	0.23
Available N	g/100g	2.78	0.23
Soil organic matter	g/100g	2.62	0.13
Temperature	℃	2.30	0.06
Total P	g/100g	1.57	0.03

3.4.4 Model for human-influenced variation of biomass at the 500 m scale

At the 500 m scale, we used distance to settlements as a proxy of human-influence intensity. Distances to watering points or settlements have been widely used as proxies for grazing intensity in various grassland systems with long pastoral histories (Fernandez-Gimenez and Allen-Diaz, 2001; Manthey and Peper, 2010; Wang et al., 2017). On the QTP, the grazing pressure increased over the past three decades near to the settlements because pasture management was transferred from nomadic to semi-nomadic pastoralism or privatized (Meyer et al., 2013; Wang et al., 2017). Therefore, areas closer to settlements experience more intensive human activities, including higher grazing density, construction work and tourism activities.

Human influences on biomass were analyzed within 8 km neighborhoods around settlements at a spatial resolution of 500 m based on previous findings that human influence can be neglected beyond 8 km on the QTP (Liu et al., 2006; Wang et al., 2015). This limit was determined in a breakpoint analysis (see next paragraph). Human activities of grazing, trampling and infrastructure near settlements can directly influence grassland biomass by removal or disturbance, although this may be conterbalanced by compensatory regrowth. Within the range of distances from 0–8 km, a positive correlation between biomass and distance to settlements indicates that biomass is lower near settlements, which suggests a negative human influence on biomass. In contrast, a negative correlation indicates that biomass is higher near settlements, suggesting a positive human influence on biomass. If biomass stays stable along distance to settlements this indicates that human activities do not have a profound influence on biomass. However, beyond the limit distance of 8 km to settlements, the direct human influence on grassland biomass should be small (Liu et al., 2006). Nevertheless, biomass may tend to decrease beyond the limit distance because people avoid areas where potential biomass is low due to harsh environmental conditions (Figure 3A.1). Figure 3.3 illustrates the above scenarios of changes of biomass along distance to settlements. A supplementary video shows examples of changes of biomass along distance to settlements (https://www.sciencedirect.com/science/article/pii/S0048969719303705), where a turning point can be observed showing the potential human influential distance and indicating a breakpoint in the relationship between biomass and distance to settlements. The influence of human activities on biomass at the 500 m scale was mapped based on these scenarios.

In order to find the specific human influential distance, the *breakpoints* function and *F* statistics test in the R package strucchange were applied (Zeileis et al., 2003), which have been widely used for detecting and monitoring structural changes in (linear) regression models (Zeileis et al., 2003). We configured the algorithm to detect the one most influential breakpoint for each pixel using a moving-window method. We assumed that the maximum human influential distance could be as large as 15 km, according to the 12 km of human influential distance reported from an area in the east of the QTP (Liu et al., 2006). The detected breakpoint distances were averaged across all pixels to get a single estimate for the entire QTP. This yielded the above-mentioned limit distance of 8 km to settlements beyond which direct human influence related to settlements could no longer be detected (Figure 3.4).

To detect the spatial variation of human influence on biomass at the 500 m scale, a moving-window method was applied between distance to settlements and biomass. Specifically, we used local Pearson moving-window regression to show positive and negative influences of human activities on biomass. The selected window size with a radius of 8 km for the local Pearson regression was based on the breakpoint analysis explained above. The area covered by settlements has no biomass value and was therefore excluded from the analysis, that is, the human influential distance was calculated to the boundary of a settlement, not an inside point. We finally linked the local Pearson correlation coefficients that represent the human-influenced spatial patterns at the 500 m scale with livestock density. Figure 3.5 summarizes all data and processing steps as a flowchart.

3.5 Results

3.5.1 Spatial variation in biomass attributed to environmental drivers at the 10 km scale

The biomass data derived from the Landsat-8 NDVI data showed a decreasing gradient from the east to the west of the QTP and additionally varied strongly within the gradient (Figure 3.6a). The overall spatial variation in biomass across the QTP was decomposed into three parts: 1) variation explained by environmental variables (Figure 3.6b), 2) variation due to spatial autocorrelation unexplained by environmental variables but potentially correlated with variation in human influences (Figure 3.6c and Section 4.2) and 3) residual variation neither explained by

environmental variables nor by spatial autocorrelation (Figure 3A.2).

The model developed from environmental variables including climatic variables, soil properties, topographical variables and eco-regions explained 70% (coefficients of determination $R^2 = 0.70$) of the spatial biomass variation with an accuracy of 27% as measured by the rRMSE. The biomass predicted by these environmental variables clearly showed the decreasing trend towards the west described in the previous paragraph. Among different environmental variables, elevation played the most important role in explaining biomass variation, followed by precipitation and soil available nitrogen (Table 3.1). The relatively lower importance of temperature than elevation was probably due to the higher temperature but low biomass in the Qaidam basin, which was opposite to the general trend of decreasing temperature and biomass along increasing elevation (Figure 3A.3).

The biomass predicted by environmental variables shows a sharp transition from high to low biomass along the east-to-west gradient (Figure 3.6b). This sharp transition was caused by eco-region boundaries and showed the relevance of including eco-regions in the model.

3.5.2 Spatial variation in biomass potentially due to human-influence at the 10 km scale

The random effects component accounting for spatial autocorrelation in biomass at the 10 km scale, which could not be attributed to variation in environmental variables was potentially related to variation in human influences. This spatial autocorrelation component accounts for 16% of the spatial variation of biomass. Negative spatial autocorrelations in biomass values occurred on the northern part of Qinghai-lake and in the southern part of the QTP. Positive spatial autocorrelations were mainly found in the eastern part of the QTP (Figure 3.6c). Both the positive and the negative autocorrelations were clearer in the eastern part of the QTP where human activities are more intense (Figure 3.2 and Figure 3.6c). A weak positive correlation ($R^2 = 0.1$) was found between the spatial autocorrelation in biomass and the human-influence variable livestock density (Figure 3.7). No further correlation was found between residuals and livestock density (Figure 3A.4).

3.5.3 Human-influenced spatial patterns of biomass at the 500 m scale

The influences of human activities on biomass at the 500 m scale were mapped by analyzing biomass along distance to settlements using a moving window radius of 8

km. The map (Figure 3.8) shows both biomass decreases and biomass increases near settlements, indicating positive and negative human influences. Strong negative signals were detected in the Yellow River–Huangshui River Valley and around the southeastern part of Qinghai-lake, Xinghai and Tongde counties (Figure 3.8 (1)), in the Yarlung Zangbo River valley and in the central Tibetan counties of Doilungdeeqeen, Lasa and Dagze (Figure 3.8 (3)). In all these areas biomass decreased with proximity to settlements. Positive signals were detected for example in the southeastern part of the QTP, i.e. Baima and Jigzhi counties, where the biomass increased with proximity to settlements (Figure 3.8 (2)).

Across the QTP, positive signals, i.e. higher biomass values closer to settlements, occurred in areas with low livestock density at the 10 km scale. In contrast, the negative signals were correlated with high livestock density, and prevailing negative signals were detected when the regional livestock density was higher than about 22 livestock units per square kilometer (Figure 3.9), even though these regions are also the ones with more productive ecosystems (Figure 3A.5). In general, biomass was actually larger near settlements in areas with low livestock density, whereas biomass was lower near settlements in more productive areas with higher livestock density.

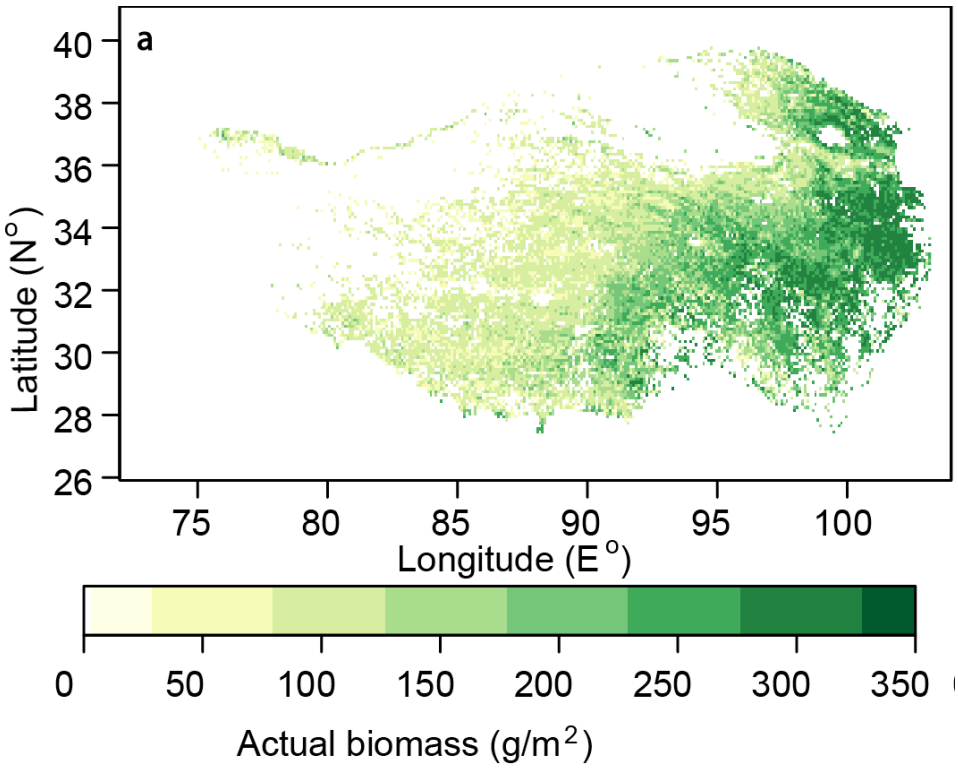

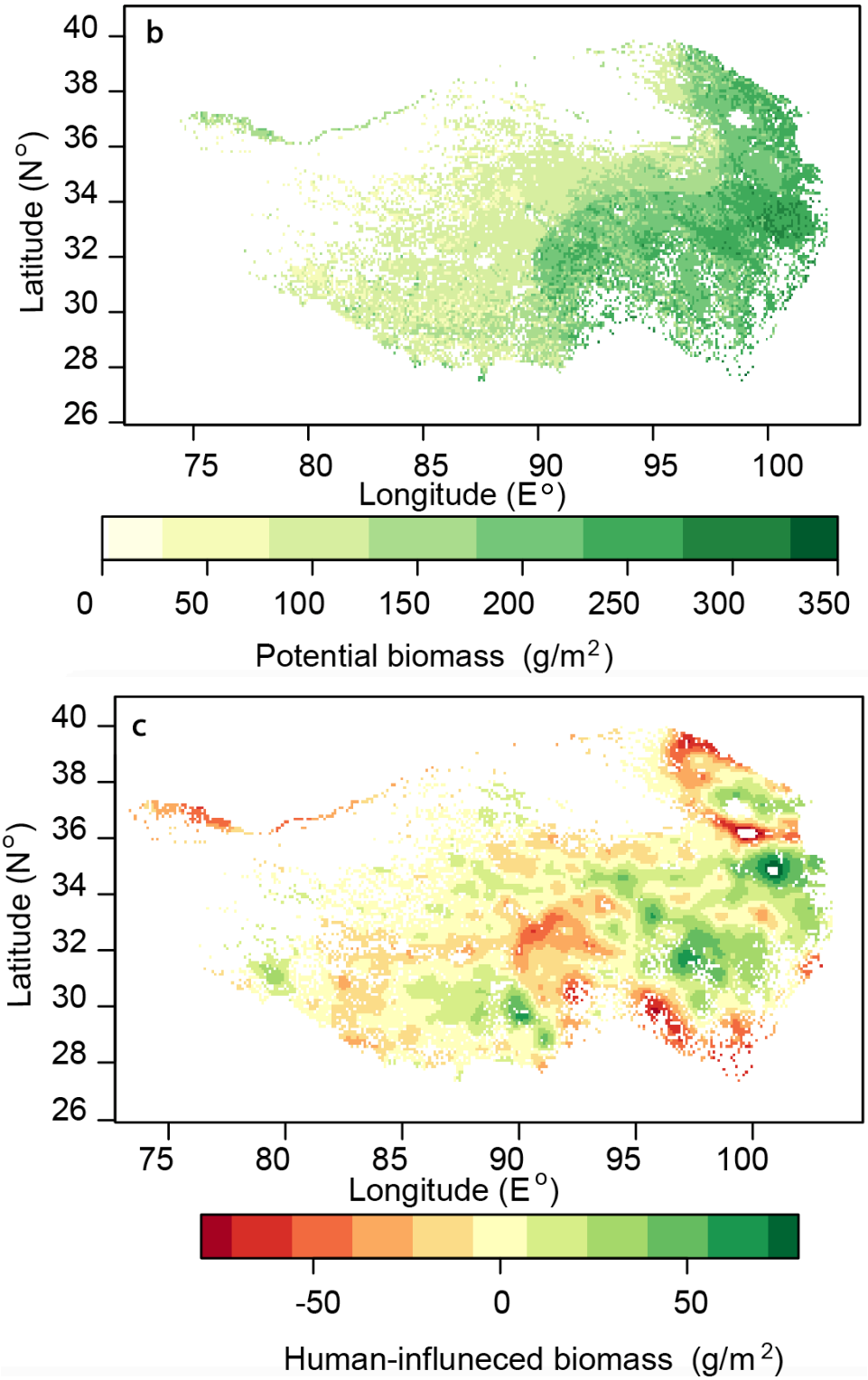

Figure 3.6. Observed biomass using Landsat-8 NDVI vegetation index (a). Biomass predicted using environmental variables (b). Spatial autocorrelation of biomass that could not be explained by environmental variables but possibly human-influence variables (c). Positive hotspots of human influences are indicated with numbers. The circle represents a positive hotspot with a positive human influence at the 500 m scale (Figure 3.7), whereas the two squares represent positive hotspots with a negative human influence at the 500 m scale.

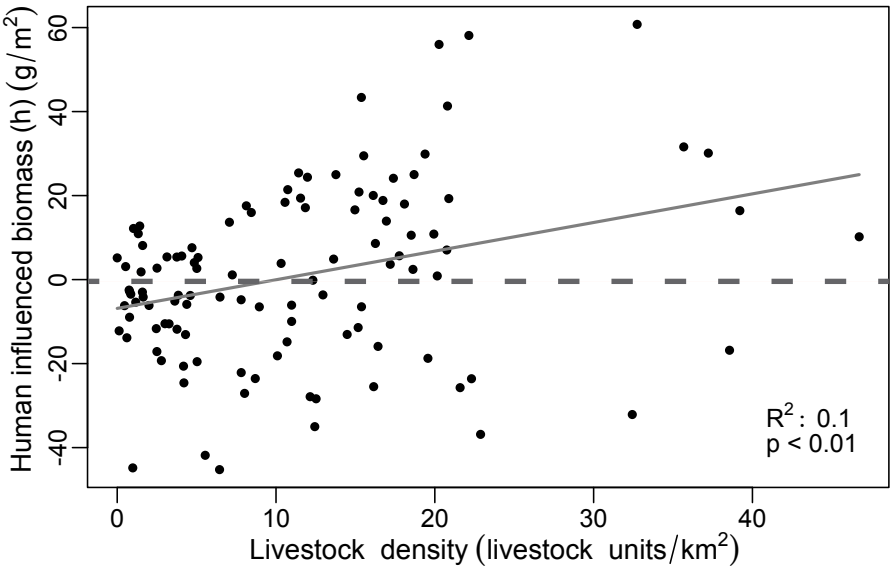

Figure 3.7. Scatterplot between human-influenced spatial pattern of grassland biomass (y) and livestock density (x).

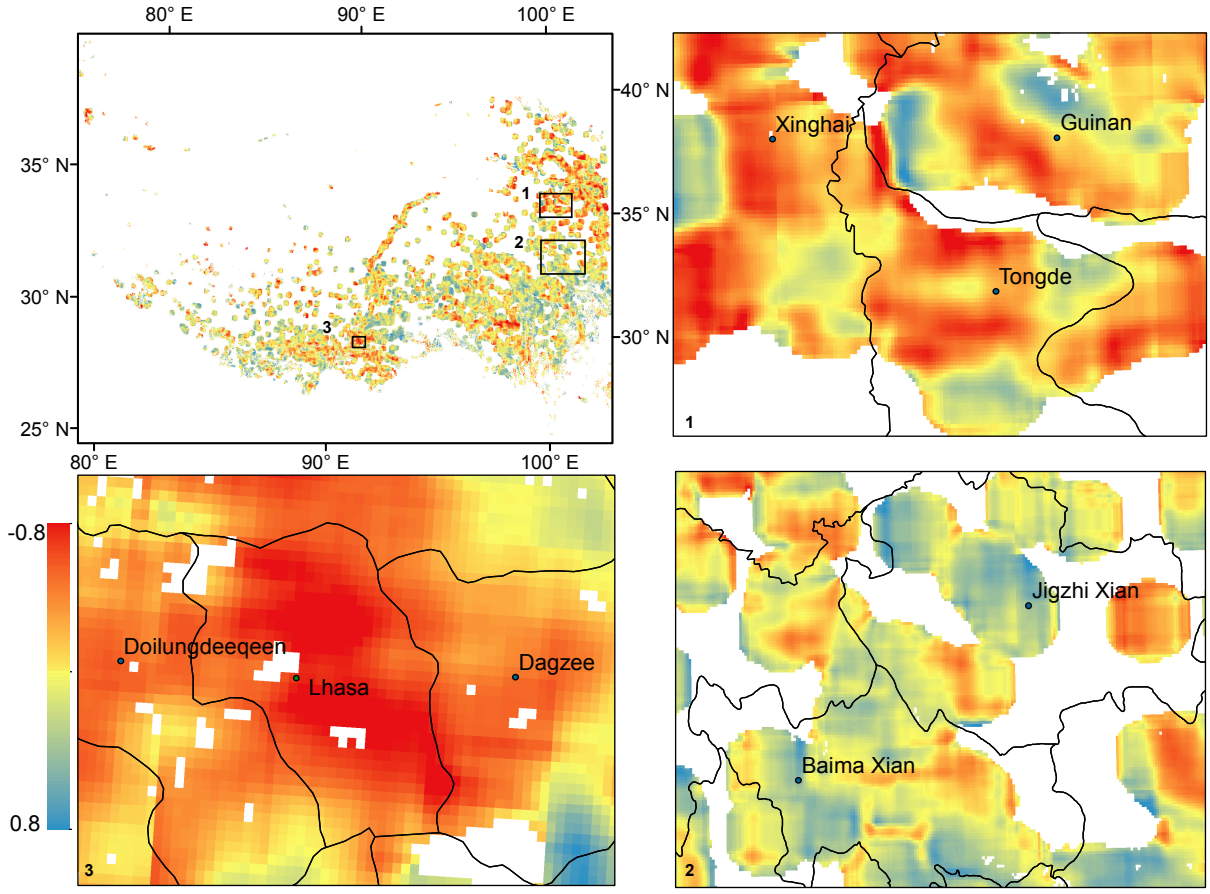

Figure 3.8. Correlation coefficients between biomass and distance to settlements (within 8 km) at grid cells of 500 m × 500 m (top left panel). A positive correlation shows biomass decreases near settlements and indicates negative human influences and vise versa. Some hotspots of negative and positive human influences area are shown in panels (1), (2), (4).

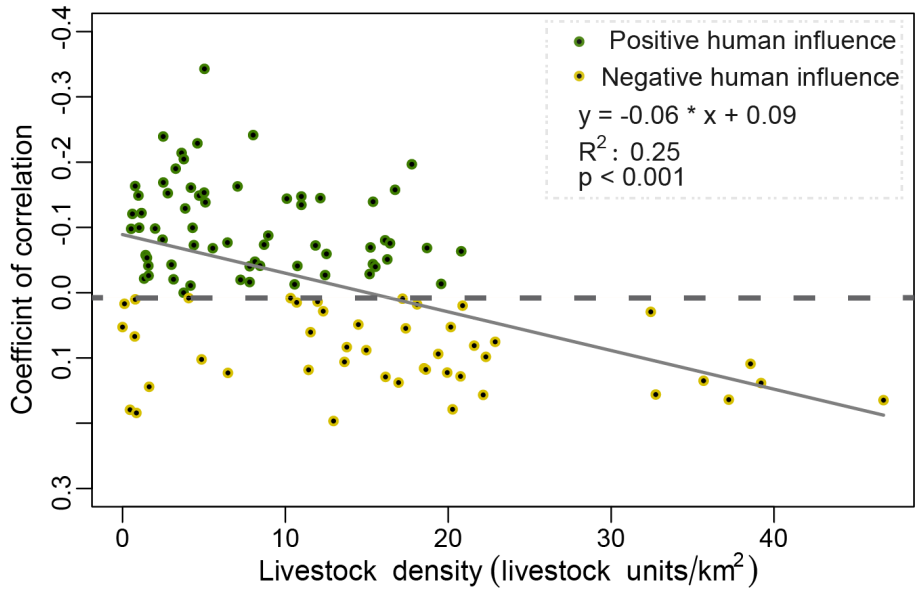

Figure 3.9. Scatterplot between human-influenced spatial biomass pattern at the 500 m scale (y) and livestock density at the 10 km scale (x). Note that a negative correlation between local biomass and distance to settlements, i.e. higher biomass close to settlements reflects a positive human influence (green dots), and vise versa. The human-influenced spatial biomass pattern was averaged per county and then regressed on the livestock density per county. The dashed line indicates the division between positive and negative human influences on local biomass.

3.6 Discussion

3.6.1 Spatial variation in biomass attributed to environmental drivers at the 10 km scale

The model developed from environmental variables explained most of the spatial variation of biomass (70%). Uncertainties of the model might stem from the limited number of environmental variables used and uncertainties within the environmental variable data, which might affect the potential biomass estimation accuracy. The influence of environmental variables such as soil moisture, soil temperature (X. Wang et al., 2016) and solar radiation (Piao et al., 2006) on biomass has become more important to affect biomass on the QTP under climate change, which should be considered in the future studies. Nevertheless, the environmental variables estimated the potential biomass without the inference of human activities. The difference between the potential biomass and actual biomass are here assumed to be linked with human-influenced variables (Haberl et al., 2007; Pan et al., 2017).

3.6.2 Human-influenced spatial patterns of biomass at the 10 km scale across the whole QTP

A continuing increase in intensity and diversity of human activities exerts spatially heterogeneous influences on grasslands on the QTP. The spatial patterns of human influence on grassland are unknown on the QTP, which are important to understand how different human activities are impacting the ecosystems and how ecosystems respond to environmental change. We mapped spatial patterns at two spatial scales and studied whether the patterns can be explained by livestock grazing density.

At the 10 km scale, we found that livestock density was positively correlated with the human-influenced spatial patterns of grassland biomass, which indicated that at large scale grazing and biomass have a positive relationship. The QTP has served as pastoral land for thousands of years (Klein et al., 2007; Lu et al., 2017). Grassland ecosystems can become adapted to grazing (Miehe et al., 2009) and major plant species are grazing-resilient (Miehe et al., 2013, 2011). Moderate grazing intensity can promote nutrient recycling and ecosystem production (Lu et al., 2017; Luo et al., 2012). Consistent with these finding, we observed that the potential biomass predicted using only environmental variables was lower than the biomass estimated from the satellite data especially in the eastern part of the QTP, where livestock grazing is the common land use. Appropriate grazing management can affect species composition and facilitate mineral uptake and hydrological processes (Schrama et al., 2013). These effects potentially boost the biomass production, especially in ecosystems that are more productive and more resilient to grazing (Milchunas and Lauenroth, 1993; Wang and Wesche, 2016), which seems to be the case in the eastern and the southeastern part of the QTP (Figure 3.6c). In summary, positive grazing effects might explain the positive correlation between livestock density and human-influenced spatial patterns in grassland biomass. The opposite causality, i.e. that livestock density is higher where biomass — unexplained by environmental variables — is higher, seems less plausible unless these higher biomass values were caused by unmeasured environmental variables.

Except for livestock grazing effects, other human activities including ongoing ecosystem restoration projects and infrastructure development might explain potential human-influenced spatial pattern in grassland biomass (Fig. 6 (b)). This is especially the case in the eastern and central areas of the QTP where human activities of land-use changes and grazing density are more widespread and more intense (S. Li et al.,

2017), whereas in the northwestern part of the QTP human activities are less widespread and less intense (Figure 3.2).

3.6.3 Human-influenced spatial patterns of biomass at the 500 m scale

The mobility of pastoralists has decreased and they have become more sedentary across the Africa, the Asia, the Middle East and the Americas (Sayre et al., 2017), which leads to increased grazing intensity near settlements (Batjargal, 1997; Vanselow et al., 2012). Distance to settlements could potentially serve as a proxy of human-influence intensity in pastoral ecosystems (Fernandez-Gimenez and Allen-Diaz, 2001; Manthey and Peper, 2010), including the QTP (Wang et al., 2017). Thus, recent studies report that livestock-grazing pressure has been increased around settlements on the QTP (Dorji et al., 2013; Hafner et al., 2012; Lehnert et al., 2014b). Here we analyzed how distance to settlements served as a proxy of human-influence intensity correlated with grassland biomass across the entire QTP.

Increased biomass closer to settlements might suggest positive grazing effects, including effects of increased input of nutrients with cattle manure (Lehnert et al., 2014a). On the other hand, implemented ecosystem restoration projects may also contribute to increased biomass near settlements in some areas, for example in the area of south Sanjiangyuan Jigzhi and Baima County, where positive biomass signals close to settlements were observed (Figure 3.8 (4) and previous studies of Cai et al., 2015; Xu et al., 2011). However, negative biomass signals close to human settlements were observed in the Xinghai and Tongde County in spite of ecosystem restoration projects in these areas (Figure 3.8 (1)).

Typically, reduced biomass near settlements is taken as an indication of negative human influences due to overgrazing (Hafner et al., 2012). Overgrazing can lead to the reduction of vegetative cover and soil erosion (Papanastasis, 2009; Thornes, 2007), which might be the case in the two regions of the Yarlung Zangbo River valley and the Yellow River-Huangshui River Valley, where we observed negative biomass signals close to human settlements (Figure 3.8). These regions are characterized by high human population density, livestock-grazing intensity, land use and infrastructure pressure (S. Li et al., 2017). Overgrazing could be one of the main reasons for negative biomass signals near settlements, which is supported by the fact that these negative signals occurred mainly in areas with high livestock density (Figure 3.9).

The influence of grazing on ecosystem degradation on the QTP is still a topic of debate. Some studies found that heavy grazing causes severe rangeland degradation or even desertification (Song et al., 2009; Wang et al., 2012), whereas other studies found that grazing improved forage quality and extended the growing season (Chen et al., 2013; Harris, 2010; Klein et al., 2007). In this study, we argue that both situations occur on the QTP, depending on the study area and the study scale. Across the whole QTP, grazing is positively related to biomass production at the 10 km scale. However, because of the limited mobility of local herders (Wang et al., 2017), overgrazing occurs near settlements in areas with high livestock density. The overgrazed area might be more vulnerable and more sensitive to climate change, which requires further attention in future ecosystem protection projects.

However, the changes of biomass with distance to settlements may also be influenced by other, unmeasured human-influence variables than only by grazing intensity and it may furthermore interact with other environmental variables such as soil properties (Papanastasis, 2009). Therefore, the observed spatial patterns need further understanding and validation by combining detailed human activity-indicators with environmental variables. In addition**,** our study is a single snapshot in time, assessing the human-influenced spatial patterns in grassland biomass in 2015. Future studies should also assess changes over time in these human-influenced spatial patterns.

3.7 Conclusions

Increased human-influenced activities including livestock grazing and township development exert spatially complex influences on grassland biomass on the QTP. Our study on spatial variation of human influences on grassland biomass on the QTP helps us to understand how these ecosystems may respond to environmental change. At the 10 km scale across the whole QTP, we estimated spatial variation of human-influenced biomass by measuring the difference between the potential aboveground biomass without the interference of human actives and actual biomass estimated from the remote sensing data. We found both positive and negative human-influenced spatial patterns across the whole QTP. These patterns positively linked to the livestock density at the county level. At the 500 m scale, we analyzed the human influence on grassland biomass as a function of distance to settlements, used as a proxy of human-influence intensity. This was done because the socioeconomic changes of privatization of pastureland and of sedentarization of nomadic herders was

assumed to have increased livestock grazing and other pressures near settlements. We detected hotspots where the biomass decreased or increased towards settlements within a radius of 8 km, indicating both negative and positive human influences on biomass. In particular, we found that biomass decreased near settlements in areas with high livestock density at county level. Overall, our study showed both positive and negative human influences on grassland biomass at two spatial scales, demonstrating the complexity of the relationship between human-influence intensity and grassland biomass, leading to large spatial variation in the relationship across the entire QTP. As a broad generalization we conclude that livestock grazing so far had positive effects on grassland biomass across the whole QTP but overgrazing near settlements now represents a threat to the future biomass production and stability of these ecosystems.

3.8 Appendix

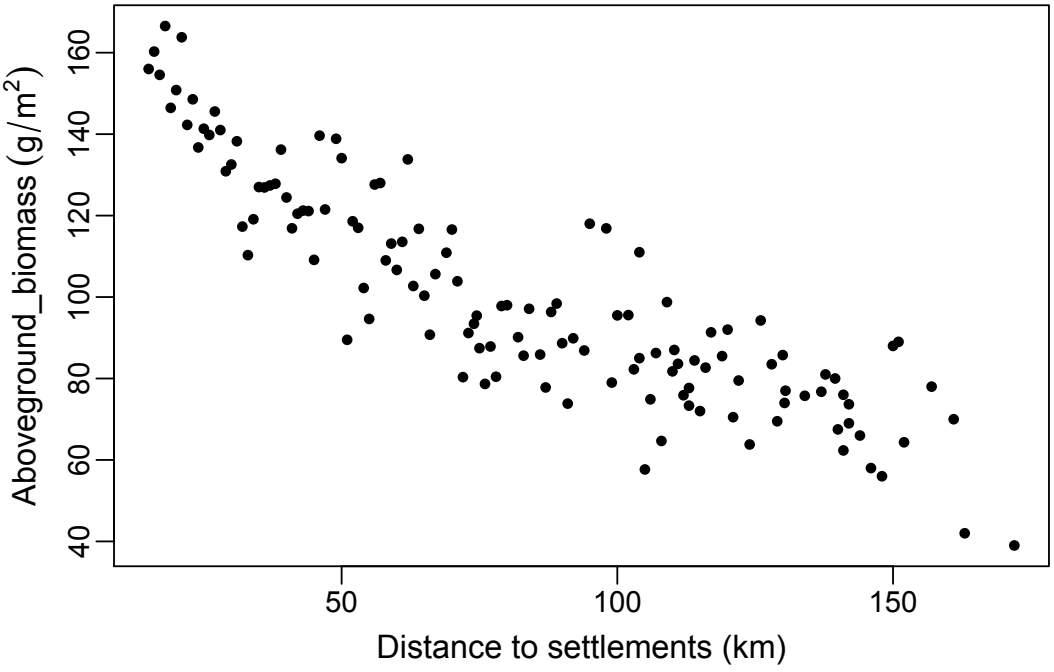

Figure 3A.1 Scatterplot between biomass and distance to settlements on the QTP, the biomass value was averaged within per kilometer.

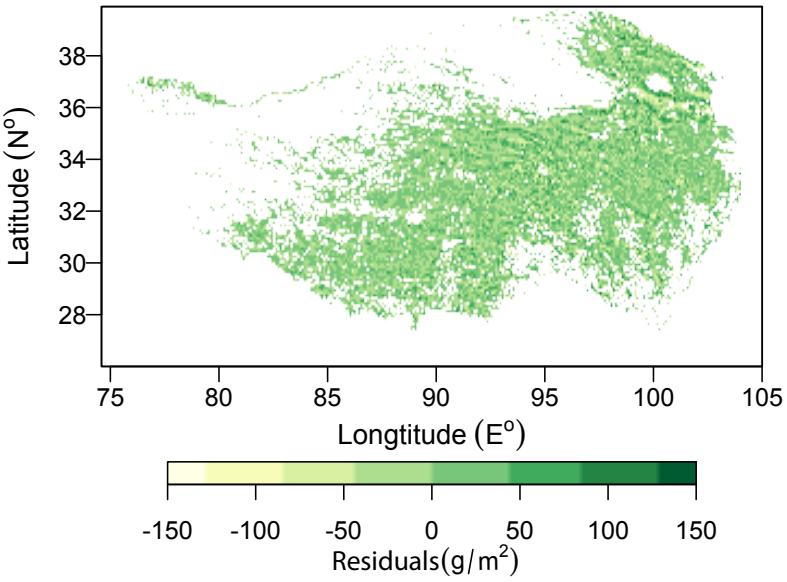

Figure 3A.2 Residuals component that is spatially uncorrelated

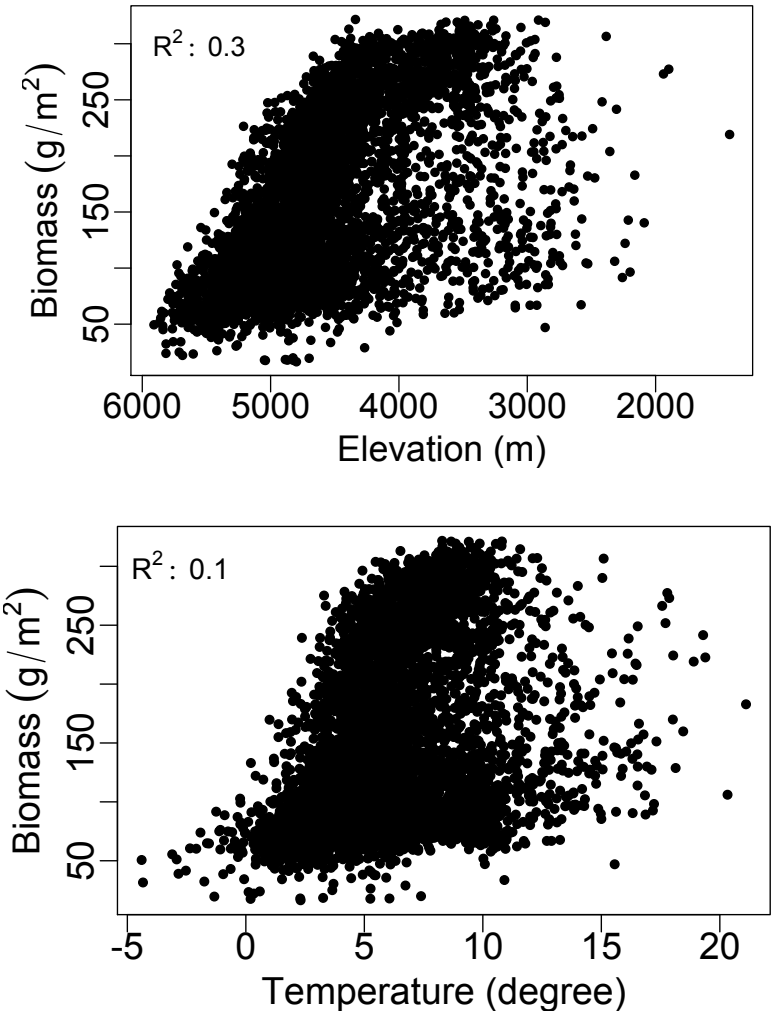

Figure 3A.3 scatterplot between biomass and elevation (up) and temperature (down). The graph shows that the elevation could better explain biomass variation. The low correlation between temperature and biomass was probably due to the higher temperature but low biomass in the Qaidam basin.

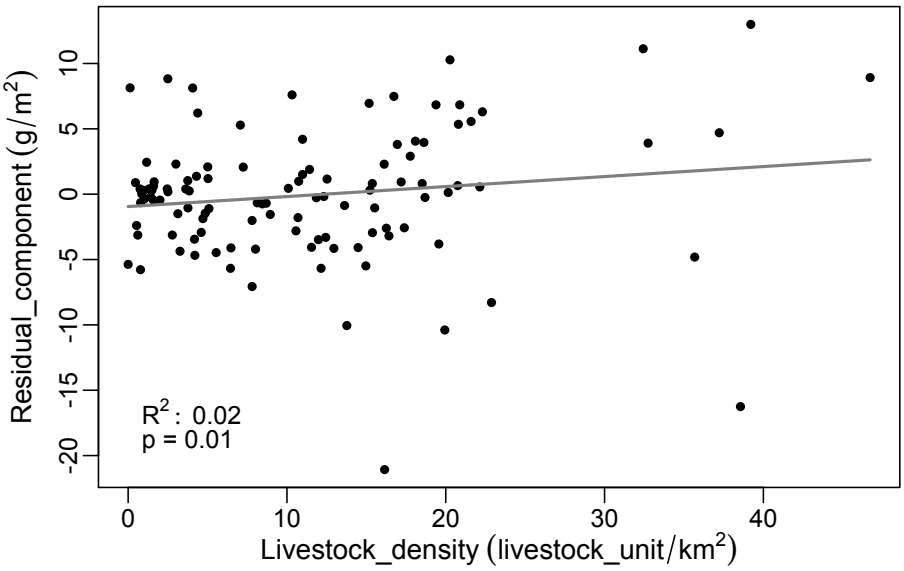

Figure 3A.4 Scatterplot between residual components (y) and livestock density (x)

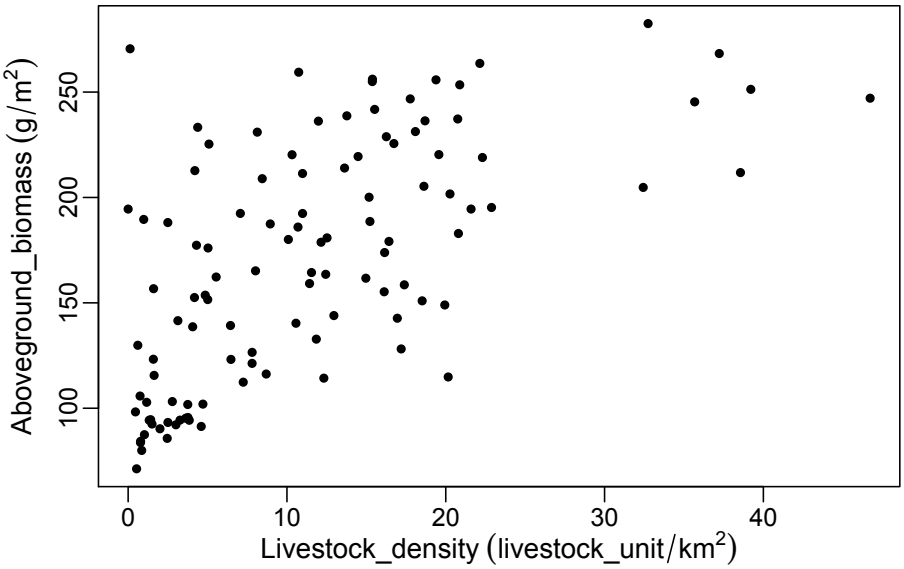

Figure 3A.5 Scatterplot between biomass and livestock density at the country level across the QTP. The livestock density is higher where biomass is higher.

3.9 Acknowledgements

The forcing climatic dataset used in this study was developed by Data Assimilation and Modeling Center for Tibetan Multi-spheres, Institute of Tibetan Plateau Research, Chinese Academy of Sciences. We acknowledge the OpenStreetMap for providing settlements spatial data. Chengxiu Li was funded by the Chinese Scholarship Council (CSC). This study was conducted in the framework of the University of Zurich Research Program on Global Change and Biodiversity (URPP GCB).

3.10 Reference

Batjargal, Z., 1997. Desertification in Mongolia. RALA Rep. No. 200 7.

Cai, H., Yang, X., Xu, X., 2015. Human-induced grassland degradation/restoration in the central Tibetan Plateau: The effects of ecological protection and restoration projects. Ecol. Eng. 83, 112–119. doi:10.1016/j.ecoleng.2015.06.031

Chen, B., Zhang, X., Tao, J., Wu, J., Wang, J., Shi, P., Zhang, Y., Yu, C., 2014. The impact of climate change and anthropogenic activities on alpine grassland over the Qinghai-Tibet Plateau. Agric. For. Meteorol. 189–190, 11–18. doi:10.1016/j.agrformet.2014.01.002

Chen, H., Zhu, Q., Peng, C., Wu, N., Wang, Y., Fang, X., Gao, Y., Zhu, D., Yang, G., Tian, J., Kang, X., Piao, S., Ouyang, H., Xiang, W., Luo, Z., Jiang, H., Song, X., Zhang, Y., Yu, G., Zhao, X., Gong, P., Yao, T., Wu, J., 2013. The impacts of climate change and human activities on biogeochemical cycles on the Qinghai-Tibetan Plateau. Glob. Chang. Biol. 19, 2940–2955. doi:10.1111/gcb.12277

Chen, X., An, S., Inouye, D.W., Schwartz, M.D., 2015. Temperature and snowfall trigger alpine vegetation green-up on the world's roof. Glob. Chang. Biol. 21, 3635–3646. doi:10.1111/gcb.12954

Chen, Y., Yang, K., He, J., Qin, J., Shi, J., Du, J., He, Q., 2011. Improving land surface temperature modeling for dry land of China. J. Geophys. Res. Atmos. 116, 1–15. doi:10.1029/2011JD015921

Chuang, L., Ruixiang, S., Wenbo, C., 2014. Eco-regional boundary data of the Roof of the World. Acta Geogr. Sin. 69, 140–143. doi:10.3974/Global

Conant, R.T., Cerri, C.E.P., Osborne, B.B., Paustian, K., 2017. Grassland management impacts on soil carbon stocks: a new synthesis. Ecol. Appl. 27, 662–668. doi:10.1002/eap.1473

de Jong, R., Schaepman, M.E., Furrer, R., de Bruin, S., Verburg, P.H., 2013. Spatial relationship between climatologies and changes in global vegetation activity. Glob. Chang. Biol. 19, 1953–1964. doi:10.1111/gcb.12193

Dorji, T., Totland, Ø., Moe, S.R., 2013. Are droppings, distance from pastoralist camps, and pika burrows good proxies for local grazing pressure? Rangel. Ecol. Manag. 66, 26–33. doi:10.2111/REM-D-12-00014.1

Duan, A.M., Wu, G.X., 2005. Role of the Tibetan Plateau thermal forcing in the summer climate patterns over subtropical Asia. Clim. Dyn. 24, 793–807. doi:10.1007/s00382-004-0488-8

Ellis, E.C., 2015. Ecology in an anthropogenic biosphere. Ecol. Monogr. 85, 287–331. doi:10.1890/14-2274.1

Ellis, E.C., Haff, P.K., 2009. Earth science in the anthropocene: New Epoch, new Paradigm, new responsibilities. Eos (Washington. DC). 90, 473. doi:10.1029/2009EO490006

Ellis, E.C., Ramankutty, N., 2008. Putting people in the map: Anthropogenic biomes of the world. Front. Ecol. Environ. 6, 439–447. doi:10.1890/070062

Farr, T., Rosen, P., Caro, E., Crippen, R., Duren, R., Hensley, S., Kobrick, M., Paller, M., Rodriguez, E., Roth, L., Seal, D., Shaffer, S., Shimada, J., Umland, J., Werner, M., Oskin, M., Burbank, D., Alsdorf, D., 2007. The shuttle radar topography mission. Rev. Geophys. 45, 1–33. doi:10.1029/2005RG000183.1.INTRODUCTION

Fassnacht, F.E., Li, L., Fritz, A., 2015. Mapping degraded grassland on the Eastern Tibetan Plateau with multi-temporal Landsat 8 data - where do the severely degraded areas occur? Int. J. Appl. Earth Obs. Geoinf. 42, 115–127. doi:10.1016/j.jag.2015.06.005

Fernandez-Gimenez, M., Allen-Diaz, B., 2001. Vegetation change along gradients from water sources in three grazed Mongolian ecosystems. Plant Ecol. 157, 101–118. doi:10.1023/A:1014519206041

Fisk, M.C., Schmidt, S.K., Seastedt, T.R., 1998. Topographic patterns of above- and belowground poduction and nitrogen cycling in alpine tundra. Ecology 79, 2253–2266. doi:10.1890/0012-9658(1998)079[2253:TPOAAB]2.0.CO;2

Foggin, J.M., 2008. Depopulating the Tibetan Grasslands. Mt. Res. Dev. 28, 26–31. doi:10.1659/mrd.0972

Gao, J., Li, S., Zhao, Z., 2009. Validating the demarcation of eco-geographical regions: A geostatistical application. Environ. Earth Sci. 59, 1327–1336. doi:10.1007/s12665-009-0120-7

Gorelick, N., Hancher, M., Dixon, M., Ilyushchenko, S., Thau, D., Moore, R., 2017. Google Earth Engine: Planetary-scale geospatial analysis for everyone. Remote Sens. Environ. doi:10.1016/j.rse.2017.06.031

Grömping, U., 2006. Relative importance for linear regression in R: the package relaimpo. J. Stat. Softw. 17, 139–147. doi:10.1016/j.foreco.2006.08.245

Guo, D., Wang, H., 2013. Simulation of permafrost and seasonally frozen ground conditions on the Tibetan Plateau, 1981-2010. J. Geophys. Res. Atmos. 118, 5216–5230. doi:10.1002/jgrd.50457

Guo, L.B., Gifford, R.M., 2002. Soil carbon stocks and land use change: A meta analysis. Glob. Chang. Biol. 8, 345–360. doi:10.1046/j.1354-1013.2002.00486.x

Haberl, H., Erb, K.-H., Krausmann, F., 2014. Human Appropriation of Net Primary Production: Patterns, Trends, and Planetary Boundaries. Annu. Rev. Environ. Resour. 39, 363–391. doi:10.1146/annurev-environ-121912-094620

Haberl, H., Erb, K.H., Krausmann, F., Gaube, V., Bondeau, A., Plutzar, C., Gingrich, S., Lucht, W., Fischer-Kowalski, M., 2007. Quantifying and mapping the human appropriation of net primary production in earth's terrestrial ecosystems. Proc. Natl. Acad. Sci. 104, 12942–12947. doi:10.1073/pnas.0704243104

Hafner, S., Unteregelsbacher, S., Seeber, E., Lena, B., 2012. Effect of grazing on carbon stocks and assimilate partitioning in a Tibetan montane pasture revealed by 13 CO 2 pulse labeling 528–538. doi:10.1111/j.1365-2486.2011.02557.x

Haklay, M., Weber, P., 2008. OpenStreet map: User-generated street maps. IEEE Pervasive Comput. 7, 12–18. doi:10.1109/MPRV.2008.80

Harris, R.B., 2010. Rangeland degradation on the Qinghai-Tibetan plateau: A review of the evidence of its magnitude and causes. J. Arid Environ. 74, 1–12. doi:10.1016/j.jaridenv.2009.06.014

Harris, R.B., Samberg, L.H., Yeh, E.T., Smith, A.T., Wenying, W., Junbang, W., Gaerrang, Bedunah, T.L.D.J., 2016. Rangeland responses to pastoralists' grazing management on a Tibetan steppe grassland, Qinghai Province, China. Rangel. J. 38, 1–15. doi:10.1071/RJ15040

Harris, R.B., Wenying, W., Badinqiuying, Smith, A.T., Bedunah, D.J., 2015. Herbivory and competition of Tibetan steppe vegetation in winter pasture: Effects of livestock exclosure and plateau pika reduction. PLoS One 10. doi:10.1371/journal.pone.0132897

Huffman, G.J., Bolvin, D.T., Nelkin, E.J., Wolff, D.B., Adler, R.F., Gu, G., Hong, Y., Bowman, K.P., Stocker, E.F., 2007. The TRMM Multisatellite Precipitation Analysis (TMPA): Quasi-Global, Multiyear, Combined-Sensor Precipitation Estimates at Fine Scales. J. Hydrometeorol. 8, 38–55. doi:10.1175/JHM560.1

Jia, W., Liu, M., Yang, Y., He, H., Zhu, X., Yang, F., Yin, C., Xiang, W., 2016. Estimation and uncertainty analyses of grassland biomass in Northern China: Comparison of multiple remote sensing data sources and modeling approaches. Ecol. Indic. 60, 1031–1040. doi:10.1016/j.ecolind.2015.09.001

Klein, J.A., Harte, J., Zhao, X.Q., 2007. Experimental warming, not grazing, decreases rangeland quality on the Tibetan Plateau. Ecol. Appl. 17, 541–557. doi:10.1890/05-0685

Krausmann, F., Erb, K.-H., Gingrich, S., Haberl, H., Bondeau, A., Gaube, V., Lauk, C., Plutzar, C., Searchinger, T.D., 2013. Global human appropriation of net primary production doubled in the 20th century. Proc. Natl. Acad. Sci. 110, 10324–10329. doi:10.1073/pnas.1211349110

Lehnert, L.W., Meyer, H., Meyer, N., Reudenbach, C., Bendix, J., 2014a. A hyperspectral indicator system for rangeland degradation on the Tibetan Plateau: A case study towards spaceborne monitoring. Ecol. Indic. 39, 54–64. doi:10.1016/j.ecolind.2013.12.005

Lehnert, L.W., Meyer, H., Meyer, N., Reudenbach, C., Bendix, J., 2014b. A hyperspectral indicator system for rangeland degradation on the Tibetan Plateau: A case study towards spaceborne monitoring. Ecol. Indic. 39, 54–64. doi:10.1016/j.ecolind.2013.12.005

Lehnert, L.W., Wesche, K., Trachte, K., Reudenbach, C., Bendix, J., 2016. Climate variability rather than overstocking causes recent large scale cover changes of Tibetan pastures. Sci. Rep. 6, 24367. doi:10.1038/srep24367

Li, C., Wulf, H., Schmid, B., He, J., Schaepman, M.E., Member, S., 2018. Estimating Plant Traits of Alpine Grasslands on the Qinghai-Tibetan Plateau Using Remote Sensing 1–13.

Li, L., Fassnacht, F.E., Storch, I., B??rgi, M., 2017. Land-use regime shift triggered the recent degradation of alpine pastures in Nyanpo Yutse of the eastern Qinghai-Tibetan Plateau. Landsc. Ecol. 1–17. doi:10.1007/s10980-017-0510-2

Li, L., Zhang, Y., Liu, L., Wu, J., Li, S., Zhang, H., Zhang, B., Ding, M., Wang, Z., Paudel, B., 2018. Current challenges in distinguishing climatic and anthropogenic contributions to alpine grassland variation on the Tibetan Plateau. Ecol. Evol. 8, 5949–5963. doi:10.1002/ece3.4099

Li, S., Wu, J., Gong, J., Li, S., 2018. Human footprint in Tibet: Assessing the spatial layout and

effectiveness of nature reserves. Sci. Total Environ. 621, 18–29. doi:10.1016/j.scitotenv.2017.11.216

Li, S., Zhang, Y., Wang, Z., Li, L., 2017. Mapping human influence intensity in the Tibetan Plateau for conservation of ecological service functions. Ecosyst. Serv. doi:10.1016/j.ecoser.2017.10.003

Liu, J.G., Xie, Z.H., 2013. Improving simulation of soil moisture in China using a multiple meteorological forcing ensemble approach. Hydrol. Earth Syst. Sci. 17, 3355–3369. doi:10.5194/hess-17-3355-2013

Liu, L., Zhang, Y., Bai, W., Yan, J., Ding, M., Shen, Z., Li, S., Zheng, D., 2006. Characteristics of grassland degradation and driving forces in the source region of the Yellow River from 1985 to 2000. J. Geogr. Sci. 16, 131–142. doi:10.1007/s11442-006-0201-4

Liu, S., Zhang, F., Du, Y., Guo, X., Lin, L., Li, Y., Li, Q., Cao, G., 2016. Ecosystem carbon storage in alpine grassland on the Qinghai Plateau. PLoS One 11, e0160420. doi:10.1371/journal.pone.0160420

Lu, X., Kelsey, K.C., Yan, Y., Sun, J., Wang, X., Cheng, G., Neff, J.C., 2017. Effects of grazing on ecosystem structure and function of alpine grasslands in Qinghai-Tibetan Plateau: A synthesis. Ecosphere 8. doi:10.1002/ecs2.1656

Luo, G., Han, Q., Zhou, D., Li, L., Chen, X., Li, Y., Hu, Y., Li, B.L., 2012. Moderate grazing can promote aboveground primary production of grassland under water stress 11, 126–136. doi:10.1016/j.ecocom.2012.04.004

Luo, T., Pan, Y., Ouyang, H., Shi, P., Luo, J., Yu, Z., Lu, Q., 2004. Leaf area index and net primary productivity along subtropical to alpine gradients in the Tibetan Plateau. Glob. Ecol. Biogeogr. 13, 345–358. doi:10.1111/j.1466-822X.2004.00094.x

Manthey, M., Peper, J., 2010. Estimation of grazing intensity along grazing gradients - the bias of nonlinearity. J. Arid Environ. 74, 1351–1354. doi:10.1016/j.jaridenv.2010.05.007

Meyer, H., Lehnert, L.W., Wang, Y., Reudenbach, C., Bendix, J., 2013. Measuring pasture degradation on the Qinghai-Tibet Plateau using hyperspectral dissimilarities and indices. Proc. SPIE 8893, 88931F–88931F–13. doi:10.1117/12.2028762

Miehe, G., Miehe, S., Bach, K., Nölling, J., Hanspach, J., Reudenbach, C., Kaiser, K., Wesche, K., Mosbrugger, V., Yang, Y.P., Ma, Y.M., 2011. Plant communities of central Tibetan pastures in the Alpine Steppe/Kobresia pygmaea ecotone. J. Arid Environ. 75, 711–723. doi:10.1016/j.jaridenv.2011.03.001

Miehe, G., Miehe, S., Bach, K., Wesche, K., Seeber, E., Behrendes, L., Kaiser, K., Reudenbach, C., Nölling, J., Hanspach, J., Herrmann, M., Yaoming, M., Mosbrugger, V., 2013. Resilience or vulnerability? Vegetation patterns of a Central Tibetan pastoral ecotone. Steppe Ecosyst. Biol. Divers. Manag. Restor. 111–151.

Miehe, G., Miehe, S., Kaiser, K., Liu, J., Zhao, X., 2008. Status and dynamics of the Kobresia pygmaea ecosystem on the Tibetan plateau. Ambio 37, 272–279. doi:10.1579/0044-7447(2008)37[272:SADOTK]2.0.CO;2

Miehe, G., Miehe, S., Kaiser, K., Reudenbach, C., Behrendes, L., La Duo, Schlütz, F., 2009. How old is pastoralism in Tibet? An ecological approach to the making of a Tibetan landscape. Palaeogeogr. Palaeoclimatol. Palaeoecol. 276, 130–147. doi:10.1016/j.palaeo.2009.03.005

Milchunas, D.G., Lauenroth, W.K., 1993. Quantitative effects of grazing on vegetation and soils over a global range of environmnents. Ecol. Monogr. 63, 327–366. doi:10.2307/2937150

Milchunas, D.G., Sala, O.E., Lauenroth, W.K., 1988. A Generalized Model of the Effects of Grazing by Large Herbivores on Grassland Community Structure. Am. Nat. 132, 87–106.

National Bureau of Statistics of China, 2015. China STATISTICAL YEARBOOK 2015. China Statistical Press, Beijing.

Neter, J., Kutner, M.H., Nachtsheim, C.J., Wasseman, W., 1996. Applied Linear Statistical Models, 4th ed. McGraw-Hill.

Ni, J., 2002. Carbon storage in grasslands of China. J. Arid Environ. 50, 205–218. doi:10.1006/jare.2001.0902

Pan, T., Zou, X., Liu, Y., Wu, S., He, G., 2017. Contributions of climatic and non-climatic drivers to grassland variations on the Tibetan Plateau. Ecol. Eng. 108, 307–317. doi:10.1016/j.ecoleng.2017.07.039

Papanastasis, V.P., 2009. Restoration of degraded grazing lands through grazing management: Can it work? Restor. Ecol. 17, 441–445. doi:10.1111/j.1526-100X.2009.00567.x

Piao, S., Fang, J., Jinsheng, H.E., 2006. Variations in vegetation net primary production in the Qinghai-

Xizang Plateau, China, from 1982 to 1999. Clim. Change 74, 253–267. doi:10.1007/s10584-005-6339-8

R Core Team, 2018. R: A language and environment for statistical computing. R Found. Stat. Comput. Vienna, Austria.

Sayre, N.F., Davis, D.K., Bestelmeyer, B., Williamson, J.C., 2017. Rangelands: Where Anthromes Meet Their Limits. Land 6, 31. doi:10.3390/land6020031

Schrama, M., Veen, G.F.C., Bakker, E.S.L., Ruifrok, J.L., Bakker, J.P., Olff, H., 2013. An integrated perspective to explain nitrogen mineralization in grazed ecosystems. Perspect. Plant Ecol. Evol. Syst. 15, 32–44. doi:10.1016/j.ppees.2012.12.001

Shang, Z., Long, R., 2007. Formation causes and recovery of the "black Soil Type" degraded alpine grassland in Qinghai-Tibetan Plateau. Front. Agric. China 1, 197–202. doi:10.1007/s11703-007-0034-7

Shangguan, W., Dai, Y., Liu, B., Zhu, A., Duan, Q., Wu, L., Ji, D., Ye, A., Yuan, H., Zhang, Q., Chen, D., Chen, M., Chu, J., Dou, Y., Guo, J., Li, H., Li, J., Liang, L., Liang, X., Liu, H., Liu, S., Miao, C., Zhang, Y., 2013. A China data set of soil properties for land surface modeling. J. Adv. Model. Earth Syst. 5, 212–224. doi:10.1002/jame.20026

Smith, A.C., Koper, N., Francis, C.M., Fahrig, L., 2009. Confronting collinearity: Comparing methods for disentangling the effects of habitat loss and fragmentation. Landsc. Ecol. 24, 1271–1285. doi:10.1007/s10980-009-9383-3

Song, X., Yang, G., Yan, C., Duan, H., Liu, G., Zhu, Y., 2009. Driving forces behind land use and cover change in the Qinghai-Tibetan Plateau: A case study of the source region of the Yellow River, Qinghai Province, China. Environ. Earth Sci. 59, 793–801. doi:10.1007/s12665-009-0075-8

Sun, J., Cheng, G.W., Li, W.P., 2013. Meta-analysis of relationships between environmental factors and aboveground biomass in the alpine grassland on the Tibetan Plateau. Biogeosciences 10, 1707–1715. doi:10.5194/bg-10-1707-2013

Thornes, J.B., 2007. Modelling soil erosion by grazing: Recent developments and new approaches. Geogr. Res. 45, 13–26. doi:10.1111/j.1745-5871.2007.00426.x

Tucker, C.J., 1979. Red and photographic infrared linear combinations for monitoring vegetation. Remote Sens. Environ. 8, 127–150. doi:10.1016/0034-4257(79)90013-0

Vanselow, K.A., Kraudzun, T., Samimi, C., 2012. Grazing Practices and Pasture Tenure in the Eastern Pamirs. Mt. Res. Dev. 32, 324–336. doi:10.1659/MRD-JOURNAL-D-12-00001.1

Wang, P., Lassoie, J.P., Morreale, S.J., Dong, S., 2015. A critical review of socioeconomic and natural factors in ecological degradation on the Qinghai-Tibetan Plateau, China. Rangel. J. 37, 1–9. doi:10.1071/RJ14094

Wang, P., Wolf, S.A., Lassoie, J.P., Poe, G.L., Morreale, S.J., Su, X., Dong, S., 2016. Promise and reality of market-based environmental policy in China: Empirical analyses of the ecological restoration program on the Qinghai-Tibetan Plateau. Glob. Environ. Chang. 39, 35–44. doi:10.1016/j.gloenvcha.2016.04.004

Wang, S., Duan, J., Xu, G., Wang, Y., Zhang, Z., Rui, Y., Luo, C., Xu, B., Zhu, X., Chang, X., Cui, X., Niu, H., Zhao, X., Wang, W., 2012. Effects of warming and grazing on soil N availability, species composition, and ANPP in an alpine meadow. Ecology 93, 2365–2376. doi:10.1890/11-1408.1

Wang, X., Yi, S., Wu, Q., Yang, K., Ding, Y., 2016. The role of permafrost and soil water in distribution of alpine grassland and its NDVI dynamics on the Qinghai-Tibetan Plateau. Glob. Planet. Change 147, 40–53. doi:10.1016/j.gloplacha.2016.10.014

Wang, Y., Heberling, G., Görzen, E., Miehe, G., Seeber, E., Wesche, K., 2017. Combined effects of livestock grazing and abiotic environment on vegetation and soils of grasslands across Tibet. Appl. Veg. Sci. 20, 327–339. doi:10.1111/avsc.12312

Wang, Y., Wesche, K., 2016. Vegetation and soil responses to livestock grazing in Central Asian grasslands: a review of Chinese literature. Biodivers. Conserv. 25, 2401–2420. doi:10.1007/s10531-015-1034-1

Wang, Z., Zhang, Y., Yang, Y., Zhou, W., Gang, C., Zhang, Y., Li, J., An, R., Wang, K., Odeh, I., Qi, J., 2016. Quantitative assess the driving forces on the grassland degradation in the Qinghai-Tibet Plateau, in China. Ecol. Inform. 33, 32–44. doi:10.1016/j.ecoinf.2016.03.006

Wessels, K.J., Prince, S.D., Frost, P.E., Van Zyl, D., 2004. Assessing the effects of human-induced land degradation in the former homelands of northern South Africa with a 1 km AVHRR NDVI

time-series. Remote Sens. Environ. 91, 47–67. doi:10.1016/j.rse.2004.02.005

Xu, J., Grumbine, R.E., Shrestha, A., Eriksson, M., Yang, X., Wang, Y., Wilkes, A., 2009. The melting Himalayas: Cascading effects of climate change on water, biodiversity, and livelihoods. Conserv. Biol. 23, 520–530. doi:10.1111/j.1523-1739.2009.01237.x

Xu, W., Gu, S., Zhao, X., Xiao, J., Tang, Y., Fang, J., Zhang, J., Jiang, S., 2011. High positive correlation between soil temperature and NDVI from 1982 to 2006 in alpine meadow of the Three-River Source Region on the Qinghai-Tibetan Plateau. Int. J. Appl. Earth Obs. Geoinf. 13, 528–535. doi:10.1016/j.jag.2011.02.001

Xu, X., Lu, C., Shi, X., Gao, S., 2008. World water tower: An atmospheric perspective. Geophys. Res. Lett. 35, 1–5. doi:10.1029/2008GL035867

Yang, Y.H., Fang, J.Y., Pan, Y.D., Ji, C.J., 2009. Aboveground biomass in Tibetan grasslands. J. Arid Environ. 73, 91–95. doi:10.1016/j.jaridenv.2008.09.027

Yatagai, A., Arakawa, O., Kamiguchi, K., Kawamoto, H., 2009. A 44-Year Daily Gridded Precipitation Dataset for Asia. Sola 5, 3–6. doi:10.2151/sola.2009

Zeileis, A., Kleiber, C., Walter, K., Hornik, K., 2003. Testing and dating of structural changes in practice. Comput. Stat. Data Anal. 44, 109–123. doi:10.1016/S0167-9473(03)00030-6

Zhang, B., Zhang, L., Xie, D., Yin, X., Liu, C., Liu, G., 2016. Application of synthetic NDVI time series blended from landsat and MODIS data for grassland biomass estimation. Remote Sens. 8, 10. doi:10.3390/rs8010010

Zhaoli, Y., Ning, W., Dorji, Y., Jia, R., 2005. A REVIEW OF RANGELAND PRIVATISATION AND ITS IMPLICATIONS IN THE TIBETAN PLATEAU, CHINA. Nomad. People. 9, 31–51.

Zhou, L., Tucker, C.J., Kaufmann, R.K., Slayback, D., Shabanov, N. V., Myneni, R.B., 2001. Variations in northern vegetation activity inferred from satellite data of vegetation index during 1981 to 1999. J. Geophys. Res. Atmos. 106, 20069–20083. doi:10.1029/2000JD000115

Chapter 4

Changes in grassland cover and spatial heterogeneFiguredegradation on the Qinghai-Tibetan Plateau

This chapter is in review with:
Li, C., de Jong, R., Schmid, B., Wulf, H., & Schaepman, M.E. (2019). Changes in grassland cover and spatial heterogeneity indicate degradation on the Qinghai-Tibetan Plateau. Ecological Indicators, in review
Paper reprinted as submitted and in review.

Authors' contributions (alphabetical order): BS, CL, HW, MES, RJ designed the study and developed the methodology. CL collected the data. All authors performed the analysis and wrote the manuscript and provided critical feedback and helped shape the research, analysis and manuscript.

4.1 Abstract

Arid grassland ecosystems undergo degradation because of increasing environmental and human pressures. Degraded grasslands show vegetation cover reduction and soil-patch development, leading to grassland fragmentation and changes in spatial heterogeneity. In this study, we hypothesized that vegetation cover, its spatial heterogeneity and changes thereof over time can identify grassland development and degradation stages. To test the hypothesis, we studied these attributes from 2000–2016 and related them to previously described degradation categories in the eastern Qinghai-Tibetan Plateau (QTP) in 2004.

We found that lower vegetation cover does not always indicate a more severe degradation; instead, higher spatial heterogeneity is a better correlate of degradation. Combined temporal changes in grassland cover and its spatial heterogeneity are related to literature-defined degradation categories. We found that grassland areas in the eastern QTP have moved into new degradation stages from 2000–2016 using changes in grassland cover and its spatial heterogeneity as indicators. The normalized difference vegetation index (NDVI) as a proxy for grassland cover declined over time in the literature-defined degraded areas but increased in the desert areas from 2000–2016. Spatial heterogeneity generally increased across different degradation categories from 2000–2016; however, this increase was less pronounced in severely degraded and slightly deserted areas. Our newly defined degradation categories in 2016 included degradation, desertification, and improving categories. Across our study area 63% were classified as degraded and 2% at risk of desertification; 35% classified as improving and re-growing occurred in higher-elevation or previously severely degraded grassland. Our study demonstrates that a combination of changes in grassland cover and in its spatial heterogeneity can be used to map grassland degradation stages and as an early-warning signal to indicate desertification threats.

4.2 Introduction

Human activities and climate change are causing ecosystem degradation, especially in arid ecosystems where degradation has affected the livelihood of a large part of the world's population (Berdugo et al., 2017; Kéfi et al., 2007). Arid-ecosystem degradation is commonly characterized by vegetation fragmentation interspersed with small bare-soil patches at the early stage of degradation and eventually large bare soil-patch development that potentially leads to desertification with increasing environmental and human pressure (Bestelmeyer et al., 2013; Kéfi et al., 2007). Vegetation fragmentation and bare soil-patch development result in changes in vegetation cover and spatial heterogeneity, which have been used as indicators of arid-ecosystem degradation (Kéfi et al., 2014, 2007; Lin et al., 2010; Maestre and Escudero, 2009; Rietkerk et al., 2004), and may even serve as early-warning signals of desertification in drylands (Berdugo et al., 2017; Lin et al., 2010; Maestre and Escudero, 2009; Rietkerk et al., 2004).

Grassland ecosystems of the Qinghai-Tibetan Plateau (QTP) have been degraded, as reflected by the increasing number and size of "black soil patches" and increase in non-edible and poisonous plants (Cai et al., 2015; Chen et al., 2017; Liu et al., 2008; Wang et al., 2015). This ecosystem degradation resulted in soil erosion, rangeland productivity reduction (Dong et al., 2013), and hydrological disturbances (Harris, 2010). Severe degradation occurred in the "Three-River Headwaters" region (X. Li et al., 2018), the source region of Asia's major rivers Yangtze, Yellow River and Mekong in the eastern part of the QTP (Figure 4.1). Degraded ecosystems have caused soil erosion and reduced water quality in this region that are threatening the livelihoods of a large part of the world's population, especially people living in downstream areas depending on freshwater coming from the QTP (Lehnert et al., 2014; Liang et al., 2013).

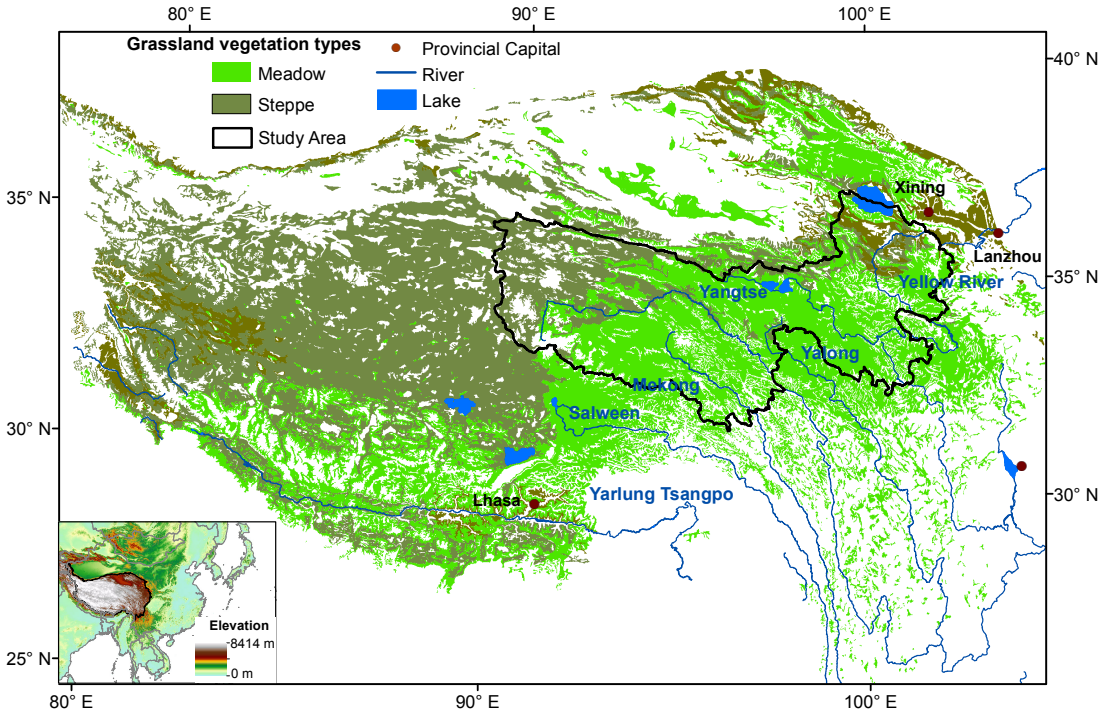

Figure 4.1. Map of the Qinghai-Tibetan Plateau indicating main grassland vegetation types and major rivers and lakes. Our study area of the "Three-River Headwaters" region on the eastern part of QTP is indicated by the black outline. Inset indicates elevation data of the extended area based on the NASA Shuttle Radar Topographic Mission (SRTMVersion 4) (Farr et al., 2007).

For the above reasons, monitoring grassland degradation stages on the QTP is important for sustainable ecosystem management. Previous researchers have studied soil organic matter, species composition, plant production, number of small-mammals, and plant cover to identify different levels of moderate, severe and extreme degradation in the field (Guo and Wang, 2013; Wang et al., 2010; Feng et al., 2005; Wang et al., 2010). However, these field studies were focused on small areas and therefore providing limited insights in grassland degradation stages on a larger scale. Such a large-scale assessment, however, can be achieved using satellite data. Vegetation cover and changes therein have been considered as indicators of degradation levels by interpreting satellite images from different years (Fassnacht et al., 2015; X. L. Li et al., 2014; Liu et al., 2008). Both, positive (Zhang et al., 2014; Zhong et al., 2010) and negative trends have been reported in past decades (Song et al., 2009; Wang et al., 2011). However, these studies were limited in both spatial and temporal scale, and the importance of changes in grassland spatial heterogeneity has not been considered for many remote-sensing applications. In this study, we

hypothesized that vegetation cover; its spatial heterogeneity and changes thereof over time can identify grassland development and degradation stages. To test the hypothesis, we studied these attributes from 2000–2016 and related them to previously described degradation-level categories in the "Three-River Headwaters" region (Liu et al., 2008). We further used the changes in vegetation cover and spatial heterogeneity to derive new degradation categories for 2016.

4.3 Data

Grassland cover and its spatial heterogeneity can be derived from the satellite data of the Normalized Difference Vegetation Index (NDVI) for large spatial extents. We used the Moderate Resolution Imaging Spectroradiometer (MODIS) bidirectional reflectance distribution function (BRDF) Adjusted Reflectance (MCD43A4) product (Schaaf et al., 2002). This product has removed view angle effects and minimized cloud and aerosol contaminations (Xulu et al., 2018). The MCD43A4 NDVI product is available every 8 days and has a spatial resolution of 500 m.

Road network data from OpenStreetMap (Haklay and Weber, 2008) and river network data extracted from hydrological data (HydroSHEDS: Hydrological data and maps based on SHuttle Elevation Derivatives at multiple Scales) (Lehner et al., 2008) were used to mask higher spatial heterogeneity value caused by roads and rivers. Elevation data were obtained from the National Aeronautics and Space Administration (NASA) Shuttle Radar Topographic Mission (SRTM) Version 4 (Farr et al., 2007).

A grassland degradation-categories dataset (Figure 4A.1) covering the study area for 2004 (Liu et al., 2008) was used as a reference to classify changes in NDVI and spatial heterogeneity into new degradation categories for 2016. Grassland cover and vegetation-patch size were used for the 2004 grassland-degradation classification along with field photos, topography maps, land-use maps, and vegetation-type maps (Liu et al., 2008). The authors classified grasslands into (1) areas without degradation, (2) areas with grassland fragmentation, (3) desertification/salinization, (4) cover decline, (5) drying swamp, and (6) areas with improving grasslands. Each degradation category had been subdivided into the three intensity levels slight, medium, and severe. In this study, we focus on the first three categories (no degradation, grassland fragmentation, and desertification/salinization) that are characteristic for soil-patch development and together account for 90% of the study area. We refer to these three categories as (1) non-degraded, (2) degraded and (3) desertified.

4.4 Methods

4.4.1 Grassland spatial heterogeneity

Fragmentation of grassland with bare-soil patches causes spatially discontinuous grassland cover and therefore possibly increased spatial heterogeneity. Grassland cover and its spatial heterogeneity can be measured from satellite data for large spatial extents. The NDVI spectral index was introduced to map vegetation cover (Kennedy, 1989; F. Li et al., 2014; Purevdorj et al., 1998; Tucker, 1979). NDVI is a well-developed and easily available product from MODIS and widely used for monitoring grassland cover on the QTP (Gao et al., 2010; Zhang et al., 2013). The coefficient of variation (CV) of NDVI within a 3 x 3-pixel moving-window of 1500 x 1500 m was calculated to represent spatial heterogeneity of vegetation cover, which is a leading indicator of ecosystem heterogeneity (Carpenter and Brock, 2006) and spatial variance (Kéfi et al., 2014).

In this study, we assessed grassland heterogeneity in terms of the spatial distribution of vegetation and bare-soil patches. On the QTP such patches can be observed from a fine spatial scale of 0.5 m up to larger scales of 1.5 km (Figure 4.2) depending on topography, soil properties and vegetation types (Chen et al., 2017). Considering the patch size and grid size of satellite images, measuring spatial heterogeneity at 1.5 km scale is reasonable for detecting grassland heterogeneity for our purpose of large-scale degradation mapping. The corresponding 3 x 3-pixel moving window provides nine NDVI samples with a grid size of 500 m, which is statistically sufficient to calculate the coefficient of variation. Furthermore, a 3 x 3-pixel window size allows to capture the locality of the spatial heterogeneity as the output of spatial heterogeneity becomes spatially smoother with increasing window size. High spatial heterogeneity around rivers and roads may not indicate degradation as commonly understood but represent more heterogeneous land-cover types. We identified these using buffers of river and road networks and excluded them when calculating the CV of NDVI. In the end, all land-cover types other than grasslands were masked out.

4.4.2 Temporal changes in NDVI and spatial heterogeneity

The median NDVI and its CV within 3 x 3-pixel moving windows during the growing season (June–September) were calculated for each year from 2000–2016. We applied linear regression to analyze their change trends over this period, which is the most common method to study long-term changes in vegetation greenness and cover (de

Jong et al., 2011; Piao et al., 2005). To analyze and visualize differences of NDVI and spatial heterogeneity among degradation categories identified by the literature, we calculated their means and plotted their distributions. Both significant values of changes in NDVI and in its spatial heterogeneity were extracted for the above analysis (Figure 4A.2).

4.4.3 Combining temporal changes in NDVI and spatial heterogeneity to map new degradation categories for 2016

Our study is based on the hypothesis that the combination of changes in NDVI and in its spatial heterogeneity can be used to identify grassland development and degradation stages. This hypothesis is based on the fact that soil patches have developed in the degraded grassland in the study area. The soil patches can be observed both in the field and from satellites (Figure 4.2 (a-c)). The development of soil patches results in increased spatial heterogeneity from intact to degraded grassland (Figure 4A.3) but decreased spatial heterogeneity in severely degraded grassland or in the stage of desertification (Figure 4A.3). The grassland cover does not always decline with degradation level in the case of invasive species. The invasive species increase vegetation cover but indicate degradation because the species are unpalatable for livestock or even toxic (Figure 4.2 (d)). Therefore, the changes in vegetation cover and spatial heterogeneity are not linearly correlated with degradation level but the combination of the two variables can indicate different degradation stages. In the following we introduce our hypothesis in detail.

4.4.3.1 Increases in NDVI and decreases in spatial heterogeneity combined represent improving conditions

The increase of NDVI and decrease of spatial heterogeneity indicate that grasslands become more productive and homogeneous, indicating improving conditions (Figure 4A.3 (a)).

4.4.3.2 Increases in NDVI and spatial heterogeneity combined represent re-growing conditions or slight degradation

Combined increases in NDVI and spatial heterogeneity may indicate two different cases. In desert or non-vegetated regions where average NDVI is normally lower than 0.2 (Piao et al., 2011; Zhang et al., 2013) increases in NDVI and in its spatial heterogeneity reflect regrowth of vegetation. In vegetated areas (NDVI > 0.2)

increases in spatial heterogeneity typically are related to the development of bare-soil patches (X. L. Li et al., 2014). Increases in NDVI can be correlated with the colonization of vegetation patches by invasive species that are characteristic of higher plant cover compared with native species *Kobresia pygmaea* (Milton and Siegfried, 1994; Wang et al., 2015) (Figure 4.2 (d)). The invasive species are not favored by domestic livestock and therefore result in a reduction of grassland forage quality. Therefore, increases in NDVI combined with increases in its spatial heterogeneity can be a sign of initial or slight degradation.

4.4.3.3 Decreases in NDVI and increases in spatial heterogeneity combined represent medium degradation

In fragmented grasslands, the bare-soil patches increase in number and size with increasing environmental and grazing pressures, which further increases the spatial heterogeneity and reduces the vegetation cover, and therefore result in negative NDVI trends. Therefore decreases in NDVI and increases in spatial heterogeneity lead to medium levels of degradation (Figure 4A.3 (b)).

4.4.3.4 Decreases in NDVI and decreases in spatial heterogeneity combined represent severe degradation or desertification

Vegetation-patch sizes decrease and bare-soil patches become larger and connected as degradation becomes more severe (Figure 4A.3 (c and d)); this is reflected in reduced vegetation cover and spatial heterogeneity. In the sparsely vegetated area where vegetation cover is relatively low (NDVI < 0.2), combined decreases in NDVI and spatial heterogeneity indicate that vegetation shifts from a patchy stage to bare soil, i.e. the stage of desertification (Milton and Siegfried, 1994; Ma et al. 1999; Rietkerk et al., 2004).

Examples of invasive species and degraded grasslands with bare-soil patches at different scales are displayed in Figure 4.2. We summarize the above characteristics of grassland development and degradation stages with the decision tree shown in Figure 4.3. Here we use this decision tree for assigning areas with particular NDVI mean and CV trends to the six new degradation categories

Figure 4.2 Example images of degraded grasslands. a) and b): pictures of fragmented grassland with bare-soil patches at Zekog, Zequ county in July 2015 and at Bange County in August 2016, respectively. c): satellite image of fragmented grassland representing grassland heterogeneity at larger scale in Madoi county (Sentinel-2 image ID: 20160819T040552_20160819T093629). The image was extracted from the Google Earth Engine platform. (d): picture showing that invasive species might strengthen the NDVI signal but reduce grassland forage quality at Naqu on 8 August 2016.

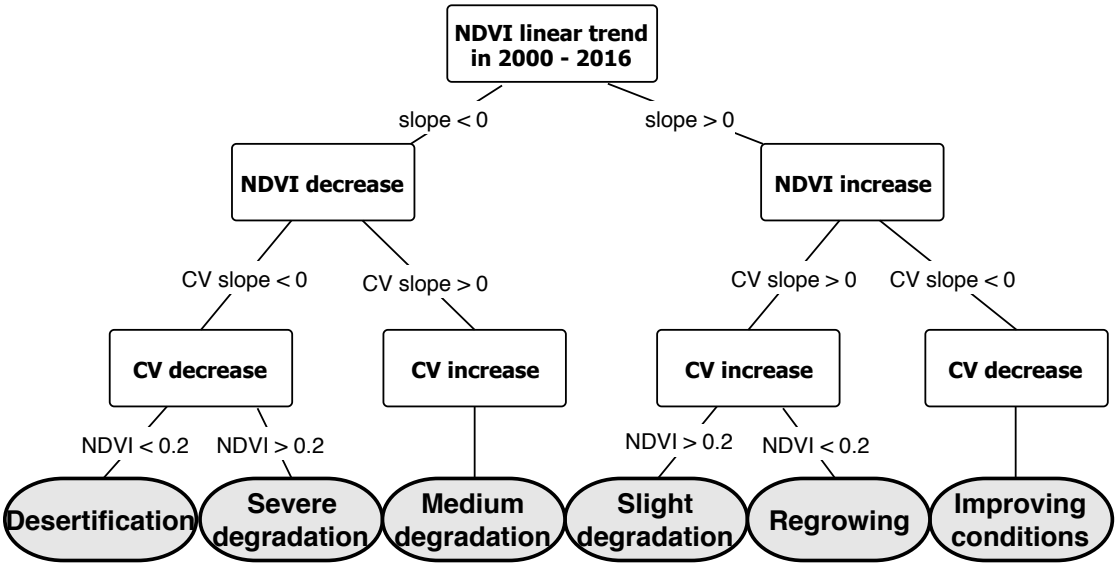

Figure 4.3 Flowchart for defining new degradation categories in 2016 based on linear trends of NDVI and spatial heterogeneity (measured as CV of NDVI in 3 x 3-pixel moving windows of 1500 x 1500 m). For further details see section 3.3 and the discussion in section 5.2.

4.5 Results

4.5.1 Linking grassland cover and spatial heterogeneity to degradation levels

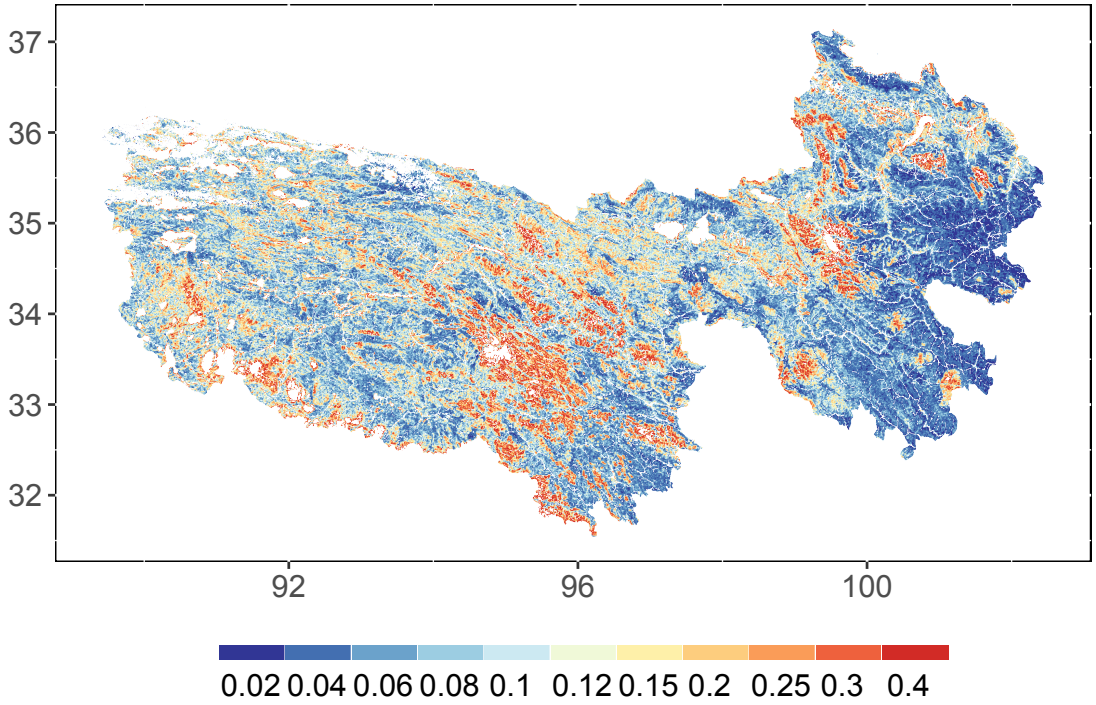

Figure 4.4. Spatial heterogeneity of grasslands in the "Three-River Headwaters" region of the QTP in 2016. Spatial heterogeneity was calculated as the CV of NDVI within a 3 x 3-pixel moving window (with the median NDVI value for the growing season from June to September).

We mapped spatial heterogeneity of grassland cover represented by the CV of NDVI within a 3 x 3-pixel moving window in an area of 1500 x 1500 m (Figure 4.4). Lower spatial heterogeneity was found in the eastern meadow-dominated regions, higher spatial heterogeneity in the northwestern steppe-dominated and mountainous regions (Figure 4.1 and Figure 4.4). Spatial heterogeneity increased with slope and was lowest at medium elevations of 3000–4500 m (Figure 4.5 (a)).

We analyzed differences in NDVI and its spatial heterogeneity for the different degradation categories defined in Liu et al. (2008) (Figure 4.6). We found the mean NDVI was lower in non-degraded compared with degraded areas, and higher in degraded and severely desertified areas (Figure 4.6 (a)). This shows that the mean NDVI was not sufficient to order areas into a monotonic sequence of degradation levels. Adding the CV of NDVI, we found higher spatial heterogeneity in more severely fragmented and deserted areas (Figure 4.6 (b)). However, it did not show a linear trend with the increased literature-derived degradation categories from no degradation to severe degradation and desertification.

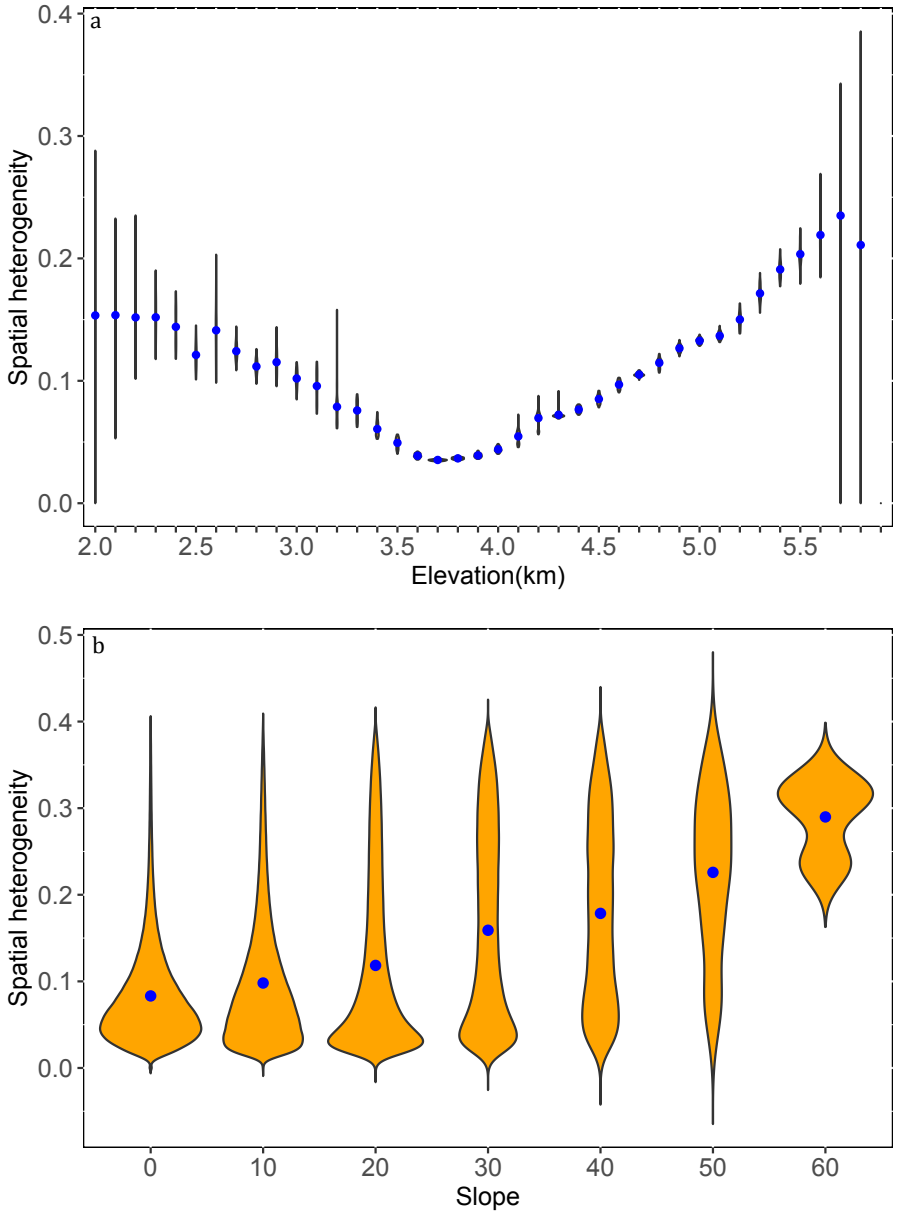

Figure 4.5. Distribution and mean (blue dots) of spatial heterogeneity of grassland cover along elevation (a) and slope (b) gradients in 2016. Spatial heterogeneity was calculated as the CV of NDVI within a 3 x 3-pixel moving window.

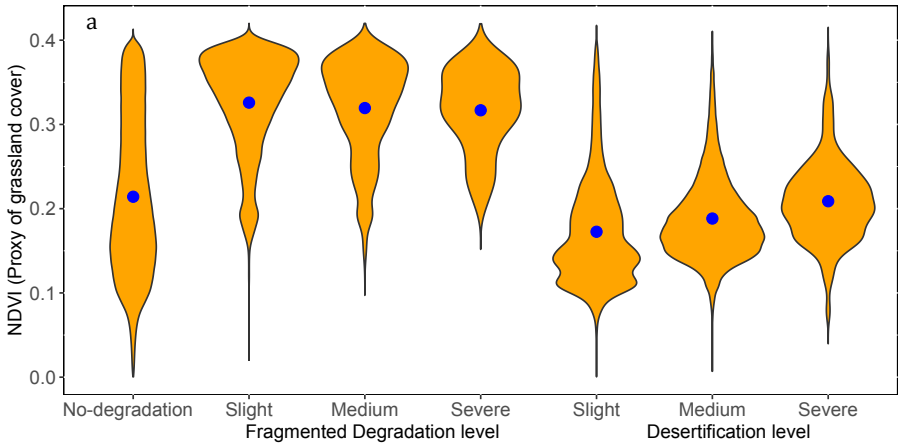

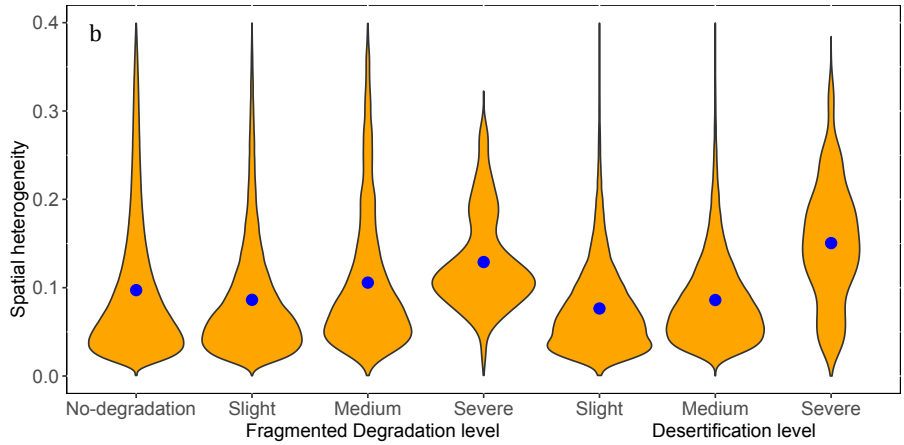

Figure 4.6. Grassland cover (NDVI) (a) and spatial heterogeneity (CV of NDVI) (b) in 2004 along increasing degradation levels from non-degraded to degraded and desertified categories as defined in Liu et al. (2008). Violin bars show the distribution of NDVI and CV, blue dots show the mean of NDVI and CV.

4.5.2 Temporal changes in NDVI and spatial heterogeneity among different degradation categories

NDVI temporal trends over 2000–2016 varied spatially (Figure 4.7 (a)), being negative in the central and southern regions (Figure 4.7) and positive in the northeastern region of the study area. Spatial heterogeneity showed mainly increasing trends from 2000–2016 (Figure 4.7 (b)), with an exception in the northeastern region, where it decreased in areas with increasing mean NDVI values (overlapping green areas in Figure 4.7 (a) and (b)). Less than 0.01% of the total area showed no detectable changes in NDVI and its spatial heterogeneity from 2000–2016. These areas were not considered when classifying new degradation categories. Examples of time-series analyses of change trends of NDVI and CV from 2000–2016 are shown in the supplementary material (Figure 4A.4, Figure 4A.5).

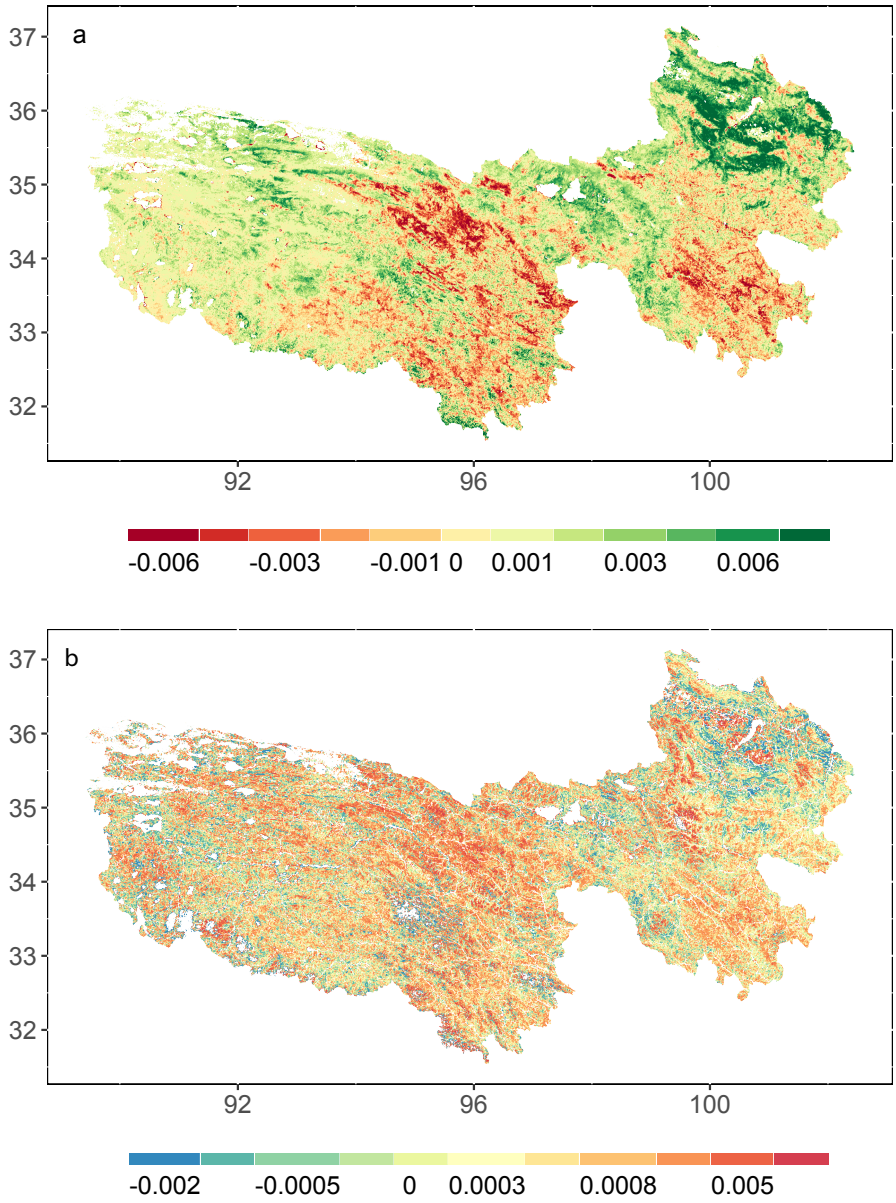

Figure 4.7. Linear temporal changes (including significant and non-significant ones) in NDVI (a) and spatial heterogeneity (b) from 2000–2016. The changes with only significant values can be found in the supplemented Figure 4A.2

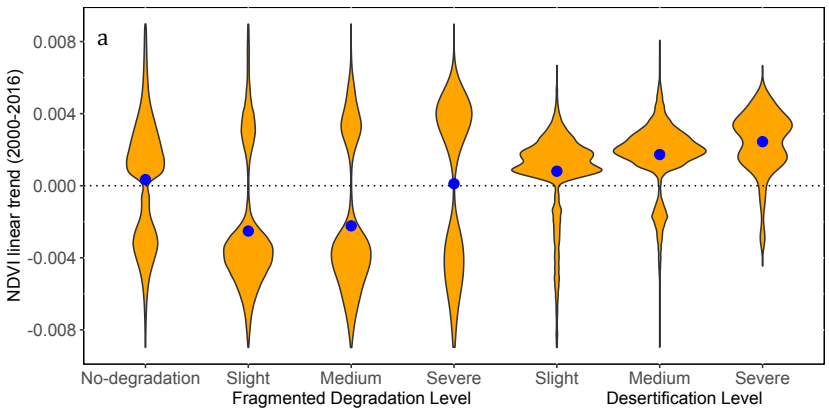

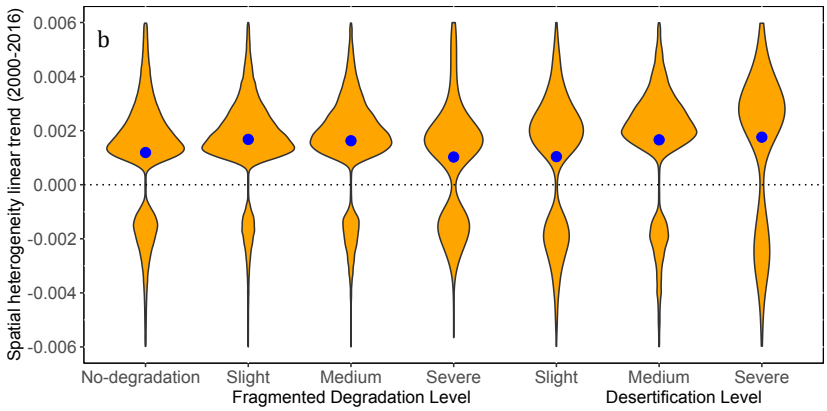

Figure 4.8. Significant ($P < 0.05$) linear temporal trends in means (a) and CVs (spatial heterogeneity) (b) of NDVI from 2000–2016 along increased degradation levels from non-degraded to fragmented and desertification categories defined in Liu et al. (2008). Violin bars show the distribution of NDVI and CV linear trends, blue dots show their mean values.

We analyzed changes in NDVI and its spatial heterogeneity in different degradation categories as defined in 2004 by Liu et al. (2008). Trends of NDVI and its spatial heterogeneity varied between but also largely within the degradation categories. In non-degraded areas that accounted for 75.3% of the study region, both decreasing and increasing NDVI trends were found, while spatial heterogeneity mostly increased (Figure 4.8). In fragmented-grassland areas that covered 10.3% of the entire study area, the NDVI mainly decreased and spatial heterogeneity mainly increased. In desertification areas, both the NDVI and its spatial heterogeneity generally increased (Figure 4.8). Desertification areas are characteristic of low cover and low NDVI. Thus combined increases in NDVI and in its spatial heterogeneity over the study period may indicate re-growing conditions. Overall, the vegetation cover represented by NDVI showed decreasing trends from 2000–2016 in slightly- to medium-fragmented areas, which contrasted with the increasing trends in desertification areas. The spatial heterogeneity of grassland cover generally increased over time and this increase was weakest in severely degraded areas and early stages of desertification, i.e. slightly deserted areas (Figure 4.8).

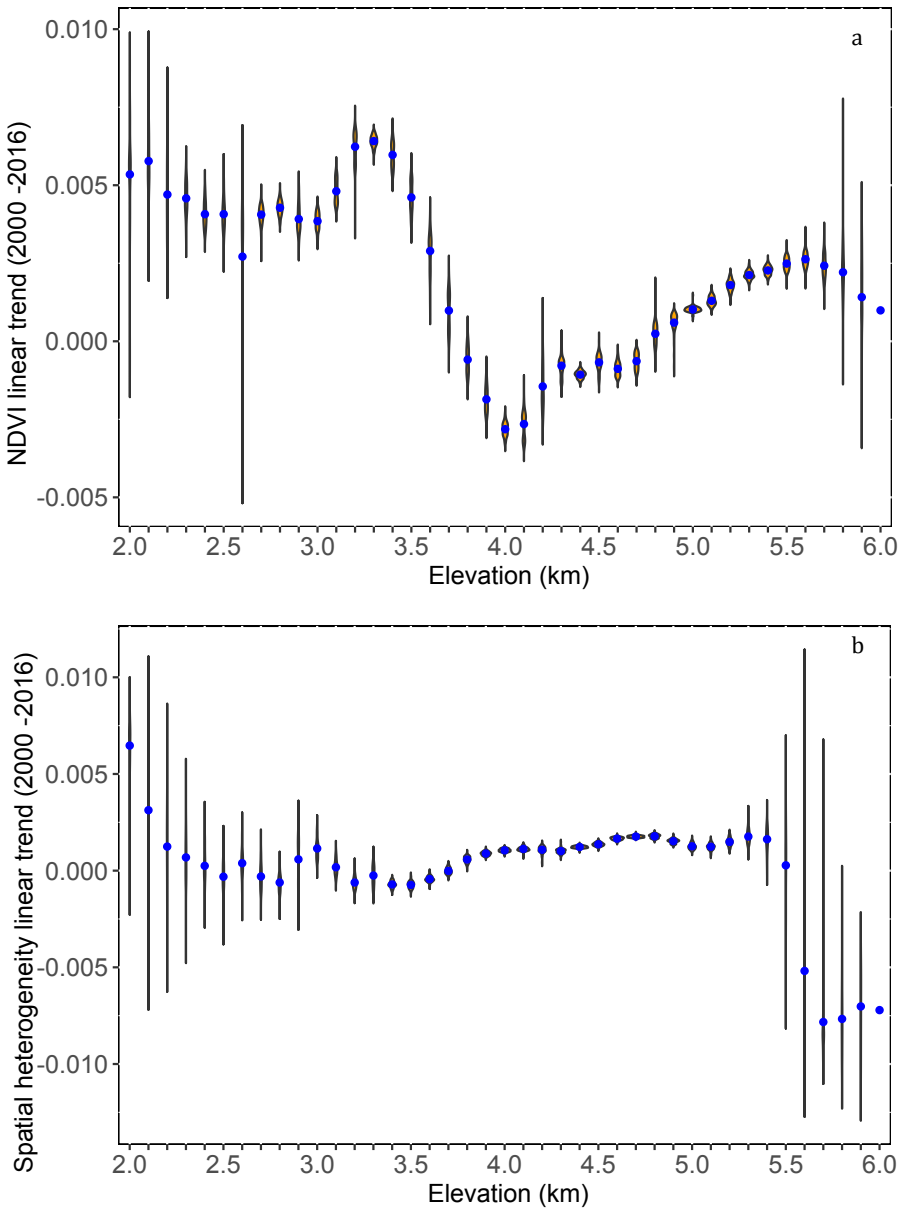

Figure 4.9. Average of significant NDVI trends (a) and trends in spatial heterogeneity (CV of NDVI) (b) along the elevation gradient.

The temporal trends of NDVI and its spatial heterogeneity were found to be elevation-dependent (Figure 4.9). The NDVI decreased at intermediate elevations and increased in lower and higher elevations. The spatial heterogeneity increased in most elevation zones except for areas above 5500 m. When correlating the NDVI trends with its spatial heterogeneity trends, we found an overall negative correlation between them. Increasing NDVI trends occurred both in areas with decreasing and increasing spatial heterogeneity.

4.5.3 Combining temporal changes in NDVI and spatial heterogeneity to map new degradation categories for 2016

NDVI and its spatial heterogeneity changed in most of the study area. These changes

indicated which grassland areas may have moved into new degradation stages over the studied time interval. We used these changes to define degradation categories and mapped them for 2016 (Figure 4.10). Compared with the earlier study of Liu et al. (2008), who classified 75% of the total study area as non-degraded grassland, we found that these grasslands have been degraded to different levels. Spatial heterogeneity mostly increased from 2000–2016 and NDVI showed both increasing and decreasing trends. We interpret the combination of increasing NDVI and increasing spatial heterogeneity as indicator of slight degradation in the vegetated area, and the combination of decreasing NDVI and increasing spatial heterogeneity as indicator of medium degradation in these areas (see Figure 4.3 and section 3.3). According to our degradation classification framework, we found that 21% of the total study area became slightly degraded and 34% and 8% became medium degraded and severely degraded, respectively. These degraded areas mainly occur in meadow-dominated regions (Figure 4.1 and Figure 4.10). Increasing NDVI and decreasing spatial-heterogeneity trends showed that grasslands have become more productive and less fragmented, indicating improving conditions across 24% of the total study area. In the sparsely vegetated areas where NDVI was less than 0.2, increases in NDVI and spatial heterogeneity indicated re-growing conditions and these occurred across 11% of the total study area (Figure 4.10). In the western part of the study area, on the other hand, decreases in NDVI and its spatial heterogeneity indicated that vegetation shifted from a patchy stage to bare soil (2% of our study area), indicating risk of desertification.

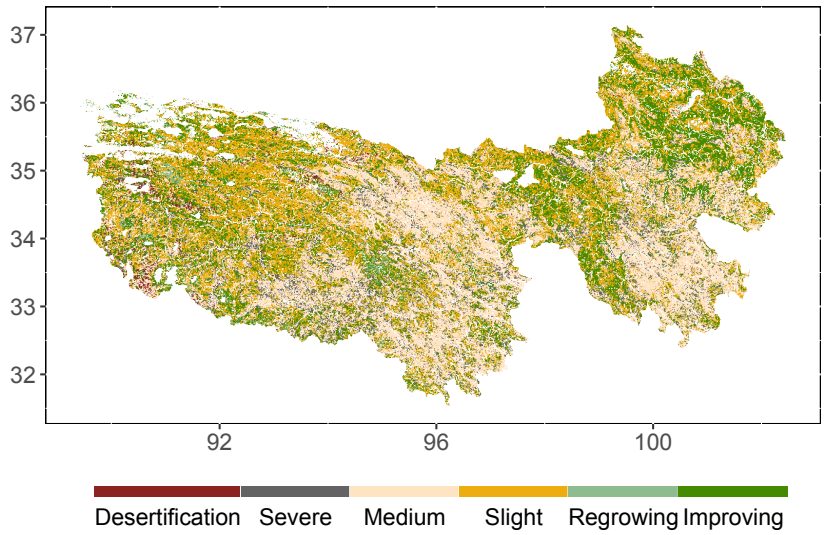

Figure 4.10. Spatial distribution of grassland-development ("re-growing", "improving") and degradation ("slight", "medium", "severe", "desertification") categories identified with the classification system presented in Figure 4.3.

4.6 Discussion

4.6.1 Heterogeneity in grassland cover as a degradation indicator

We found that lower vegetation cover does not always suggest more severe degradation of grassland because vegetation cover could actually be higher in some degraded areas than in non-degraded areas. Considering that lower vegetation cover is a characteristic of grassland ecosystems on the western QTP due to harsh environmental conditions, we argue that vegetation cover at one single time is not a representative indicator of grassland-degradation level and spatial heterogeneity of vegetation cover could be a better degradation indicator on the QTP. Our new findings point to limitations of previous degradation assessments based mainly on vegetation cover (e.g. X. L. Li et al., 2014).

We found that in areas identified as severely degraded in a reference study from 2004 (Liu et al., 2008) the spatial heterogeneity of vegetation cover was generally high, suggesting that this measure could be used as an indicator of grassland-degradation level. On the QTP the high spatial heterogeneity in degraded grasslands indicates the presence of bare-soil patches, likely caused by heavy livestock grazing and small mammal activities (Chen et al., 2017; Wei et al., 2007). Heavy grazing has caused grassland cover reduction, which facilitates small-mammal activities and the creation of bare-soil patches (Wen et al., 2013) and with that the increase of spatial heterogeneity. The presence of larger bare-soil patches combined with wind erosion can enhance desertification risks (Dong et al., 2009). Such degradation and desertification processes are more obvious in steeper areas where soil erosion is higher and spatial heterogeneity is also higher (Figure 4.5(b)). However, due to the spatial resolution of the satellite data used, small-scale bare-soil patches related to the activities of small mammal might not have been easily detected in this study.

4.6.2 Combining temporal changes in NDVI and spatial heterogeneity to map new degradation categories for 2016

We found that a combination of changes in vegetation cover and in its spatial heterogeneity could better indicate grassland degradation levels than vegetation cover alone. Existing studies have shown that a negative temporal trend of vegetation activity indicates degradation and a positive trend indicates restoration (Z. Wang et al., 2016). Based on these criteria, these and other authors concluded that vegetation that accounts for 61.2% of the QTP had been recovering (Z. Wang et al., 2016, Fan et

al., 2010; Xu et al., 2011). In contrast, we found that a large fraction of the area with increasing NDVI also shows increases in spatial heterogeneity, which may indicate an early stage of degradation instead of improvement. Invasive species (Zeng et al., 2013) colonization in degraded grasslands and bare-soils patches might explain the increasing spatial heterogeneity and therefore indicate the early stage of grassland degradation. These invasive species are generally higher and have larger leaf area than indigenous species, which increases the vegetation cover (Figure 4.2) and thus NDVI and contributes to changes in spatial heterogeneity. Previously, the decline of vegetation cover was commonly used as a degradation indicator. Here we caution that if vegetation cover increases due to the invasion of poisonous plant species it can actually be a sign of degradation (Liu et al., 2015). We therefore suggest that in vegetated areas the increase of spatial heterogeneity is an indicator of the early stage of degradation — even if the NDVI shows increasing trends.

Field investigations of vegetation cover, soil properties (soil organic carbon) and species composition have shown that grassland has been degrading on the QTP in the past decades (Liu et al., 2018a; Zeng et al., 2013). However, studies based on satellite observations showed increasing NDVI trends, which suggested the opposite process of grassland recovery and restoration (Z. Wang et al., 2016). We suggest that substantial parts of the non-degraded areas in 2004 have been degrading, as suggested by the combination of temporal changes in NDVI and its spatial heterogeneity, which is more consistent with the results from field studies (Liu et al., 2018a; Zeng et al., 2013).

In the slightly and medium-degraded areas in 2004 (Liu et al., 2008), we found that NDVI mostly decreased and spatial heterogeneity increased from 2000–2016 (Figure 4.8), showing that the grasslands have been fragmented and more soil patches have developed, therefore indicating more severe degradation. With the increasing environmental and grazing pressures, the severely degraded and sparsely vegetated areas would have been under risk of desertification with reduced vegetation cover, making recovery over short time-scales unlikely (Kéfi et al., 2007).

Areas that were classified as desertified in 2004 showed an increasing NDVI and spatial heterogeneity trend over time (Figure 4.8), suggesting grasslands to be re-growing. This condition was most apparent in the medium and severely desertified areas. Warming and wetter climate and sustainable grazing density might improve vegetation growth (Huang et al., 2016), especially climate warming facilitating

vegetation growth by reducing growth constraints and increasing photosynthetic rates (Peng et al., 2012; X. Wang et al., 2016). This might explain the improving conditions indicated by increasing NDVI (Zhang et al., 2014; Zhong et al., 2010) and decreasing spatial heterogeneity.

We found that degraded grasslands were more dominant at elevations of 3500–4500 m, indicated by increased spatial heterogeneity and decreased vegetation cover, which is consistent with a previous study that found more severe degradation in this elevation range (Wang et al., 2015). At elevation above 5000 m, we found that the NDVI increased and spatial heterogeneity decreased over time, suggesting an improvement of grasslands, possibly due to particularly strong warming effects at elevations above 5000 m. A previous study found that the warming rate is larger at higher elevation, which could enhance vegetation growth in these areas (Liu et al., 2019).

Our results suggest that the grasslands in the eastern part of the QTP have undergone degradation during the study period. The degradation levels vary depending on climate, soils and the regionally different impacts of rangeland management change (Wang et al., 2018). Climate change, rodent damage, and human factors such as overstocking, population increases and land-use change have been discussed as causes of grassland degradation (Harris, 2010; Lehnert et al., 2016; Miehe et al., 2019). Specifically, climate variability of rising air temperature combined with declining precipitation could be explanations of vegetation cover decline on the QTP (Lehnert et al., 2016). Increasing human disturbance via road and township development and grassland privatization (S. Li et al., 2018) resulted in grassland loss, furthermore, overgrazing in the vicinity of human settlements caused vegetation cover reductions (Li et al., 2019). Reduced vegetation cover creates a favorable condition for the invasion of pikas, which cause soil-patch development and increases grassland degradation (Li et al., 2013). Heavy grazing and intensive pika activity further resulted in increases in unpalatable and poisonous weeds (Wen et al., 2013). However, many of these are speculative explanations and further research is needed on the cause of the here observed grassland degradation on the QTP.

Defining globally accepted criteria for classifying grassland degradation levels is challenging because of the wide range of grassland types and conditions (White et al., 2000). On the QTP, varying standards and indicator systems have been used to define degradation at different spatial scales, resulting in uncertainties about the real

situation and trends of grassland degradation (Liu et al., 2018b; Miehe et al., 2019). In this study, we propose indicators of defining grassland degradation stages on the landscape scale using remote sensing, that is the combination of changes in NDVI and in its spatial heterogeneity. The combination of these indicators can better indicate grassland degradation and its trends than it was previously possible with NDVI alone. Our new indicators may serve as early warning signals for grassland degradation and desertification.

4.7 Conclusion and outlook

We studied whether vegetation cover, spatial heterogeneity, and their changes can be used to define grassland degradation levels in the eastern QTP. We found that a combination of changes in vegetation cover and spatial heterogeneity during 2000–2016 could best indicate previously defined degradation levels (Liu et al., 2008). Grassland cover and its spatial heterogeneity have changed in most of the study area, indicating that grassland areas have moved into new degradation stages over the studied time interval.

Areas classified as degraded in 2004 generally became more degraded, as suggested by decreasing vegetation cover and increasing spatial heterogeneity from 2000–2016, due to the reduction of vegetation patch sizes and the increase in the number of bare-soil patches. However, areas classified as desertified in 2004 showed signs of recovery or re-growth, as suggested by increasing vegetation cover and increasing spatial heterogeneity. Based on these observations, we define new degradation categories for the QTP grasslands in 2016. Our results suggest that large parts of the total study area (63%) have undergone at least slight degradation during the study period, and 2% of the western part of the study area is at risk of desertification. Nevertheless, 24% and 11% of the total study area have been improving or recovering, respectively, and these areas are concentrated in high elevation or severely degraded grasslands.

We studied spatial heterogeneity at the 500 m scale, although soil patches occur on the QTP at scales varying from less than 0.1 m to more than 500 m. Therefore, monitoring changes in spatial heterogeneity at different scales is important for understanding how the soil patches relate to the different drivers like small-mammal activities. Satellite data with higher resolution such as Landsat (30 m) and Sentinel-2 (10-20 m) could be used to map and monitor spatial heterogeneity that relates to bare-

soil patches smaller than 30 m. The proposed indicators for monitoring grassland development may also be applicable to other arid ecosystems where the development of bare-soil patches also has been widely observed (Aguiar and Sala, 1999; Bestelmeyer et al., 2013; Kéfi et al., 2007).

However, grassland degradation is a complicated process that not only involves changes in vegetation cover and spatial heterogeneity, but also changes in soil properties and species composition, among other factors (Zhang et al., 2018). Therefore, the proposed new indicators for classifying grassland degradation categories can only give a broad estimate of the specific situation in a particular area. The suggested combination of the above two indicators allows monitoring of grassland degradation on a large scale using remote sensing. Future studies should focus on different scales to better understand degradation process. For example, understanding how soil properties have changed over the past decades, especially how permafrost degradation may have contributed to grassland degradation, and what drives invasive species encroachment at the field scale will help to more accurately predict future grassland degradation risks and develop mitigation strategies.

4.8 Appendix

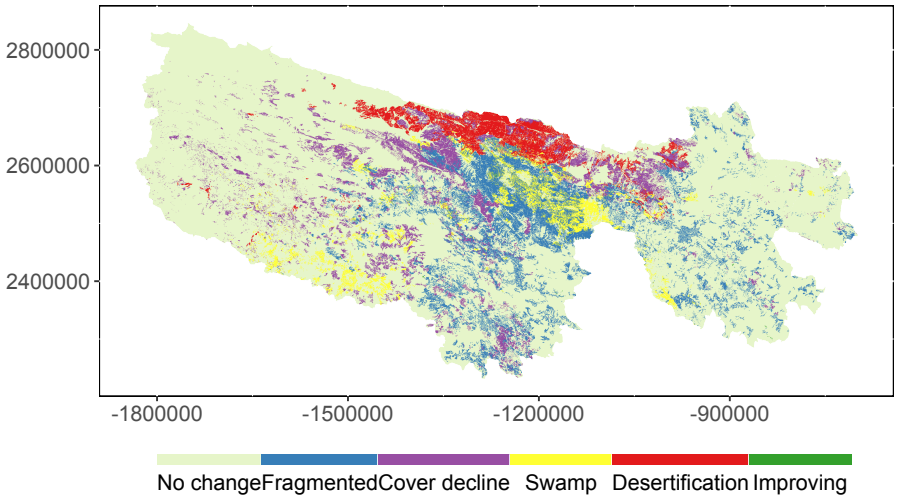

Figure 4A.1 Grassland degradation-level categories in 2004 from the literature(Liu et al., 2008).

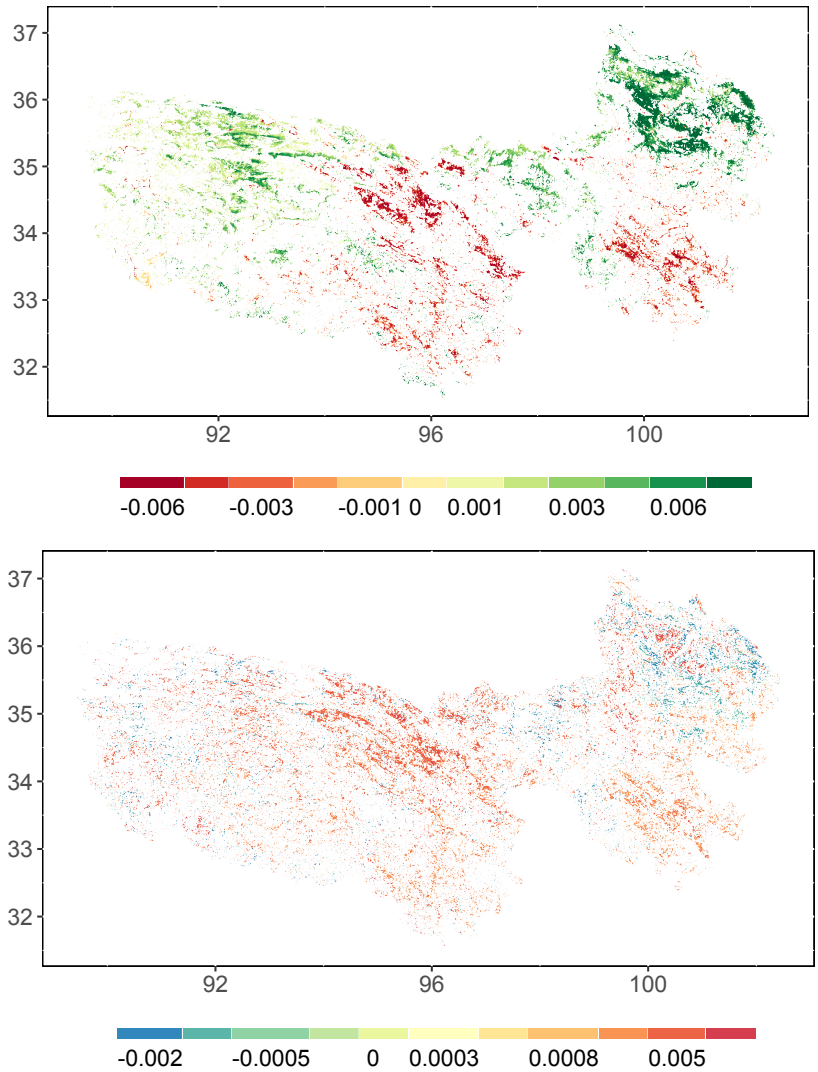

Figure 4A.2. Significant linear temporal changes of NDVI (a) and its spatial heterogeneity (b) from 2000–2016.

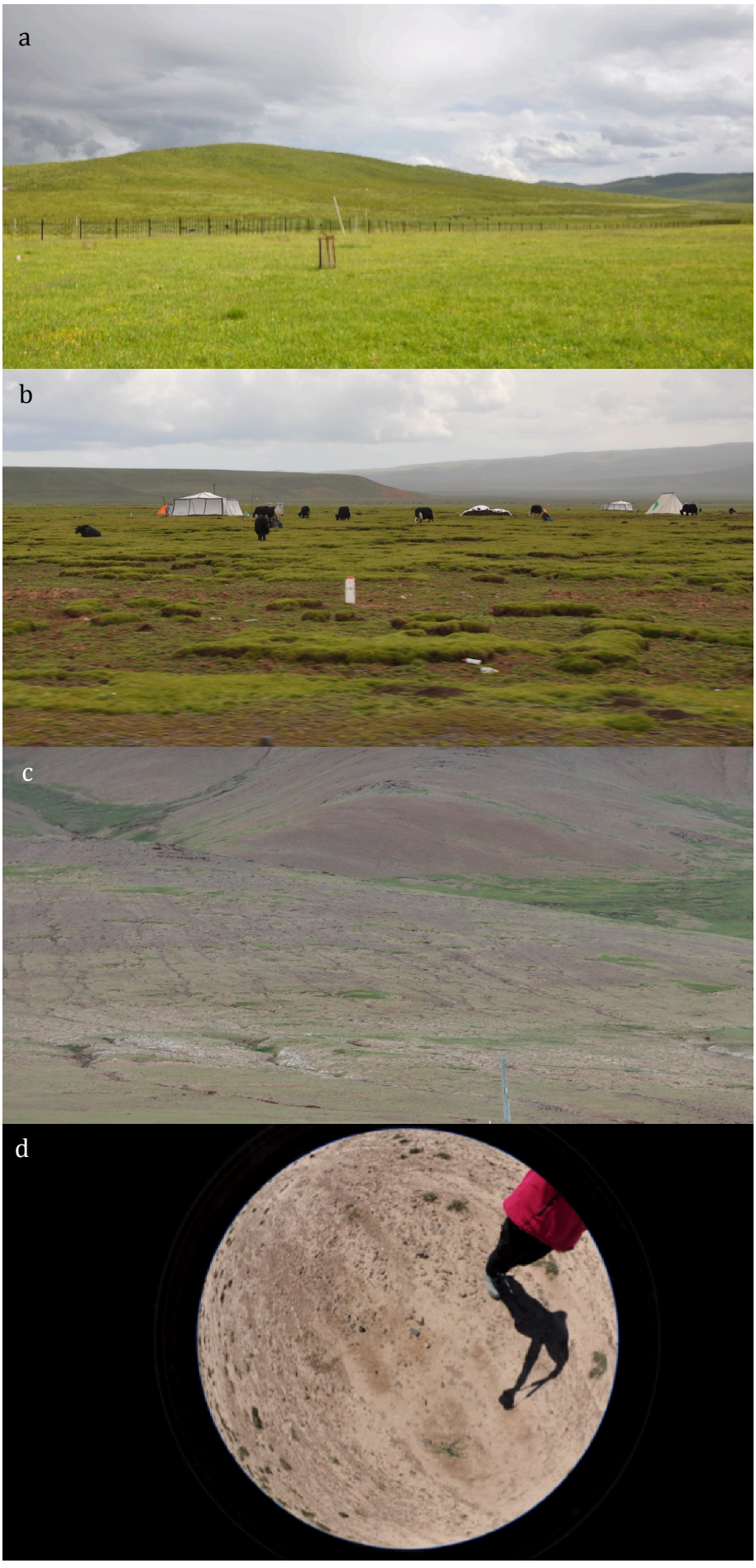
a
b
c
d

Figure 4A.3 Example pictures of grasslands show the change of spatial heterogeneity at different degradation stages. The pictures illustrate that the change of spatial heterogeneity is not linear with degradation level. The spatial heterogeneity first increases with degradation level and then decreases at severe degradation and desertification stages.

a) Intact grassland showing the typically homogeneous landscape in the northeastern QTP in July 2015.

b) Degraded grassland with bare-soil patches showing increased spatial heterogeneity in the eastern QTP in July 2015.

c) Severely degraded grassland showing vegetation-patch sizes decrease and bare-soil patches become larger and connected at Wudaoliang, Qinghai province in August 2016.

d) Desertification stage of grassland dominated by bare soil showing decreased spatial heterogeneity at Wulan, northeastern QTP in August 2016.

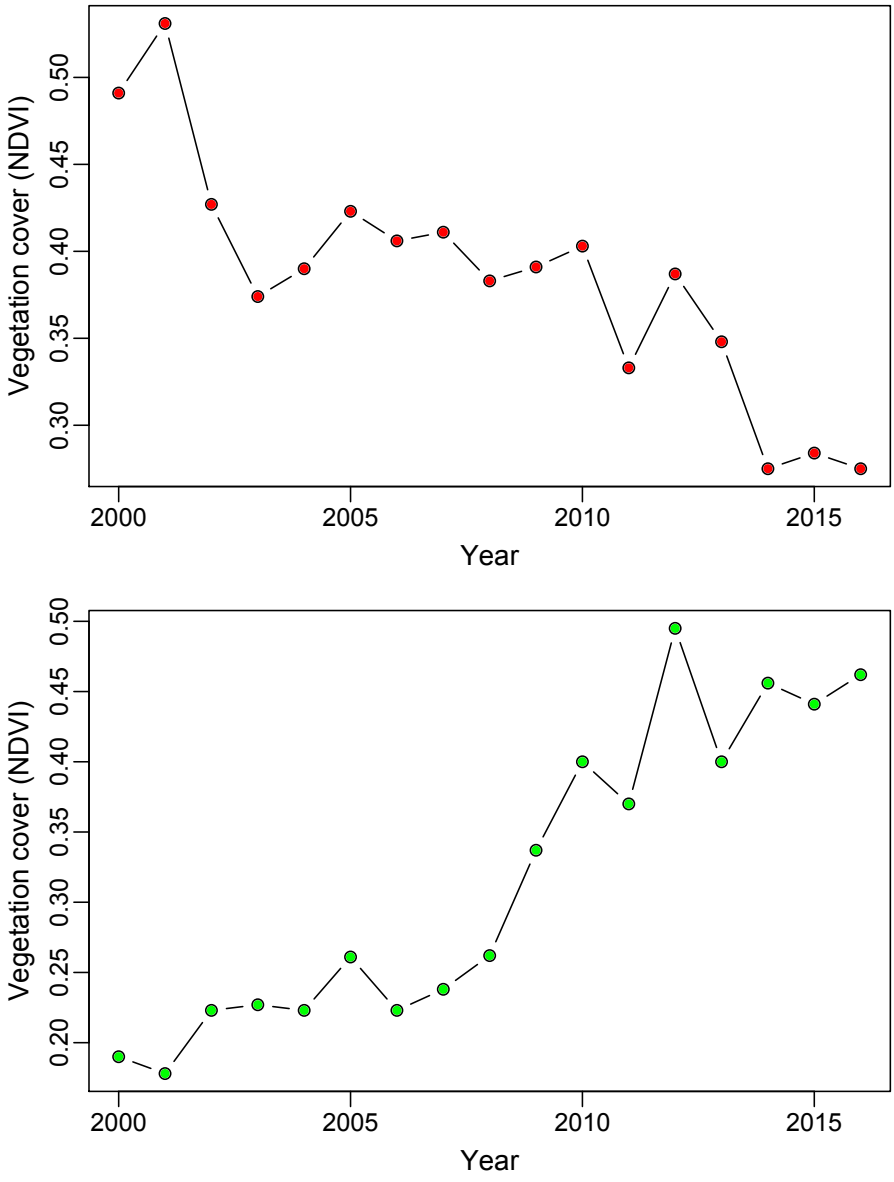

Figure 4A.4. Examples of increasing and decreasing trends of NDVI from 2000–2016 in the central (95.782° E, 34.631° N) and northeastern (99.9272° E, 36.1119° N) parts of the study area, respectively.

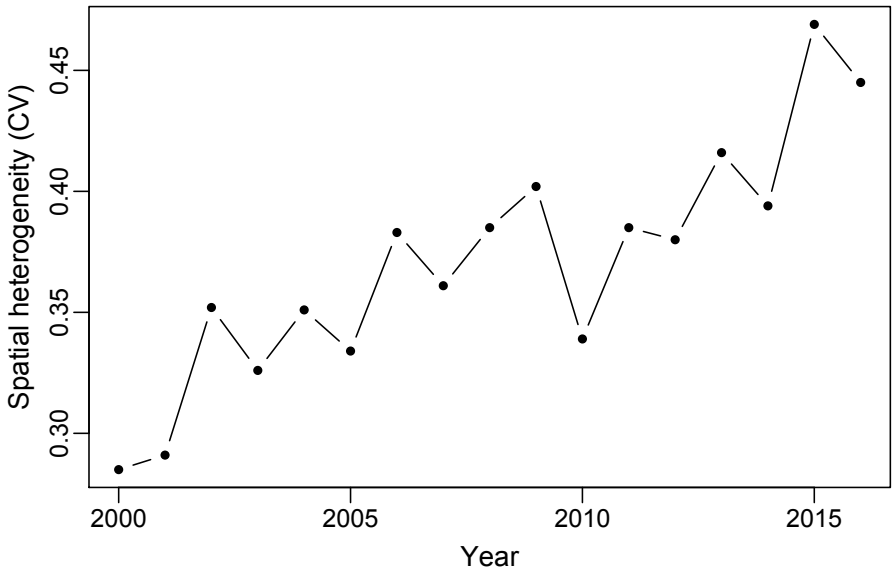

Figure 4A.5 Example of increasing trend of the CV of NDVI from 2000–2016 in the central part of study area (95.4793° E, 34.8999° N).

4.9 Acknowledgments

The degradation dataset is from the Rescourse and enivronmental data cloud platform, Chinese Academy of Science (http://www.resdc.cn/DOI),2018.DOI:10.12078/2018062101). Chengxiu Li was funded by the Chinese Scholarship Council (CSC). This study was conducted in the framework of the University of Zurich Research Program on Global Change and Biodiversity (URPP GCB). We acknowledge the OpenStreetMap for providing settlements spatial data.

4.10 References

Aguiar, M.R., Sala, O.E., 1999. Patch structure, dynamics and implications for the functioning of arid ecosystems. Trends Ecol. Evol. 14, 273–277. doi:10.1016/S0169-5347(99)01612-2

Berdugo, M., Kéfi, S., Soliveres, S., Maestre, F.T., 2017. Plant spatial patterns identify alternative ecosystem multifunctionality states in global drylands. Nat. Ecol. Evol. 1, 1–7. doi:10.1038/s41559-016-0003

Bestelmeyer, B.T., Duniway, M.C., James, D.K., Burkett, L.M., Havstad, K.M., 2013. A test of critical thresholds and their indicators in a desertification-prone ecosystem: More resilience than we thought. Ecol. Lett. 16, 339–345. doi:10.1111/ele.12045

Cai, H., Yang, X., Xu, X., 2015. Human-induced grassland degradation/restoration in the central Tibetan Plateau: The effects of ecological protection and restoration projects. Ecol. Eng. 83, 112–119. doi:10.1016/j.ecoleng.2015.06.031

Carpenter, S.R., Brock, W.A., 2006. Rising variance: A leading indicator of ecological transition. Ecol. Lett. 9, 308–315. doi:10.1111/j.1461-0248.2005.00877.x

Chen, J., Yi, S., Qin, Y., 2017. The contribution of plateau pika disturbance and erosion on patchy alpine grassland soil on the Qinghai-Tibetan Plateau: Implications for grassland restoration. Geoderma 297, 1–9. doi:10.1016/j.geoderma.2017.03.001

Dong, Q.M., Zhao, X.Q., Wu, G.L., Shi, J.J., Ren, G.H., 2013. A review of formation mechanism and restoration measures of "black-soil-type" degraded grassland in the Qinghai-Tibetan Plateau. Environ. Earth Sci. 70, 2359–2370. doi:10.1007/s12665-013-2338-7

Dong, Z., Hu, G., Yan, C., Wang, W., Lu, J., 2009. Aeolian desertification and its causes in the Zoige Plateau of China's Qinghai-Tibetan Plateau. Environ. Earth Sci. 59, 1731–1740. doi:10.1007/s12665-009-0155-9

Duong, T., 2007. ks: Kernel Density Estimation and Kernel Discriminant Analysis for Multivariate Data in R. J. Stat. Softw. 21, 1–16. doi:10.18637/jss.v068.c02

Fan, J.W., Shao, Q.Q., Liu, J.Y., Wang, J.B., Harris, W., Chen, Z.Q., Zhong, H.P., Xu, X.L., Liu, R.G., 2010. Assessment of effects of climate change and grazing activity on grassland yield in the Three Rivers Headwaters Region of Qinghai-Tibet Plateau, China. Environ. Monit. Assess. 170, 571–584. doi:10.1007/s10661-009-1258-1

Farr, T., Rosen, P., Caro, E., Crippen, R., Duren, R., Hensley, S., Kobrick, M., Paller, M., Rodriguez, E., Roth, L., Seal, D., Shaffer, S., Shimada, J., Umland, J., Werner, M., Oskin, M., Burbank, D., Alsdorf, D., 2007. The shuttle radar topography mission. Rev. Geophys. 45, 1–33. doi:10.1029/2005RG000183.1.INTRODUCTION

Fassnacht, F.E., Li, L., Fritz, A., 2015. Mapping degraded grassland on the Eastern Tibetan Plateau with multi-temporal Landsat 8 data - where do the severely degraded areas occur? Int. J. Appl. Earth Obs. Geoinf. 42, 115–127. doi:10.1016/j.jag.2015.06.005

Feng, J., Wang, T., Qi, S., Xie, C., 2005. Land degradation in the source region of the Yellow River, northeast Qinghai-Xizang Plateau: Classification and evaluation. Environ. Geol. 47, 459–466. doi:10.1007/s00254-004-1161-6

Guo, D., Wang, H., 2013. Simulation of permafrost and seasonally frozen ground conditions on the Tibetan Plateau, 1981-2010. J. Geophys. Res. Atmos. 118, 5216–5230. doi:10.1002/jgrd.50457

Haklay, M., Weber, P., 2008. OpenStreet map: User-generated street maps. IEEE Pervasive Comput. 7, 12–18. doi:10.1109/MPRV.2008.80

Harris, R.B., 2010. Rangeland degradation on the Qinghai-Tibetan plateau: A review of the evidence of its magnitude and causes. J. Arid Environ. 74, 1–12. doi:10.1016/j.jaridenv.2009.06.014

Kéfi, S., Guttal, V., Brock, W.A., Carpenter, S.R., Ellison, A.M., Livina, V.N., Seekell, D.A., Scheffer, M., Van Nes, E.H., Dakos, V., 2014. Early warning signals of ecological transitions: Methods for spatial patterns. PLoS One 9, 10–13. doi:10.1371/journal.pone.0092097

Kéfi, S., Rietkerk, M., Alados, C.L., Pueyo, Y., Papanastasis, V.P., ElAich, A., De Ruiter, P.C., 2007. Spatial vegetation patterns and imminent desertification in Mediterranean arid ecosystems. Nature 449, 213–217. doi:10.1038/nature06111

Kennedy, P., 1989. Monitoring the vegetation of Tunisian grazing lands using the normalized difference vegetation index. Ambio 18, 119–123.

Lehner, B., Verdin, K., Jarvis, A., 2008. New global hydrography derived from spaceborne elevation data. Eos (Washington. DC). 89, 93–94. doi:10.1029/2008EO100001

Lehnert, L.W., Meyer, H., Meyer, N., Reudenbach, C., Bendix, J., 2014. A hyperspectral indicator system for rangeland degradation on the Tibetan Plateau: A case study towards spaceborne monitoring. Ecol. Indic. 39, 54–64. doi:10.1016/j.ecolind.2013.12.005

Li, F., Chen, W., Zeng, Y., Zhao, Q., Wu, B., 2014. Improving estimates of grassland fractional vegetation cover based on a pixel dichotomy model: A case study in Inner Mongolia, China. Remote Sens. 6, 4705–4722. doi:10.3390/rs6064705

Li, S., Wu, J., Gong, J., Li, S., 2018. Human footprint in Tibet: Assessing the spatial layout and effectiveness of nature reserves. Sci. Total Environ. 621, 18–29. doi:10.1016/j.scitotenv.2017.11.216

Li, X., Gao, J., Zhang, J., 2018. A topographic perspective on the distribution of degraded meadows and their changes on the Qinghai-Tibet Plateau, West China. L. Degrad. Dev. 29, 1574–1582. doi:10.1002/ldr.2952

Li, X.L., Perry, G.L.W., Brierley, G., Sun, H.Q., Li, C.H., Lu, G.X., 2014. Quantitative assessment of degradation classifications for degraded alpine meadows (Heitutan), Sanjiangyuan, western China. L. Degrad. Dev. 25, 417–427. doi:10.1002/ldr.2154

Liang, L., Li, L., Liu, C., Cuo, L., 2013. Climate change in the Tibetan plateau three rivers source region: 1960-2009. Int. J. Climatol. 33, 2900–2916. doi:10.1002/joc.3642

Lin, Y., Han, G., Zhao, M., Chang, S.X., 2010. Spatial vegetation patterns as early signs of desertification: A case study of a desert steppe in Inner Mongolia, China. Landsc. Ecol. 25, 1519–1527. doi:10.1007/s10980-010-9520-z

Liu, J., Xu, X., Shao, Q., 2008. Grassland degradation in the "Three-River Headwaters" region, qinghai province. J. Geogr. Sci. 18, 259–273. doi:10.1007/s11442-008-0259-2

Liu, S., Zamanian, K., Schleuss, P.M., Zarebanadkouki, M., Kuzyakov, Y., 2018. Degradation of Tibetan grasslands: Consequences for carbon and nutrient cycles. Agric. Ecosyst. Environ. 252, 93–104. doi:10.1016/j.agee.2017.10.011

Maestre, F.T., Escudero, A., 2009. Is the patch size distribution of vegetation a suitable indacator of desertification processes? Ecology 90, 1729–1735. doi:10.1641/0006-3568(2001)051[0341:LNDATS]2.0.CO;2

Milton, S.J., Siegfried, W.R., 1994. A Conceptual Model of Arid Rangeland Degradation. Bioscience 44, 70–76. doi:10.2307/1312204

Peng, J., Liu, Z., Liu, Y., Wu, J., Han, Y., 2012. Trend analysis of vegetation dynamics in Qinghai-Tibet Plateau using Hurst Exponent. Ecol. Indic. 14, 28–39. doi:10.1016/j.ecolind.2011.08.011

Piao, S., Wang, X., Ciais, P., Zhu, B., Wang, T., Liu, J., 2011. Changes in satellite-derived vegetation growth trend in temperate and boreal Eurasia from 1982 to 2006. Glob. Chang. Biol. 17, 3228–3239. doi:10.1111/j.1365-2486.2011.02419.x

Purevdorj, T.S., Tateishi, R., Ishiyama, T., Honda, Y., 1998. Relationships between percent vegetation cover and vegetation indices. Int. J. Remote Sens. 19, 3519–3535. doi:10.1080/014311698213795

Rietkerk, M., Dekker, S.C., De Ruiter, P.C., Van De Koppel, J., 2004. Self-organized patchiness and catastrophic shifts in ecosystems. Science (80-.). 305, 1926–1929. doi:10.1126/science.1101867

Schaaf, C.B., Gao, F., Strahler, A.H., Lucht, W., Li, X., Tsang, T., Strugnell, N.C., Zhang, X., Jin, Y., Muller, J.P., Lewis, P., Barnsley, M., Hobson, P., Disney, M., Roberts, G., Dunderdale, M., Doll, C., D'Entremont, R.P., Hu, B., Liang, S., Privette, J.L., Roy, D., 2002. First operational BRDF, albedo nadir reflectance products from MODIS. Remote Sens. Environ. 83, 135–148. doi:10.1016/S0034-4257(02)00091-3

Song, X., Yang, G., Yan, C., Duan, H., Liu, G., Zhu, Y., 2009. Driving forces behind land use and cover change in the Qinghai-Tibetan Plateau: A case study of the source region of the Yellow River, Qinghai Province, China. Environ. Earth Sci. 59, 793–801. doi:10.1007/s12665-009-0075-8

Tucker, C.J., 1979. Red and photographic infrared linear combinations for monitoring vegetation. Remote Sens. Environ. 8, 127–150. doi:10.1016/0034-4257(79)90013-0

Wang, G., Bai, W., Li, N., Hu, H., 2011. Climate changes and its impact on tundra ecosystem in Qinghai-Tibet Plateau, China. Clim. Change 106, 463–482. doi:10.1007/s10584-010-9952-0

Wang, J., Wang, G., Hu, H., Wu, Q., 2010. The influence of degradation of the swamp and alpine meadows on CH4and CO2fluxes on the Qinghai-Tibetan Plateau. Environ. Earth Sci. 60, 537–548. doi:10.1007/s12665-009-0193-3

Wang, P., Lassoie, J.P., Morreale, S.J., Dong, S., 2015. A critical review of socioeconomic and natural factors in ecological degradation on the Qinghai-Tibetan Plateau, China. Rangel. J. 37, 1–9.

doi:10.1071/RJ14094

Wang, X., Yi, S., Wu, Q., Yang, K., Ding, Y., 2016. The role of permafrost and soil water in distribution of alpine grassland and its NDVI dynamics on the Qinghai-Tibetan Plateau. Glob. Planet. Change 147, 40–53. doi:10.1016/j.gloplacha.2016.10.014

Wang, Z., Zhang, Y., Yang, Y., Zhou, W., Gang, C., Zhang, Y., Li, J., An, R., Wang, K., Odeh, I., Qi, J., 2016. Quantitative assess the driving forces on the grassland degradation in the Qinghai-Tibet Plateau, in China. Ecol. Inform. 33, 32–44. doi:10.1016/j.ecoinf.2016.03.006

Wei, X., Li, S., Yang, P., Cheng, H., 2007. Soil erosion and vegetation succession in alpine Kobresia steppe meadow caused by plateau pika - A case study of Nagqu County, Tibet. Chinese Geogr. Sci. 17, 75–81. doi:10.1007/s11769-007-0075-0

Wen, L., Dong, S.K., Li, Y.Y., Sherman, R., Shi, J.J., Liu, D.M., Wang, Y.L., Ma, Y.S., Zhu, L., 2013. The effects of biotic and abiotic factors on the spatial heterogeneity of alpine grassland vegetation at a small scale on the Qinghai-Tibet Plateau (QTP), China. Environ. Monit. Assess. 185, 8051–8064. doi:10.1007/s10661-013-3154-y

White, R., Murray, S., Rohweder, M., 2000. Pilot Analysis of Global Ecosystems: Grassland Ecosystems, World Resources Institute. doi:10.1021/es0032881

Xu, W., Gu, S., Zhao, X.Q., Xiao, J., Tang, Y., Fang, J., Zhang, J., Jiang, S., 2011. High positive correlation between soil temperature and NDVI from 1982 to 2006 in alpine meadow of the Three-River Source Region on the Qinghai-Tibetan Plateau. Int. J. Appl. Earth Obs. Geoinf. 13, 528–535. doi:10.1016/j.jag.2011.02.001

Xulu, S., Peerbhay, K., Gebreslasie, M., Ismail, R., 2018. Drought Influence on Forest Plantations in Zululand, South Africa, Using MODIS Time Series and Climate Data. Forests 9, 528. doi:10.3390/f9090528

Zeng, C., Zhang, F., Wang, Q., Chen, Y., Joswiak, D.R., 2013. Impact of alpine meadow degradation on soil hydraulic properties over the Qinghai-Tibetan Plateau. J. Hydrol. 478, 148–156. doi:10.1016/j.jhydrol.2012.11.058

Zhang, G., Biradar, C.M., Xiao, X., Dong, J., Zhou, Y., Qin, Y., Zhang, Y., Liu, F., Ding, M., Thomas, R.J., 2018. Exacerbated grassland degradation and desertification in Central Asia during 2000-2014. Ecol. Appl. 28, 442–456. doi:10.1002/eap.1660

Zhang, G., Zhang, Y., Dong, J., Xiao, X., 2013. Green-up dates in the Tibetan Plateau have continuously advanced from 1982 to 2011. Proc. Natl. Acad. Sci. 110, 4309–4314. doi:10.1073/pnas.1210423110

Zhang, L., Guo, H.D., Wang, C.Z., Ji, L., Li, J., Wang, K., Dai, L., 2014. The long-term trends (1982-2006) in vegetation greenness of the alpine ecosystem in the Qinghai-Tibetan Plateau. Environ. Earth Sci. 72, 1827–1841. doi:10.1007/s12665-014-3092-1

Zhong, L., Ma, Y., Salama, M.S., Su, Z., 2010. Assessment of vegetation dynamics and their response to variations in precipitation and temperature in the Tibetan Plateau. Clim. Change 103, 519–535. doi:10.1007/s10584-009-9787-8

Chapter 5

Synthesis

5.1 Main findings

Plants in the alpine grasslands have developed unique strategies to adapt to the harsh environments such as low temperature and strong solar radiation. The plant adaptation strategies could be reflected by plant traits for example SLA, LDMC and Chlorophyll content. Alpine grassland ecosystems along with plant traits are vulnerable and sensitive to climate change and land use change. Global warming and increasing human activities have caused ecosystem changes including ecosystem degradation, as identified by vegetation cover reduction, changes in community composition and soil properties. This thesis aims to firstly, map the grassland plant traits at the canopy scale for better understanding of plant adaptation strategies; secondly, to map human influence on grassland ecosystems at two spatial scales and finally, to monitor ecosystem changes and degradation. Here, we review the research questions pointed out in the section 1.3.3 together with the Hypotheses.

RQ1: Can we estimate plant traits at the canopy level from remote sensing data? Are remotely-sensed plant traits comparable to the plant traits measured at the community level in the field?

We are able to estimate the plant traits at the canopy scale across the whole QTP using high-resolution satellite data and cloud-based computation platform. Chapter 2 provides an approach to estimate plant traits (Plant Dry Matter Content, Specific Plant Area, and Chlorophyll content) at the canopy level. The plant traits estimation was based on the fact that leaf-level trait measurements are close to plant-level trait measurements for the herbaceous plant in the alpine grasslands. By taking advantage of the high resolution of Landsat-8 and Sentinel-2 data, we approximate Specific Plant Area (SPA = plant area/plant dry mass) and Plant Dry Matter Content (PDMC = plant dry mass/plant fresh mass) to Community-Weighted Means (CWMs) of Specific Leaf Area (SLA) and Leaf Dry Matter Content (LDMC). The plant traits of CHL, SPA, and PDMC could be predicted using satellite data of Sentinel-2 (20 m) and Landsat-8 (30 m) as well as the MODIS LAI product (500 m), with R^2 of 0.34, 0.22, and 0.53, respectively.

Despite the different measurement methods, we found that the remotely sensed plant traits (SPA and PDMC) are comparable to the literature-derived plant traits at the community level (CWMs of SLA and LDMC) measured at the field. Both remotely sensed and field-measured results showed that alpine meadow plants reveal a wider

range and higher averages of CHL and SPA but lower PDMC compared with alpine steppe plants. These plant trait differences among vegetation types indicate tradeoffs between plant productivity and persistence, describing different plant strategies.

Chapter 2 is the first time to provide evidences that the remotely sensed plant traits are correlated to the field-measured traits at the community level. Satellite observations and field measurements have been conducted at different spatial and temporal scale, and the weak correlation might be improved if measurements were conducted at the same temporal and spatial scale.

The remotely sensed plant traits reveal a vast spatial variability across the whole QTP, showing the large difference in plant trait values even in the same vegetation type. This reflects that trait differences are widely influenced by environmental conditions and possibly by human influences. The outputs are key to understand ecosystem functioning and ecosystem process under environmental change.

RQ2: Can we map the human influence on grassland ecosystems on the QTP? What is the impact of livestock grazing on grasslands at different spatial scales?

We estimate human influences on ecosystems by modeling the differences between potential biomass and actual biomass. The potential biomass is only driven by environmental variables without the intervention of human activities therefore estimated from the environmental variables at 10-km scale. The actual biomass is estimated from the satellite observation and *in-situ* measurements. We find that the modeled human-influenced biomass at the 10-km scale has a weak-positive correlation ($R^2 = 0.1$) with grazing intensity. We further map the human influences on ecosystems at a local scale of 500 m close to settlements. This is based on the background of reduced mobility of pastoralism that exerts increasing pressures on the vegetation near to settlements (Wang et al., 2017). We approximate the distance to settlements as a proxy of human influence density. We detect hotspots where the biomass decreases or increases towards settlements within a radius of 8 km, indicating negative or positive human influences on biomass. In particular, we find that biomass decreases near settlements in areas with high livestock density at the county level.

The results suggest opposite grazing effects on biomass at two different spatial scales, showing positive grazing at the regional scale of 10 km and negative grazing effects at the local scale of 500 m close to settlements, indicating that grazing facilitates

biomass growth across the whole QTP (Lu et al., 2017) but overgrazing near settlements (Papanastasis, 2009) represents a threat to the future biomass production and stability of these ecosystems. The overgrazed area might be more vulnerable and more sensitive to climate change, which requires further attention in future ecosystem protection projects.

The human activities on the QTP not only include livestock grazing but also township development, and ecosystem restoration programs, which all together exert spatially complex influences on ecosystems. These human activities have happened at different regions and scales, therefore, showed strong spatial variation. Overall, chapter 3 shows both positive and negative human influences on grassland biomass at two spatial scales, demonstrating the complexity of the relationship between human-influence intensity and grassland biomass. This study on quantifying spatial variation of human influence on grassland ecosystems is important for better understanding ecosystem dynamics and drivers of ecosystem changes.

RQ3: How did the grassland cover and spatial heterogeneity change between 2000 and 2016? Which degradation levels can be extracted from changes in grassland cover and spatial heterogeneity?

Grassland ecosystems on the QTP have been changed because of increasing human activities and environmental changes. Degraded grasslands on the QTP have shown decreasing vegetation cover and increasing vegetation fragmentation, we monitor the changes in vegetation cover and in its spatial heterogeneity from 2000 – 2016 in chapter 4, and further test whether these changes could be used to identify grassland degradation levels.

We find that the vegetation cover represented by NDVI has increased in most parts (60%) of the study area on the eastern QTP, which is in line with increased vegetation activities reported by earlier studies (Fan et al., 2010; Xu et al., 2011). However, the areas with increasing vegetation cover also show increasing spatial heterogeneity, possibly indicating growing soil patches and unpalatable species. The changing trends of vegetation cover and spatial heterogeneity are associated with the vegetation degradation stages. In degraded areas that were identified in 2004, the vegetation cover shows decreasing trends in 2000–2016, which is contrasted with the increasing trends in desertified areas. Spatial heterogeneity has generally increased in 2000-2016;

however, this increase was weakest in the severely degraded areas and slightly deserted areas in 2004 identified from the literature (Liu et al., 2008) .

The results confirm the hypothesis that the temporal changes in grassland cover and in spatial heterogeneity are associated with literature-identified degradation categories in 2004. In general, the decreases in NDVI and increases in spatial heterogeneity indicate degradation. The increases in both NDVI and spatial heterogeneity at highly vegetated area indicate degradation because of increasing unpalatable species (Wang et al., 2015) that might strengthen the NDVI signals but serve as a sign of degradation. However, in the area where NDVI is less than 0.2, the increase in both NDVI and spatial heterogeneity indicate re-growing. Based on different changing trends in grassland cover and in spatial heterogeneity, we further define new grassland development stages and degradation categories in 2016 on the eastern QTP. The new degradation categories show that the degradation category dominates the study area, accounting for 63 % of the whole area; improving and recovering make up 24% and 11 % of the study region respectively.

The criteria for identifying grassland degradation are not clear and defining globally accepted criteria are challenging (White et al., 2000). Most studies assigned the grasslands of the QTP with low vegetation cover as degraded grasslands (Chen and Rao, 2008; Feng et al., 2005; Li et al., 2014). However, we argue that vegetation cover at one single time is not a representative indicator of grassland degradation level on the QTP. This is because lower plant cover is a characteristic of grassland ecosystems on the QTP due to the harsh environments. In chapter 4, we conclude that the changes in vegetation cover and in spatial heterogeneity serve as indicators of grassland degradation and development stages.

5.2 Main contributions

Remote sensing offers an effective way to address challenges of alpine grassland ecosystems studies in mapping plant traits, quantifying the human influence on grassland biomass and monitoring ecosystem changes. There are three main contributions of this thesis.

We firstly provide possibilities of measuring plant traits using the available high-resolution satellite data and linking the remotely-sensed plant traits with field measured traits. We find that the plant traits estimated from the satellite data at the canopy scale are comparable to the plant traits measured at the community level. In chapter 2, we estimate plant traits of alpine grasslands using statistical models and satellite data, showing possibilities of estimating herbaceous plant traits at the large scale. The spatial variation of remotely sensed plant traits on the QTP shows the prominent gradient in climate, soil properties, and human influence, which facilitates further understanding on how plants traits correlate to environmental variables and human activities.

Secondly, we provide a methodological framework for quantifying the spatial variation of human influence on biomass at two spatial scales. The framework of mapping human influence on pasture grassland ecosystems is applicable to other pastoralism ecosystems, especially these with reduced pastoralism mobility. We show that overgrazing has occurred near settlements but overall we reveal that the complex grazing effects on the QTP depends on the spatial scales. Furthermore, we suggest the critical areas where human activities have negative influences on biomass that would guide policy-makers to protect the regions that are potentially vulnerable.

Thirdly, we propose the indicators for defining grassland development and degradation levels. We find that the combined changes in vegetation cover and in spatial heterogeneity can indicate different grassland degradation levels and development stages on the QTP. The vegetation greening trend observed from the satellite data is not consistent with the widely recognized ecosystem degradation in the field (Li et al., 2018a, 2014). Either only vegetation cover in a single time or temporal changes in vegetation cover have been used to indicate ecosystem degradation levels in previous studies (Fassnacht et al., 2015; Li et al., 2014). The combined changes in vegetation cover and in spatial heterogeneity proposed in this study provides a more comprehensive picture of ecosystem degradation levels and

improving conditions in 2016. The output of ecosystem development and degradation categories on the QTP is critical to understand how ecosystems respond to environmental change and human influence. The proposed indicators for monitoring grassland development and degradation categories can be tested in other arid ecosystems where bare-soil patches have been widely developed (Aguiar and Sala, 1999; Bestelmeyer et al., 2013; Kéfi et al., 2007).

5.3 Open issues and future directions

Besides the findings of this thesis and its main contributions, there remain open issues to discuss and the next research directions to focus on.

5.3.1 Open issues

Remote sensing of plant trait can be measured at both the individual scale and further upscale to the canopy scale (Violle et al., 2007). However, the detailed understanding of the link between community plant traits and spectral information is not clear. Furthermore, reflectance patterns at the canopy scale represent the integrated effects of biochemical and structural constituents and often influenced by multiple species and functional groups (Ollinger, 2011). Various combinations of individual plant properties can yield similar whole-canopy spectra (Ollinger, 2011). Thus canopy structure affects the interpretation of canopy reflectance and traits estimation accuracy (Knyazikhin et al., 2013). The study on how spectral information at leaf and canopy levels correlate to plant traits measured at leaf and community level is important to accurately retrieve plant traits from the satellite data. Particularly, future research is needed on testing the hypothesis that leaf-level traits measurement (i.e. CWMs of SLA and LDMC) is comparable to field-measured and remotely sensed plant traits (SPA and PDMC). Strengthening the hypothesis would be beneficial for successful integration of RS observations and ecological applications (Messier et al., 2010). Physical canopy reflectance models such as PROSAIL could further be used to improve understanding on the link between community plant traits with spectral information (Feilhauer et al., 2017; Jacquemoud et al., 2009).

Second, we hypothesize that distance to settlements serves as a proxy of human influence intensity and changes in biomass along the distance was correlated to human influence intensity. However, the changes in other environmental variables such as topography and soil properties might also affect biomass. For example,

topography might affect the accessibility of the pasture and footprint of human activities. Therefore, when analyzing human influential distance, topography could be added as a weight in the model.

Furthermore, when mapping grassland degradation categories, we study the spatial heterogeneity at 500 m scale within an area of 1500 m * 1500 m, which allows the monitoring of spatial heterogeneity related to the large-scale soil patches (> 500 m). However, bare-soil patches occur on the QTP at different scales, varying from less than 0.1 m to larger than 500 m and these patches are driven by different variables like small-mammal activities and topography. Satellite data with higher resolution such as Landsat (30 m) and Sentinel-2 (10-20 m) could be used to map and monitor spatial heterogeneity related to the bare-soil patches that are less than 30 m.

5.3.2 Monitoring changes in plant traits

Vegetation spectra from remote platforms provide ways of estimating plant traits over large areas at regular intervals (Homolová et al., 2013; Kokaly et al., 2009; Ollinger, 2011). Monitoring temporal changes in plant traits is essential for predicting ecosystem functioning in response to the warming and wetting trend on the QTP (Kang et al., 2010; Yao et al., 2012; You et al., 2013) and also for predicting ecosystem functioning. In this study, we find that Sentinel-2 and Landsat-8 data provides reasonable accuracies for estimating plant traits at the canopy level. The continuous operation of these satellite observations offers the possibility to measure the plant traits (optical traits) at the canopy scale in the long-term. Combining this with increasing in-situ plant traits data availability on the QTP even at the global scale (Kattge et al., 2011) paves the way for possible large-scale and long-term plant traits estimation.

5.3.3 Monitoring changes in human influence on the QTP ecosystems

In recent years, human activities on the QTP have been growing, including increasing changes in land use, growing population and infrastructure development, which impacts on the loss of ecosystem functioning and ecosystem services (Li et al., 2017). Future studies on assessing changes in the human influence on ecosystems could include information on human activities such as land use maps, road and settlement density, and population density. Assessing changes in the human influence on ecosystems is valuable for monitoring ecosystem services and to provide guidance on implementing ecosystem protection projects. The framework of mapping human

influence proposed in this thesis could be used for this aim, which could further to help disentangling the combined effects of human activities and climate change on the ecosystem.

5.3.4 Attributing drivers for ecosystem developments and degradation on the QTP

Monitoring changes in plant traits and human influence would help to better understand changes in ecosystem degradation on the QTP. The studies on attributing variables that are causing vegetation fragmentation are important to understand potential reasons for ecosystem degradation. The reasons for ecosystem change and degradation on the QTP are complex (X. Li et al., 2018b; Harris, 2010; Miehe et al., 2019). Climate change and human activities have been widely discussed (Harris, 2010; Lehnert et al., 2016; Li et al., 2013; Miehe et al., 2019) as drivers of ecosystem changes and grassland degradation. Remote sensing data have been widely used to explore the potential drivers such as climatic factors (Wang, 2016; Wang et al., 2016) including changes in precipitation, temperature, and atmospheric CO2 concentration (Piao et al., 2012), ecological restoration projects (Sheng et al., 2019; Feng et al., 2017). However, studies on potential drivers that cause grassland fragmentation are limited. Variables that explain vegetation degradation and fragmentation may be varied at different scales, degradation stages and regions. For example, warming may cause desiccation, which can possibly increase soil erosion along with small-mammal activities at relatively low altitude. However, warming may explain the greening and improving trend of vegetation at higher altitude where vegetation growth is constrained by the low temperature (Ding et al., 2013; Piao et al., 2015; Wang, 2016). This study shows that remote sensing can provide ways to monitor the critical areas of grassland degradation and vegetation fragmentation at various scales, ranging from large to local scale. Future remote sensing studies are recommended to explore potential drivers such as climate change variables, small-mammal activities, topographical variables, and distance to human settlements and roads to explain grassland fragmentation and degradation

5.4 References

Aguiar, M.R., Sala, O.E., 1999. Patch structure, dynamics and implications for the functioning of arid ecosystems. Trends Ecol. Evol. 14, 273–277. doi:10.1016/S0169-5347(99)01612-2

Bestelmeyer, B.T., Duniway, M.C., James, D.K., Burkett, L.M., Havstad, K.M., 2013. A test of critical thresholds and their indicators in a desertification-prone ecosystem: More resilience than we thought. Ecol. Lett. 16, 339–345. doi:10.1111/ele.12045

Chen, S., Rao, P., 2008. Land degradation monitoring using multi-temporal Landsat TM/ETM data in a transition zone between grassland and cropland of northeast China. Int. J. Remote Sens. 29, 2055–2073. doi:10.1080/01431160701355280

Ding, M.J., Zhang, Y.L., Sun, X.M., Liu, L.S., Wang, Z.F., Bai, W.Q., 2013. Spatiotemporal variation in alpine grassland phenology in the Qinghai-Tibetan Plateau from 1999 to 2009. Chinese Sci. Bull. 58, 396–405. doi:10.1007/s11434-012-5407-5

Fassnacht, F.E., Li, L., Fritz, A., 2015. Mapping degraded grassland on the Eastern Tibetan Plateau with multi-temporal Landsat 8 data - where do the severely degraded areas occur? Int. J. Appl. Earth Obs. Geoinf. 42, 115–127. doi:10.1016/j.jag.2015.06.005

Feilhauer, H., Somers, B., van der Linden, S., 2017. Optical trait indicators for remote sensing of plant species composition: Predictive power and seasonal variability. Ecol. Indic. 73, 825–833. doi:10.1016/j.ecolind.2016.11.003

Feng, J., Wang, T., Qi, S., Xie, C., 2005. Land degradation in the source region of the Yellow River, northeast Qinghai-Xizang Plateau: Classification and evaluation. Environ. Geol. 47, 459–466. doi:10.1007/s00254-004-1161-6

Harris, R.B., 2010. Rangeland degradation on the Qinghai-Tibetan plateau: A review of the evidence of its magnitude and causes. J. Arid Environ. 74, 1–12. doi:10.1016/j.jaridenv.2009.06.014

Homolová, L., Malenovský, Z., Clevers, J.G.P.W., García-Santos, G., Schaepman, M.E., 2013. Review of optical-based remote sensing for plant trait mapping. Ecol. Complex. 15, 1–16. doi:10.1016/j.ecocom.2013.06.003

Jacquemoud, S., Verhoef, W., Baret, F., Bacour, C., Zarco-Tejada, P.J., Asner, G.P., François, C., Ustin, S.L., 2009. PROSPECT + SAIL models: A review of use for vegetation characterization. Remote Sens. Environ. 113, S56–S66. doi:10.1016/j.rse.2008.01.026

Kang, S., Xu, Y., You, Q., Flügel, W.-A., Pepin, N., Yao, T., 2010. Review of climate and cryospheric change in the Tibetan Plateau. Environ. Res. Lett. 5, 015101. doi:10.1088/1748-9326/5/1/015101

Kattge, J., Díaz, S., Lavorel, S., Prentice, I.C., Leadley, P., Bönisch, G., Garnier, E., Westoby, M., Reich, P.B., Wright, I.J., Cornelissen, J.H.C., Violle, C., Harrison, S.P., Van Bodegom, P.M., Reichstein, M., Enquist, B.J., Soudzilovskaia, N.A., Ackerly, D.D., Anand, M., Atkin, O., Bahn, M., Baker, T.R., Baldocchi, D., Bekker, R., Blanco, C.C., Blonder, B., Bond, W.J., Bradstock, R., Bunker, D.E., Casanoves, F., Cavender-Bares, J., Chambers, J.Q., Chapin, F.S., Chave, J., Coomes, D., Cornwell, W.K., Craine, J.M., Dobrin, B.H., Duarte, L., Durka, W., Elser, J., Esser, G., Estiarte, M., Fagan, W.F., Fang, J., Fernández-Méndez, F., Fidelis, A., Finegan, B., Flores, O., Ford, H., Frank, D., Freschet, G.T., Fyllas, N.M., Gallagher, R. V., Green, W.A., Gutierrez, A.G., Hickler, T., Higgins, S.I., Hodgson, J.G., Jalili, A., Jansen, S., Joly, C.A., Kerkhoff, A.J., Kirkup, D., Kitajima, K., Kleyer, M., Klotz, S., Knops, J.M.H., Kramer, K., Kühn, I., Kurokawa, H., Laughlin, D., Lee, T.D., Leishman, M., Lens, F., Lenz, T., Lewis, S.L., Lloyd, J., Llusià, J., Louault, F., Ma, S., Mahecha, M.D., Manning, P., Massad, T., Medlyn, B.E., Messier, J., Moles, A.T., Müller, S.C., Nadrowski, K., Naeem, S., Niinemets, Ü., Nöllert, S., Nüske, A., Ogaya, R., Oleksyn, J., Onipchenko, V.G., Onoda, Y., Ordoñez, J., Overbeck, G., Ozinga, W.A., Patiño, S., Paula, S., Pausas, J.G., Peñuelas, J., Phillips, O.L., Pillar, V., Poorter, H., Poorter, L., Poschlod, P., Prinzing, A., Proulx, R., Rammig, A., Reinsch, S., Reu, B., Sack, L., Salgado-Negret, B., Sardans, J., Shiodera, S., Shipley, B., Siefert, A., Sosinski, E., Soussana, J.F., Swaine, E., Swenson, N., Thompson, K., Thornton, P., Waldram, M., Weiher, E., White, M., White, S., Wright, S.J., Yguel, B., Zaehle, S., Zanne, A.E., Wirth, C., 2011. TRY - a global database of plant traits. Glob. Chang. Biol. 17, 2905–2935. doi:10.1111/j.1365-2486.2011.02451.x

Kéfi, S., Rietkerk, M., Alados, C.L., Pueyo, Y., Papanastasis, V.P., ElAich, A., De Ruiter, P.C., 2007. Spatial vegetation patterns and imminent desertification in Mediterranean arid ecosystems. Nature 449, 213–217. doi:10.1038/nature06111

Knyazikhin, Y., Schull, M.A., Stenberg, P., Mottus, M., Rautiainen, M., Yang, Y., Marshak, A., Latorre Carmona, P., Kaufmann, R.K., Lewis, P., Disney, M.I., Vanderbilt, V., Davis, A.B., Baret, F., Jacquemoud, S., Lyapustin, A., Myneni, R.B., 2013. Hyperspectral remote sensing of

foliar nitrogen content. Proc. Natl. Acad. Sci. 110, E185–E192. doi:10.1073/pnas.1210196109

Kokaly, R.F., Asner, G.P., Ollinger, S. V., Martin, M.E., Wessman, C.A., 2009. Characterizing canopy biochemistry from imaging spectroscopy and its application to ecosystem studies. Remote Sens. Environ. 113, S78–S91. doi:10.1016/j.rse.2008.10.018

Lehnert, L.W., Wesche, K., Trachte, K., Reudenbach, C., Bendix, J., 2016. Climate variability rather than overstocking causes recent large scale cover changes of Tibetan pastures. Sci. Rep. 6, 24367. doi:10.1038/srep24367

Li, S., Zhang, Y., Wang, Z., Li, L., 2017. Mapping human influence intensity in the Tibetan Plateau for conservation of ecological service functions. Ecosyst. Serv. doi:10.1016/j.ecoser.2017.10.003

Li, X.-L., Gao, J., Brierley, G., Qiao, Y.-M., Zhang, J., Yang, Y.-W., 2013. Rangeland Degradation on the Qinghai-Tibet Plateau: Implications for Rehabilitation. L. Degrad. Dev. 24, 72–80. doi:10.1002/ldr.1108

Li, X., Gao, J., Zhang, J., 2018a. A topographic perspective on the distribution of degraded meadows and their changes on the Qinghai-Tibet Plateau, West China. L. Degrad. Dev. 29, 1574–1582. doi:10.1002/ldr.2952

Li, X., Perry, G.L.W., Brierley, G.J., 2018b. A spatial simulation model to assess controls upon grassland degradation on the Qinghai-Tibet Plateau, China. Appl. Geogr. 98, 166–176. doi:10.1016/j.apgeog.2018.07.003

Li, X.L., Perry, G.L.W., Brierley, G., Sun, H.Q., Li, C.H., Lu, G.X., 2014. Quantitative assessment of degradation classifications for degraded alpine meadows (Heitutan), Sanjiangyuan, western China. L. Degrad. Dev. 25, 417–427. doi:10.1002/ldr.2154

Liu, J., Xu, X., Shao, Q., 2008. Grassland degradation in the "Three-River Headwaters" region, qinghai province. J. Geogr. Sci. 18, 259–273. doi:10.1007/s11442-008-0259-2

Lu, X., Kelsey, K.C., Yan, Y., Sun, J., Wang, X., Cheng, G., Neff, J.C., 2017. Effects of grazing on ecosystem structure and function of alpine grasslands in Qinghai-Tibetan Plateau: A synthesis. Ecosphere 8. doi:10.1002/ecs2.1656

Messier, J., McGill, B.J., Lechowicz, M.J., 2010. How do traits vary across ecological scales? A case for trait-based ecology. Ecol. Lett. 13, 838–848. doi:10.1111/j.1461-0248.2010.01476.x

Miehe, G., Schleuss, P.M., Seeber, E., Babel, W., Biermann, T., Braendle, M., Chen, F., Coners, H., Foken, T., Gerken, T., Graf, H.F., Guggenberger, G., Hafner, S., Holzapfel, M., Ingrisch, J., Kuzyakov, Y., Lai, Z., Lehnert, L., Leuschner, C., Li, X., Liu, J., Liu, S., Ma, Y., Miehe, S., Mosbrugger, V., Noltie, H.J., Schmidt, J., Spielvogel, S., Unteregelsbacher, S., Wang, Y., Willinghöfer, S., Xu, X., Yang, Y., Zhang, S., Opgenoorth, L., Wesche, K., 2019. The Kobresia pygmaea ecosystem of the Tibetan highlands – Origin, functioning and degradation of the world's largest pastoral alpine ecosystem: Kobresia pastures of Tibet. Sci. Total Environ. 648, 754–771. doi:10.1016/j.scitotenv.2018.08.164

Ollinger, S. V., 2011. Sources of variability in canopy reflectance and the convergent properties of plants. New Phytol. 189, 375–394. doi:10.1111/j.1469-8137.2010.03536.x

Papanastasis, V.P., 2009. Restoration of degraded grazing lands through grazing management: Can it work? Restor. Ecol. 17, 441–445. doi:10.1111/j.1526-100X.2009.00567.x

Piao, S., Tan, K., Nan, H., Ciais, P., Fang, J., Wang, T., Vuichard, N., Zhu, B., 2012. Impacts of climate and CO2changes on the vegetation growth and carbon balance of Qinghai-Tibetan grasslands over the past five decades. Glob. Planet. Change 98–99, 73–80. doi:10.1016/j.gloplacha.2012.08.009

Piao, S., Yin, G., Tan, J., Cheng, L., Huang, M., Li, Y., Liu, R., Mao, J., Myneni, R.B., Peng, S., Poulter, B., Shi, X., Xiao, Z., Zeng, N., Zeng, Z., Wang, Y., 2015. Detection and attribution of vegetation greening trend in China over the last 30 years. Glob. Chang. Biol. 21, 1601–1609. doi:10.1111/gcb.12795

Sheng, W., Zhen, L., Xiao, Y., Hu, Y., 2019. Ecological and socioeconomic effects of ecological restoration in China's Three Rivers Source Region. Sci. Total Environ. 650, 2307–2313. doi:10.1016/j.scitotenv.2018.09.265

Violle, C., Navas, M.L., Vile, D., Kazakou, E., Fortunel, C., Hummel, I., Garnier, E., 2007. Let the concept of trait be functional! Oikos 116, 882–892. doi:10.1111/j.2007.0030-1299.15559.x

Wang, C., 2016. A remote sensing perspective of alpine grasslands on the Tibetan Plateau: Better or worse under "Tibet Warming"? Remote Sens. Appl. Soc. Environ. 3, 36–44. doi:10.1016/j.rsase.2015.12.002

Wang, P., Lassoie, J.P., Morreale, S.J., Dong, S., 2015. A critical review of socioeconomic and natural

factors in ecological degradation on the Qinghai-Tibetan Plateau, China. Rangel. J. 37, 1–9. doi:10.1071/RJ14094

Wang, X., Yi, S., Wu, Q., Yang, K., Ding, Y., 2016. The role of permafrost and soil water in distribution of alpine grassland and its NDVI dynamics on the Qinghai-Tibetan Plateau. Glob. Planet. Change 147, 40–53. doi:10.1016/j.gloplacha.2016.10.014

Wang, Y., Heberling, G., Görzen, E., Miehe, G., Seeber, E., Wesche, K., 2017. Combined effects of livestock grazing and abiotic environment on vegetation and soils of grasslands across Tibet. Appl. Veg. Sci. 20, 327–339. doi:10.1111/avsc.12312

White, R., Murray, S., Rohweder, M., 2000. Pilot Analysis of Global Ecosystems: Grassland Ecosystems, World Resources Institute. doi:10.1021/es0032881

Yao, T., Thompson, L.G., Mosbrugger, V., Zhang, F., Ma, Y., Luo, T., Xu, B., Yang, X., Joswiak, D.R., Wang, W., Joswiak, M.E., Devkota, L.P., Tayal, S., Jilani, R., Fayziev, R., 2012. Third Pole Environment (TPE). Environ. Dev. 3, 52–64. doi:10.1016/j.envdev.2012.04.002

You, Q., Fraedrich, K., Ren, G., Pepin, N., Kang, S., 2013. Variability of temperature in the Tibetan Plateau based on homogenized surface stations and reanalysis data. Int. J. Climatol. 33, 1337–1347. doi:10.1002/joc.3512

Curriculum vitae

Chengxiu Li

Education

2014 – 2018 Ph.D. candidate in Earth Observation
Department of Geography, Remote Sensing Laboratories
University of Zurich (CH).

2011 – 2014 Master of Science in Geography

Institute of Glaciology and Eco-geography, Lanzhou University, China

Thesis title: *Remote sensing of snow cover and glacier area dynamics on the Qinghai-Tibetan Plateau* (in Chinese)

2006 – 2010 Bachelor of Science in Resources Science and Engineering

Beijing Normal University, China

Thesis title: *Structure and Species Diversity of Meadow Community along the Shaliu River in the Qinghai Lake Basin* (In Chinese)

Teaching and supervision

2015 – 2018 Assistant for courses within the Department of Geography, University of Zurich

GEO441 Spectroscopy of the Earth System: Advising master students on the project: "*Monitoring Phenology using Satellite Data*"

GEO 229 Small Group Teaching in Geography: Leading the group discussion and guiding students for finishing small essay.

Previous research and professional experience

Sep 2010 - Jul 2011 Geography teacher in High Middle School,
Affiliated School in Inner Mongolia Normal University, China

Jul 2011 - Aug 2011 Project Assistance in Global LAnd Surface Satellite (GLASS) product generation, College of Global Change and Earth,
Beijing Normal University, China

Graduate courses and training

- PhD Seminars I & II
- Principles and Theory in Geography
- Graduate School Retreat Seminars (I & II)
- Scientific writing

- Project management
- Voice training and presentation skills
- Time and self-management
- ECO 332 R4All. A Recipe for Success with Successful R
- ECO 331 General Linear and Linear Mixed Successful Models in R
- ESS 401 Current topics in Earth System Successful Science
- ECO 374 How to Publish in Peer-Reviewed Successful Journals
- ECO 339 Community Ecology

Peer-reviewed publications

Li, C. et al. (2019) Spatial variation of human influences on grassland biomass on the Qinghai-Tibetan Plateau. Sci. Total Environ. 665, 678–689

Li, C. et al. (2018) Estimating plant traits of alpine grasslands on the qinghai-tibetan plateau using remote sensing. IEEE J. Sel. Top. Appl. Earth Obs. Remote Sens. 11, 2263–2275.

Chengxiu Li. et al. (under revision Ecological Indicators) Changes in grassland cover and in its spatial heterogeneity indicate degradation on the Qinghai-Tibetan Plateau

Conference contributions

2017 Swiss Geoscience Meeting, Davos, Switzerland. *The impacts of human activities and environmental variables on grassland canopy traits on the Qinghai-Tibetan Plateau.*

2017 10th EARSeL Imaging Spectroscopy Workshop, Zurich (CH). *Monitoring Functional Traits of Alpine Vegetation using Remote Sensing*

2016 IGRASS IEEE International Geoscience and Remote Sensing Symposium, Beijing, China. *Monitoring Functional Traits of Alpine Vegetation on The Tibetan Plateau using Multi-Sensor Remote Sensing*

2016 American Geophysical Union AGU, San Francisco, USA. *Monitoring Functional Traits of Alpine Vegetation using Remote Sensing*

Acknowledgements

Pursuing a PhD degree far from home is very challenging but rewarding life experience. There are many people helped me along the way and to whom I would like to express my gratitude.

I am very grateful for my supervisor Prof. Michael Schaepman for providing the opportunity to undertake this PhD research in Europe. His suggestions, advices are very helpful for making progress on research. I appreciate his trust and encouragement for developing research questions independently, which not only contribute significantly to the PhD work, but also offer inspiration for my academic career path.

I would like to thank my daily supervisors Dr. Hendrik Wulf for his time on meetings and discussions. I very much appreciate his contribution on the research and support for my personal life, especially always being there to help me out and be very encouraging and warming. I am thankful to Dr. Rogier de Jong for his valuable inputs to this Ph.D. Thanks for helping with the data analysis and fruitful discussions, which are very important for the last stage of the PhD. I would especially like to thank my PhD Committee Member Prof. Bernhard Schmid for his comprehensive help on my PhD publications. I appreciate his patience, scientific enthusiasm and spirit for always pursuing better scientific quality.

My appreciation further goes to all my colleagues at RSL and URPP GCB for exchanging research ideas and many unforgettable social events. Special thanks to Carla, Fabian, Irene, Jing, Gilian, Ewa, Zhaoju, Rifat, Hossein, Peter, Shivangi for discussions and all nice time spent together. I am in particularly thankful to Sanne, Daniela and Parviz for help on programming in R, giving me support and encouragement when I got lost with PhD progress, and always caring for my personal life in Zurich. Furthermore, I would like to acknowledge the kindness of Rita Ott and Sandra Altorfer for making my life easier over the last four years.

I express my gratitude to my Chinese friends Bai Yu, Deng Ting, Shao Feng, Shao Pu, Lu Gang, Cao Xiaobao, Ling Wang, Yuanyuan, Wenjie, and Dong Wang for offering their company and time which made me feel closer to home. Further, I acknowledge my PhD funding agency China Scholarship Council (CSC).

My special thanks to Domi, you made my PhD life happier and easier. I'm thinking of you every day.

Finally my heartfelt thanks go to my parents and my sisters, my love for you grows everyday even though I am far from home.